



Experimental study of Generalised Parton Distributions at Jefferson Lab

Daria Sokhan
University of Glasgow, UK

The 11th Workshop on Hadron Physics in China and Opportunities Worldwide
Nankai University, Tianjin, China — 24th August 2019



Introduction

A constructivist view of the nucleon

Wigner distributions

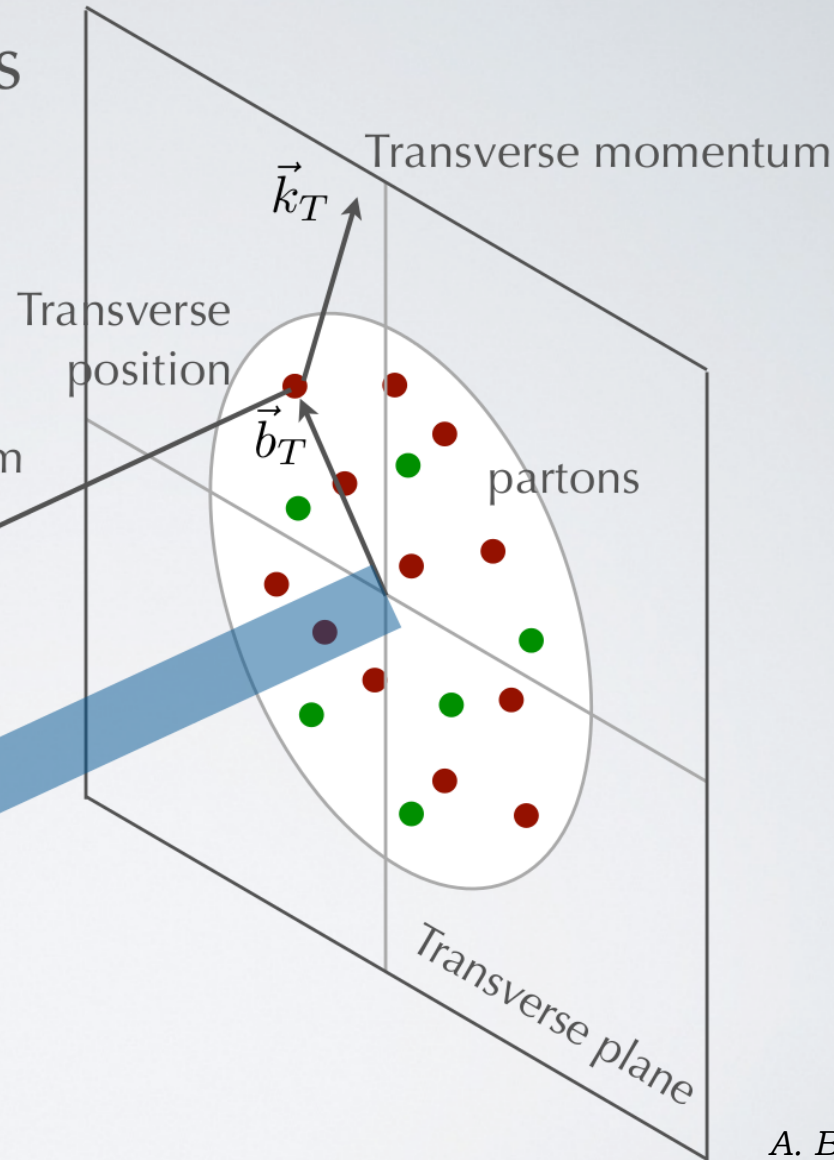
$$\rho(x, \vec{k}_T, \vec{b}_T)$$

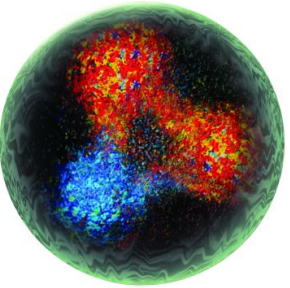
*intuitive relation to
experimental observables*

Longitudinal momentum

$$k^+ = xP^+$$

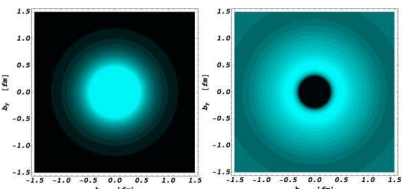
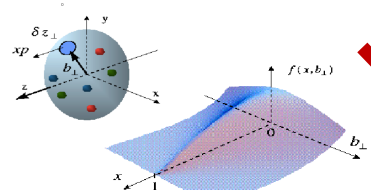
x : longitudinal
momentum
fraction carried by
struck parton





Wigner function:
full phase space parton distribution of the nucleon
Generalised Transverse Momentum Distributions (GTMDs)

Generalised Parton Distributions (GPDs)



Form Factors
eg: G_E, G_M

$\int d^2 k_T$

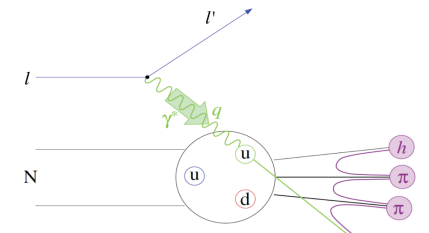
$\int d^2 b_T$

$\int dx$

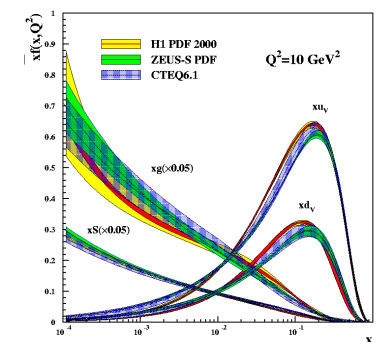
$\int d^2 b_T$

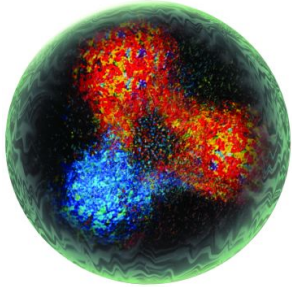
$\int d^2 k_T$

Parton Distribution Functions (PDFs)



Transverse Momentum Distributions (TMDs)

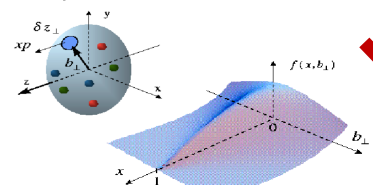




*Wigner function:
full phase space parton
distribution of the nucleon*

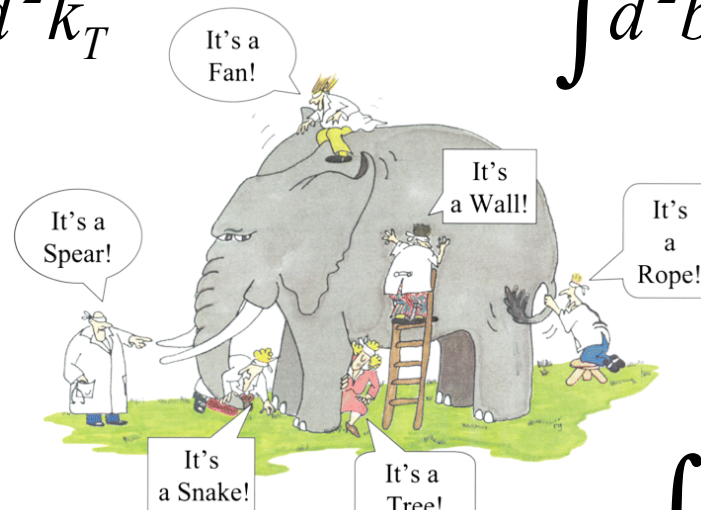
Generalised Transverse Momentum
Distributions (GTMDs)

Generalised Parton
Distributions (GPDs)



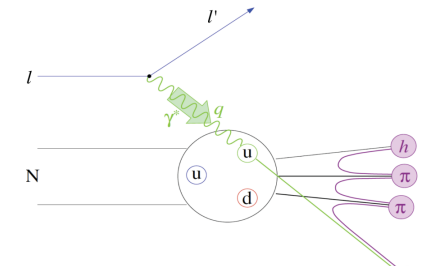
$$\int dx$$

Form Factors
eg: G_E, G_M

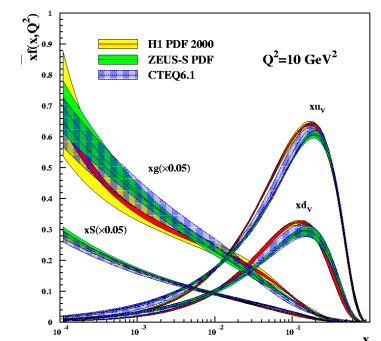


$$\int d^2 k_T$$

Parton Distribution
Functions (PDFs)



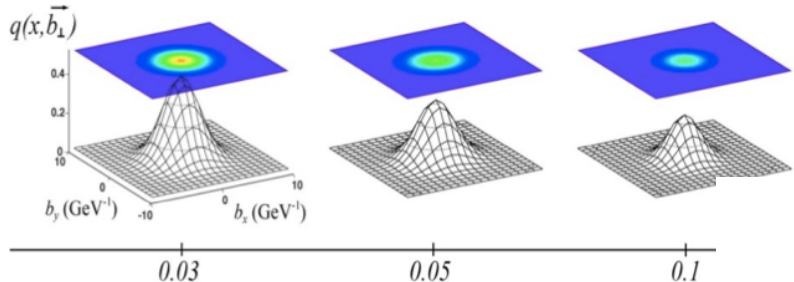
Transverse
Momentum
Distributions
(TMDs)



Generalised Parton Distributions

- proposed by Müller (1994), Radyushkin, Ji (1997).
- can be interpreted as relating, in the infinite momentum frame, transverse position of partons (impact parameter b_\perp) to longitudinal momentum fraction (x).

* **Tomography** of the nucleon:
transverse spatial distributions of quarks and gluons in longitudinal momentum space.



* Indirect access to mechanical properties of the nucleon:
possibilities of extracting **pressure distributions** within the nucleon.

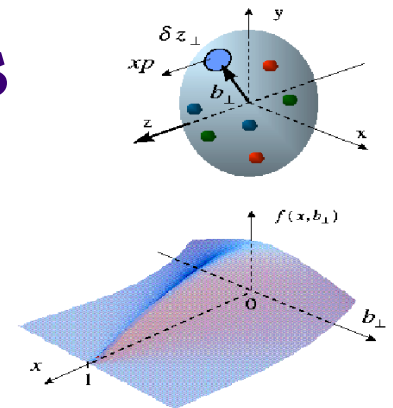
* Information on the orbital angular momentum contribution to nucleon spin:
the spin puzzle.

Ji's relation:

$$J_N = \frac{1}{2} = \frac{1}{2} \sum_q + L_q + J_g$$

$$\begin{aligned} J^q &= \frac{1}{2} - J^g \\ &= \frac{1}{2} \int_{-1}^1 x dx \left\{ H^q(x, \xi, 0) + E^q(x, \xi, 0) \right\} \end{aligned}$$

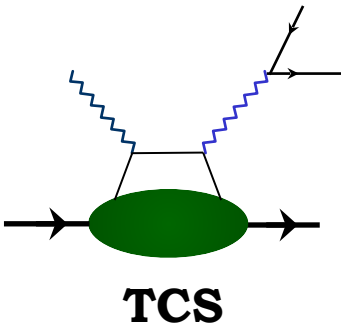
* Combine with TMDs to access **spin-orbit correlations** of quarks and gluons, study non-perturbative interactions of partons.



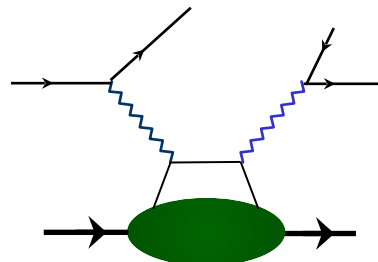
Experimental paths to GPDs in electron - hadron scattering

Accessible in *exclusive* reactions, where all final state particles are determined:

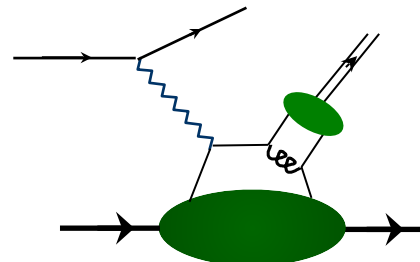
- * Deeply Virtual Compton Scattering (DVCS)
- * Deeply Virtual Meson Production (DVMP) / Hard Exclusive Meson Production (HEMP)
- * Time-like Compton Scattering (TCS)
- * Double DVCS
- * Photon-meson production
- * ...



*Virtual photon
time-like*



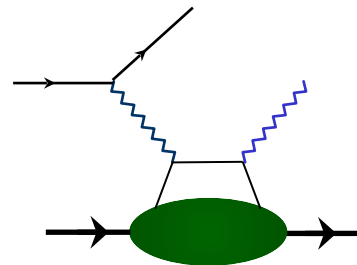
One time-like, one space-like virtual photon



Virtual photon space-like



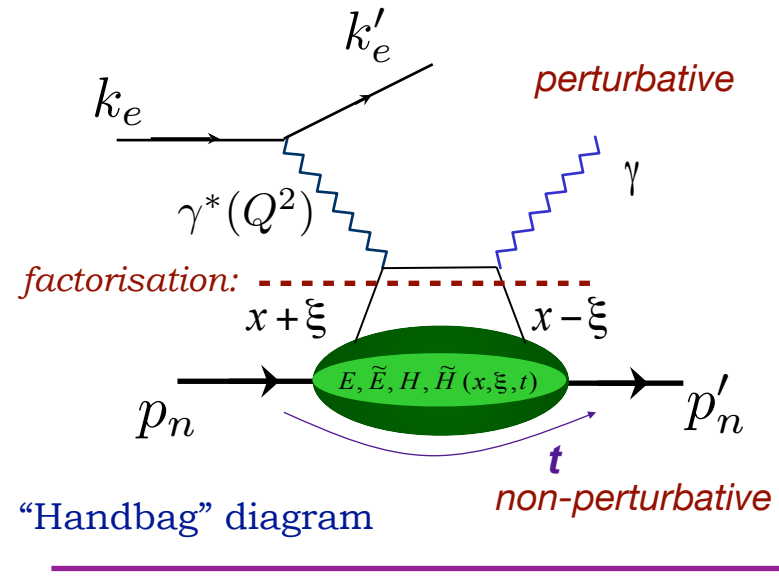
cliparts.co



*Virtual photon
space-like*

Deeply Virtual Compton Scattering

the “golden channel” for GPD extraction



$$Q^2 = -(\mathbf{k} - \mathbf{k}')^2 \quad t = (\mathbf{p}'_n - \mathbf{p}_n)^2$$

$$\text{Bjorken variable: } x_B = \frac{Q^2}{2\mathbf{p}_n \cdot \mathbf{q}}$$

$x \pm \xi$ longitudinal momentum fractions of the struck parton

$$\text{Skewness: } \xi \approx \frac{x_B}{2 - x_B}$$

- * At high exchanged Q^2 and low t access to four parton helicity-conserving, chiral-even GPDs:

$$E^q, \tilde{E}^q, H^q, \tilde{H}^q(x, \xi, t)$$

- * Can be related to PDFs:

$$H(x, 0, 0) = q(x) \quad \tilde{H}(x, 0, 0) = \Delta q(x)$$

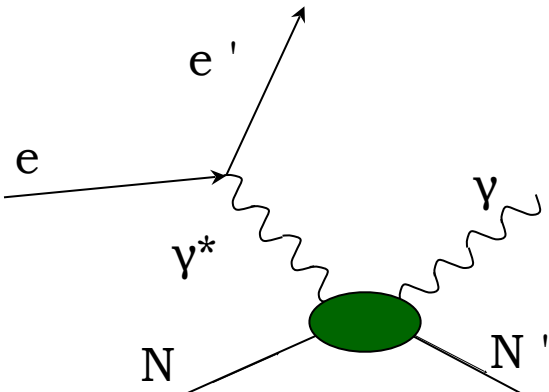
and form factors:

$$\begin{array}{ll} \int_{-1}^{+1} H dx = F_1 & \int_{-1}^{+1} \tilde{H} dx = G_A \\ \int_{-1}^{+1} E dx = F_2 & \int_{-1}^{+1} \tilde{E} dx = G_P \\ \text{(Dirac and Pauli)} & \text{(axial and pseudo-scalar)} \end{array}$$

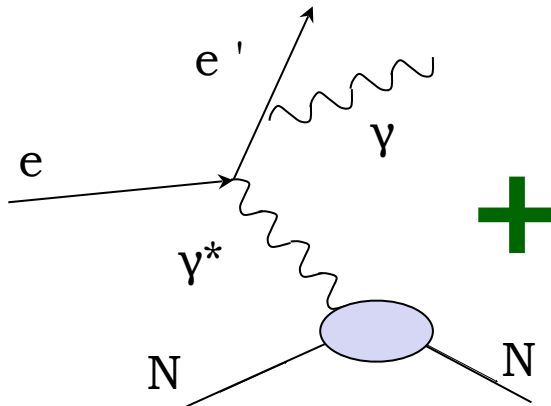
- * Small changes in nucleon transverse momentum allows mapping of transverse structure at large distances.

Measuring DVCS

- * Process measured in experiment:



DVCS



Bethe - Heitler

$$d\sigma \propto |T_{DVCS}|^2 + |T_{BH}|^2 + \underbrace{T_{BH} T^{*}_{DVCS} + T_{DVCS} T^{*}_{BH}}$$

Amplitude parameterised in terms of Compton Form Factors

Amplitude calculable from elastic Form Factors and QED

Interference term

$$|T_{DVCS}|^2 \ll |T_{BH}|^2$$

Compton Form Factors in DVCS

Experimentally accessible in DVCS cross-sections and spin asymmetries, eg:

$$A_{LU} = \frac{d\vec{\sigma} - d\bar{\sigma}}{d\vec{\sigma} + d\bar{\sigma}} = \frac{\Delta\sigma_{LU}}{d\vec{\sigma} + d\bar{\sigma}}$$

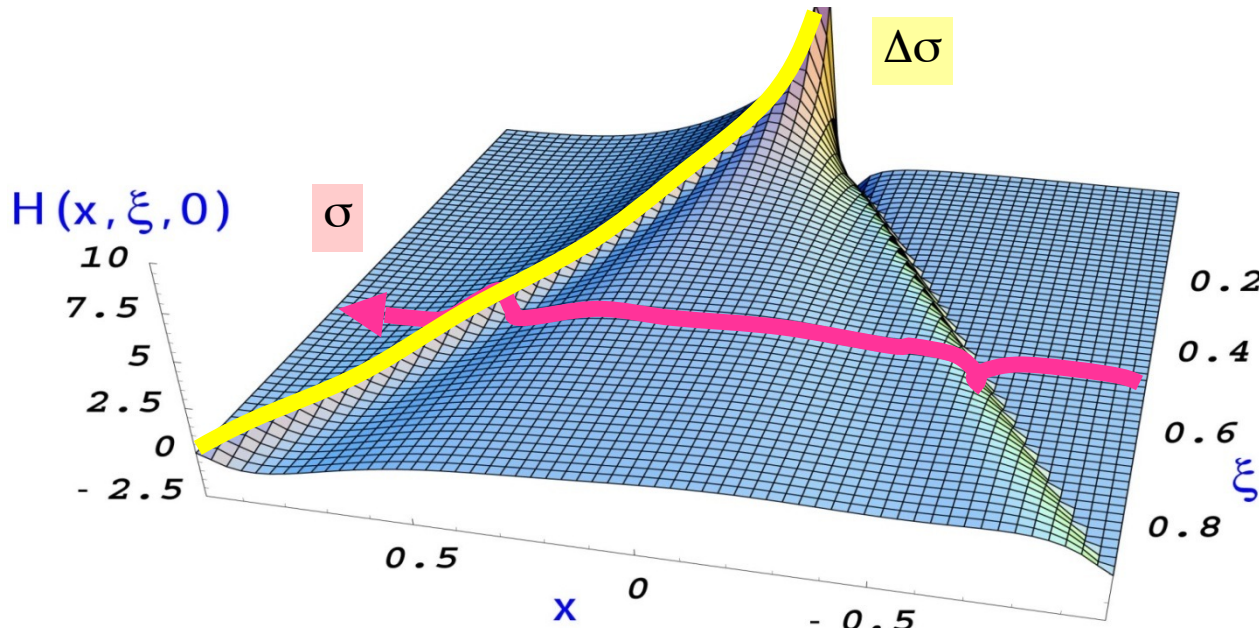
cross-sections,
beam-charge and
double polarisation asymmetries

single-spin
asymmetries

At leading twist, leading order:

$$T^{DVCS} \sim \int_{-1}^{+1} \frac{GPDs(x, \xi, t)}{x \pm \xi + i\varepsilon} dx + \dots \sim$$

$$P \int_{-1}^{+1} \frac{GPDs(x, \xi, t)}{x \pm \xi} dx \pm i\pi GPDs(\pm\xi, \xi, t) + \dots$$



Only ξ and t are accessible
experimentally!

To get information on x need
extensive measurements in Q^2 .

Need measurements off
proton and **neutron** to get
flavour separation of CFFs
in DVCS.

Jefferson Lab



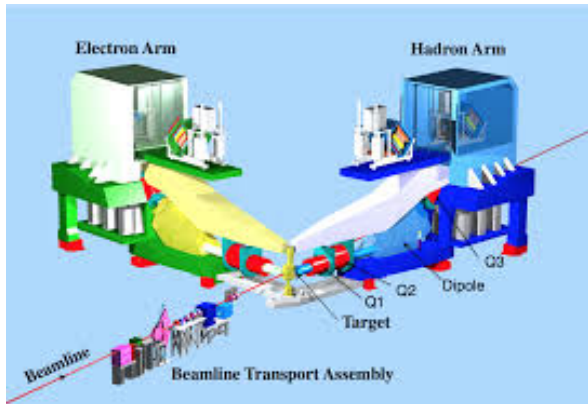
Jefferson Lab: 6 GeV era

CEBAF: Continuous Electron Beam Accelerator Facility.

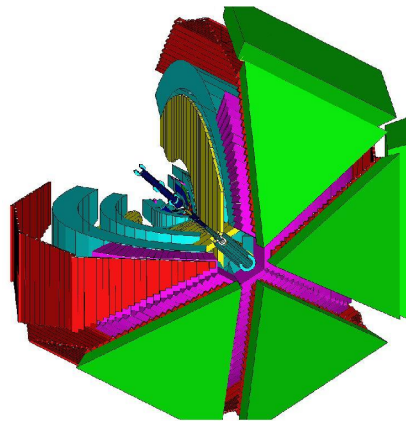
- * Energy up to ~ 6 GeV
- * Energy resolution $\delta E/E_e \sim 10^{-5}$
- * Electron polarisation up to $\sim 85\%$



Hall A:



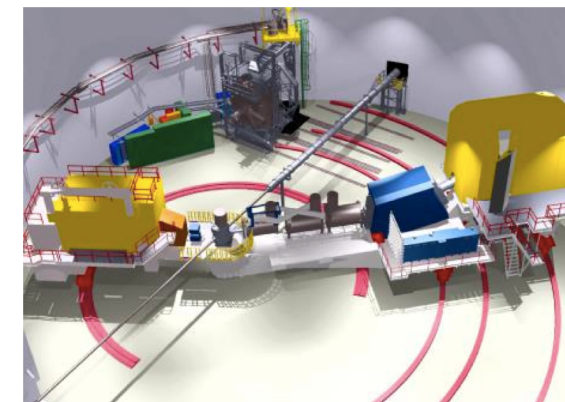
Hall B: CLAS



- * High resolution($\delta p/p = 10^{-4}$) spectrometers, very high luminosity.

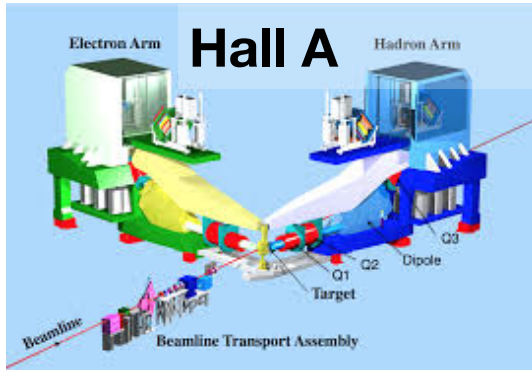
- * Very large acceptance, detector array for multi-particle final states.

Hall C:

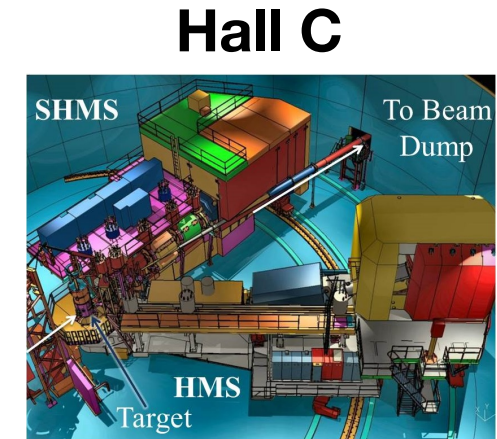
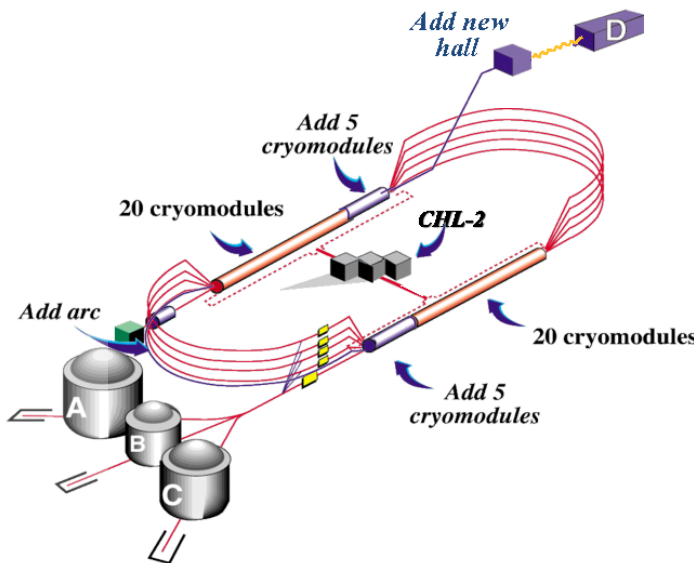


- * Two movable spectrometer arms, well-defined acceptance, high luminosity

JLab @ 12 GeV



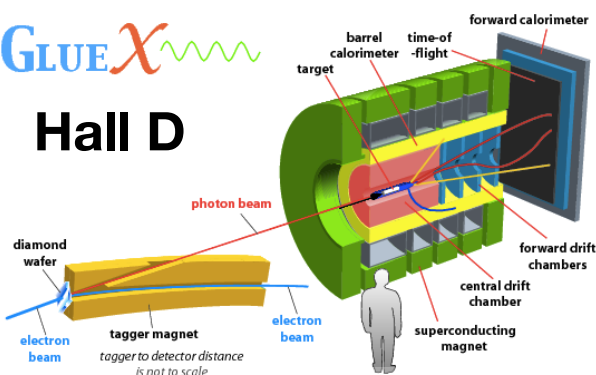
High resolution ($\delta p/p = 10^{-4}$)
spectrometers, very high
luminosity, large installation
experiments.



Two movable high
momentum
spectrometers, well-
defined acceptance,
very high luminosity.

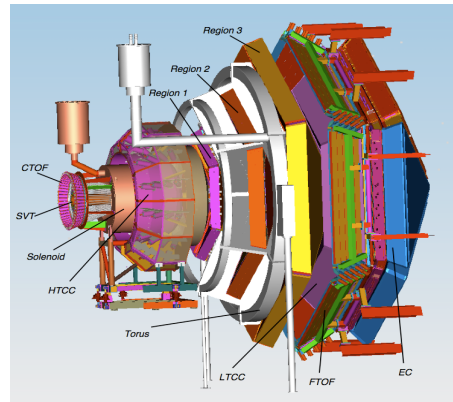
GLUEX

Hall D



9 GeV tagged polarised photons,
full acceptance

Hall B: CLAS12

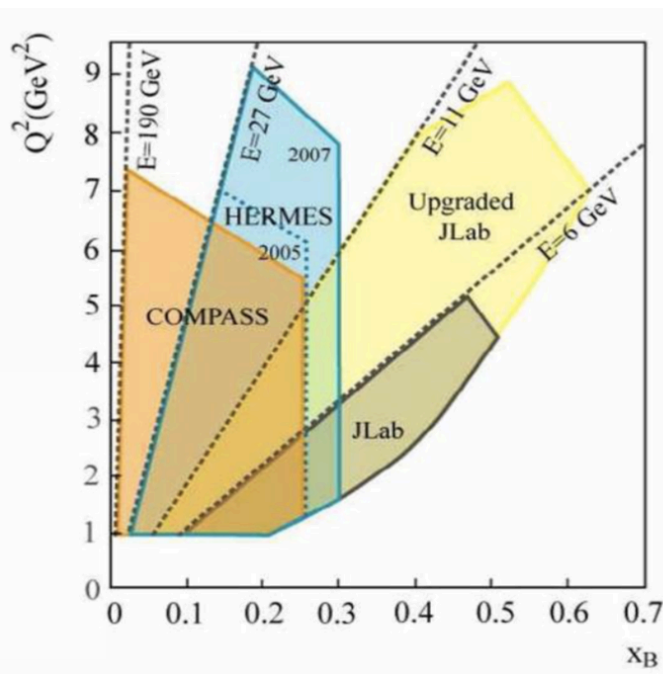


Very large acceptance,
high luminosity.

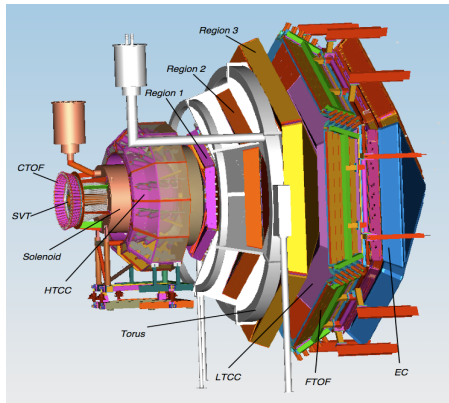
JLab @ 12 GeV



High resolution($\delta p/p = 10^{-4}$) spectrometers, very high luminosity, large installation experiments.



Hall B: CLAS12



Very large acceptance, high luminosity.

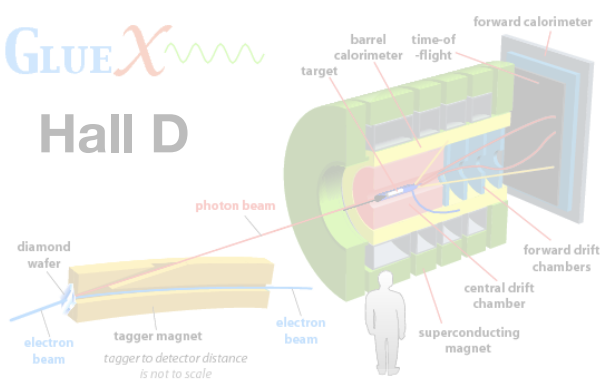


Hall C

Two movable high momentum spectrometers, well-defined acceptance, very high luminosity.

GLUE χ

Hall D



9 GeV tagged polarised photons, full acceptance

CLAS12

Design luminosity

$$L \sim 10^{35} \text{ cm}^{-2} \text{ s}^{-1}$$

High luminosity & large acceptance:

Concurrent measurement of **exclusive**, **semi-inclusive**, and **inclusive** processes

Acceptance for photons and electrons:

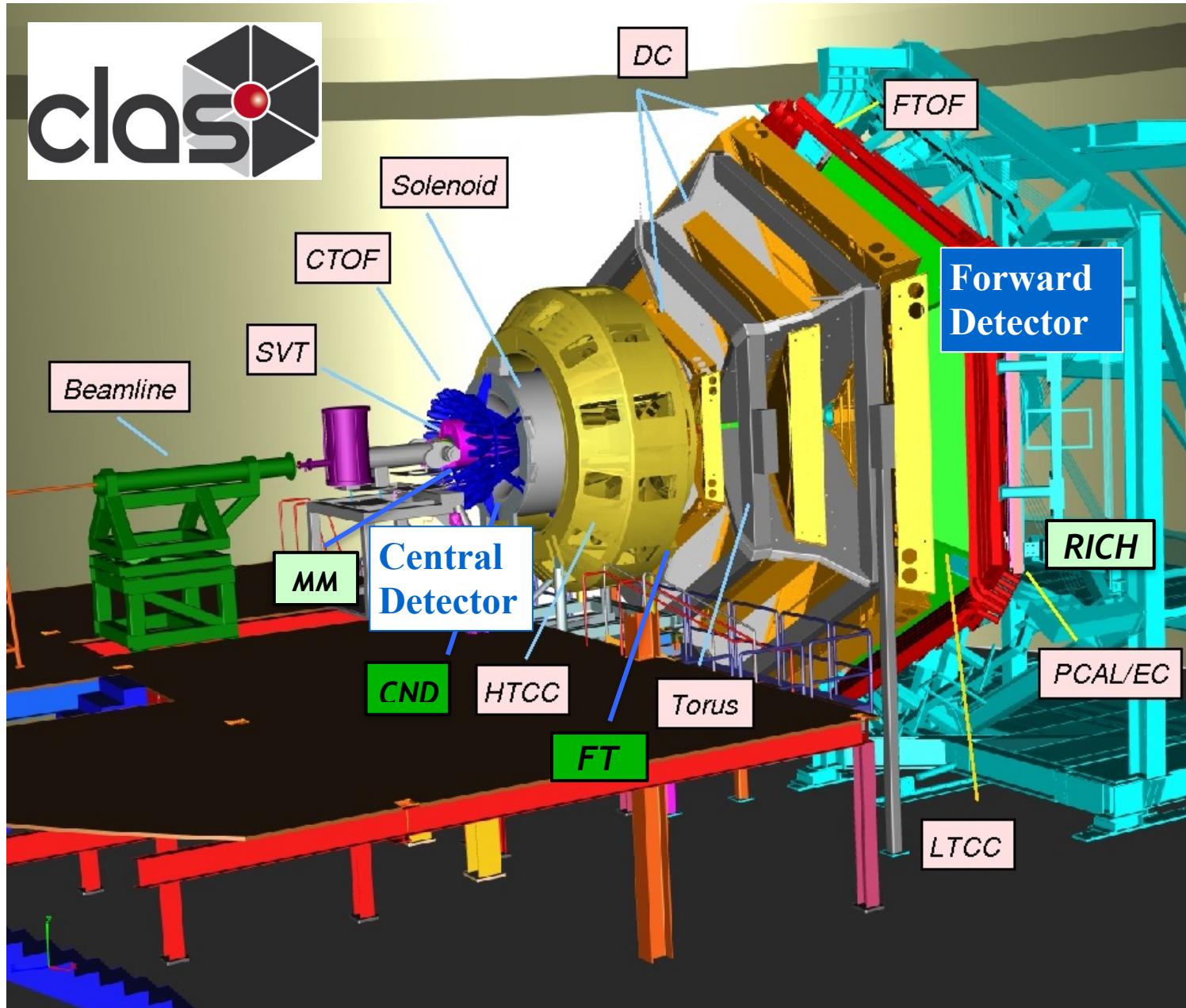
- $2.5^\circ < \theta < 125^\circ$

Acceptance for all charged particles:

- $5^\circ < \theta < 125^\circ$

Acceptance for neutrons:

- $5^\circ < \theta < 120^\circ$



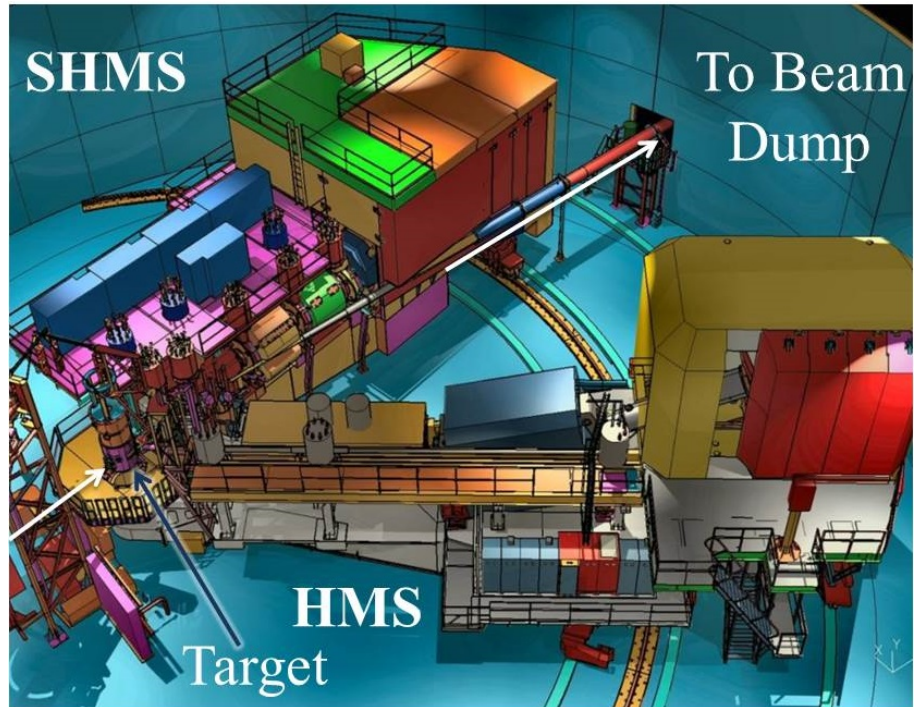
DVCS in Hall C

Detect electron with (Super) High Momentum Spectrometer, (S)HMS.

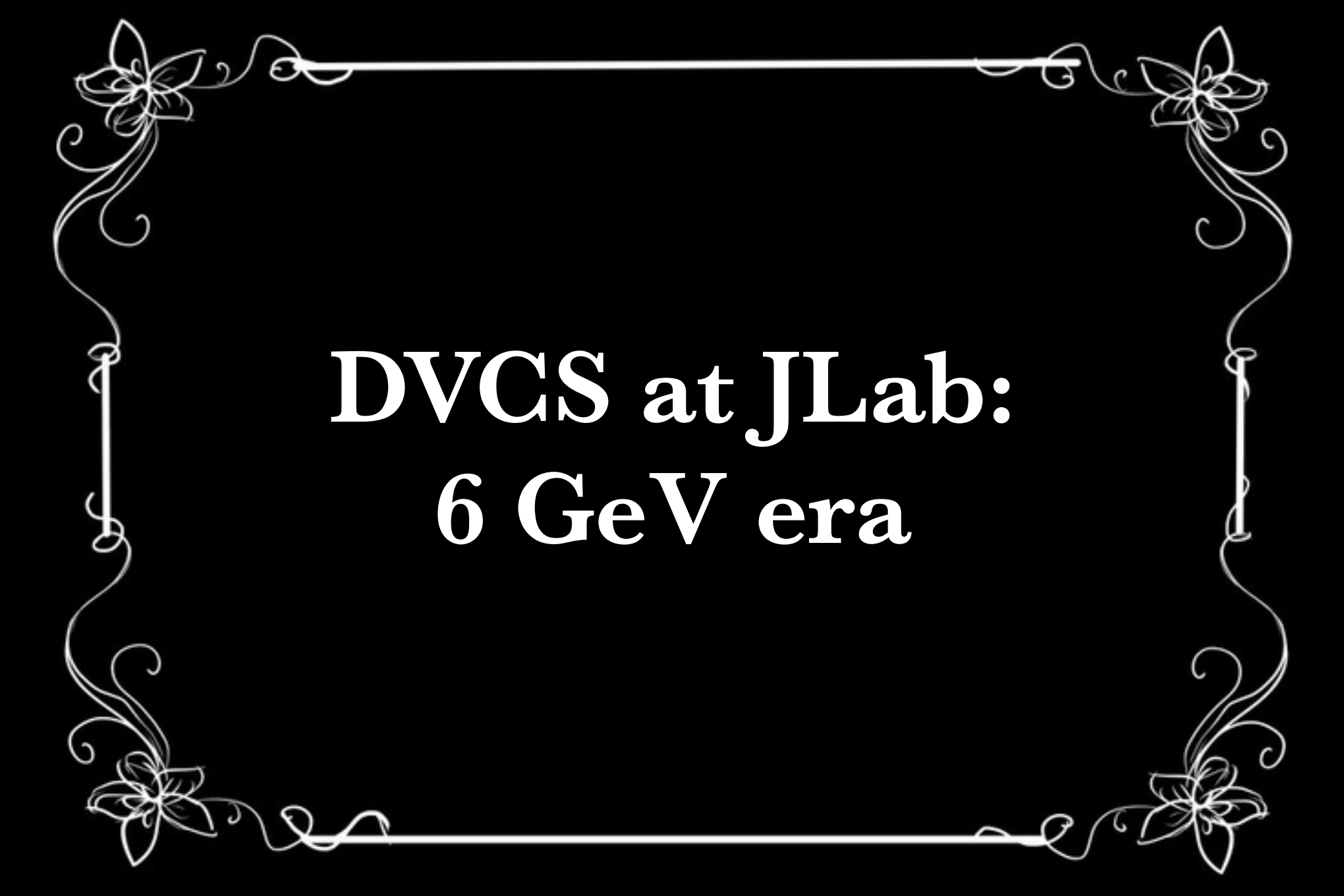
Detect photon in PbWO₄ calorimeter.

Sweeping magnet to reduce backgrounds in calorimeter.

Reconstruct recoiling proton through missing mass.



Similar principle applied in Hall A

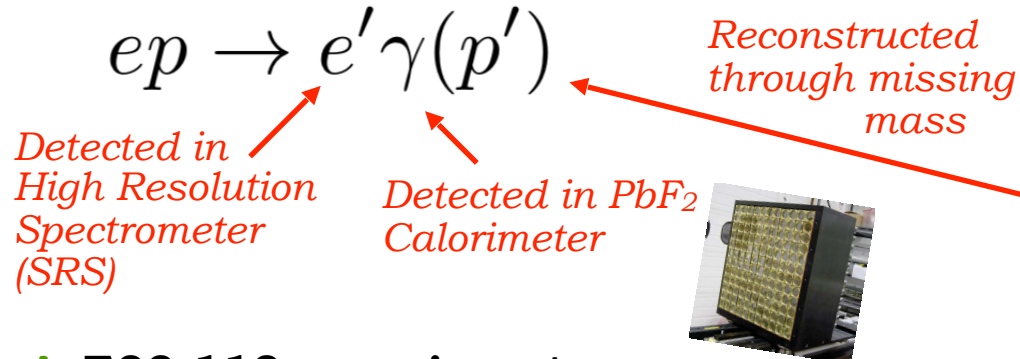


DVCS at JLab: 6 GeV era

DVCS in Hall A

- * 15 cm long liquid H_2 target

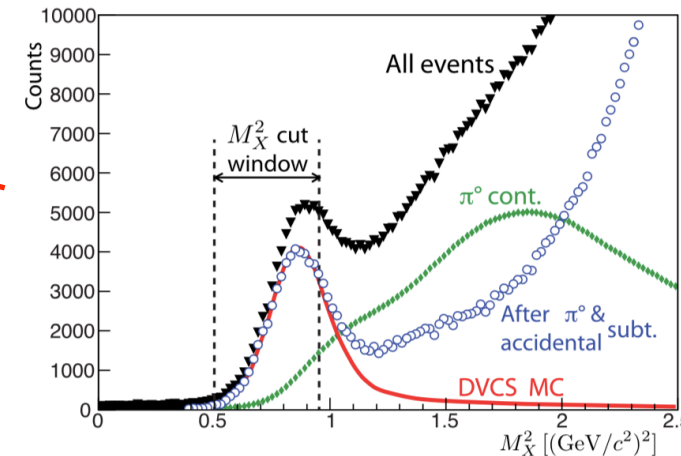
- * Luminosity = $10^{37} \text{ cm}^{-2}\text{s}^{-1}$



* E00-110 experiment

(2004): 5.75 GeV polarised electron beam

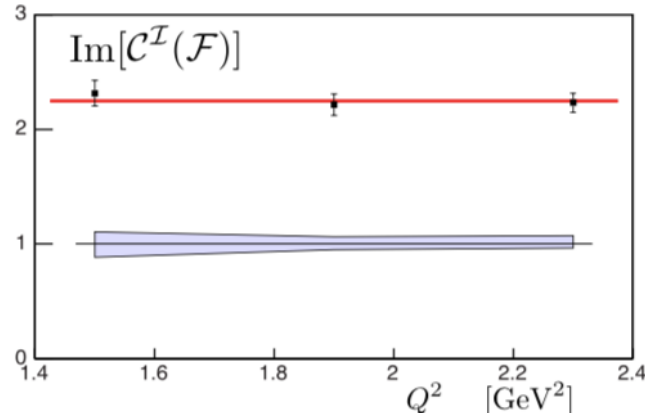
* Measure Q^2 -dependence (Q^2 : 1.5, 1.9, 2.3 GeV^2) of DVCS-BH cross-sections at fixed x_B (0.36) and x_B dependence at constant Q^2 .



M. Defurne *et al*,
PRC 92 (2015)
055202.

* E07-004 experiment (2010):

Energy scan for fixed x_B , Q^2 :

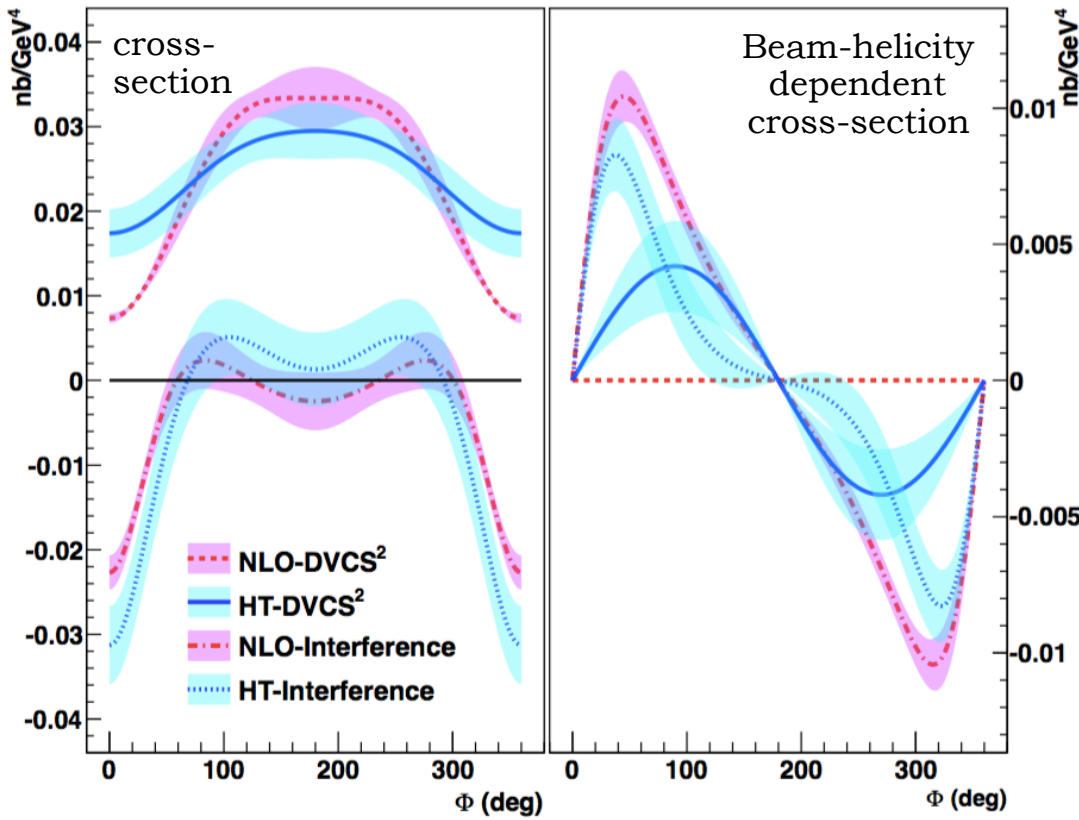


$Q^2 (\text{GeV}^2)$	x_B	$E^{\text{beam}} (\text{GeV})$	$-t (\text{GeV}^2)$
1.50	0.36	3.355	0.18, 0.24, 0.30
		5.55	
1.75	0.36	4.455	0.18, 0.24, 0.30, 0.36
		5.55	
2.00	0.36	4.455	0.18, 0.24, 0.30, 0.36
		5.55	

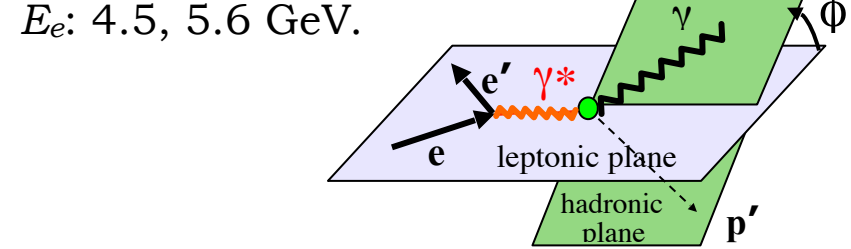
M. Defurne *et al*, PRC 92 (2015) 055202.

High-precision cross-sections: Hall A

- * High precision cross-section measurement in a small kinematic region: Generalised Rosenbluth separation of the DVCS² (scales as E_e^2) and the BH-DVCS interference (scales as E_e^3) terms. NLO and/or higher-twist improve model agreement.



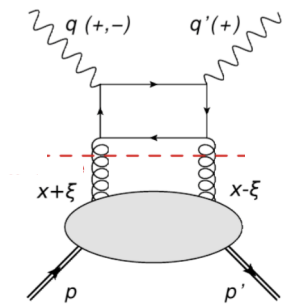
Q^2 : 1.5, 1.9, 2.3 GeV 2 at fixed x_B 0.36
 $-t$: 0.18, 0.24, 0.30



- * Significant differences between pure DVCS and interference contributions.

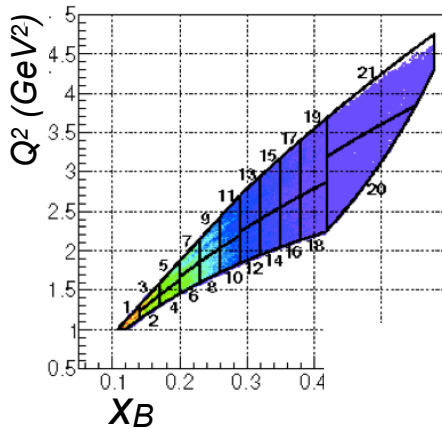
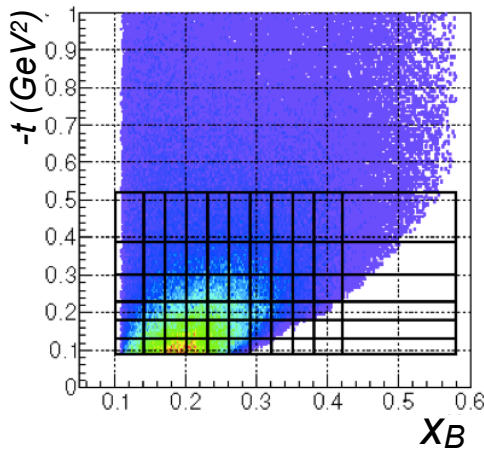
- * If NLO: sensitivity to gluons.

- * Separation of HT and NLO effects requires scans across wider ranges of Q^2 and beam energy: JLab12.



Large kinematic coverage: CLAS

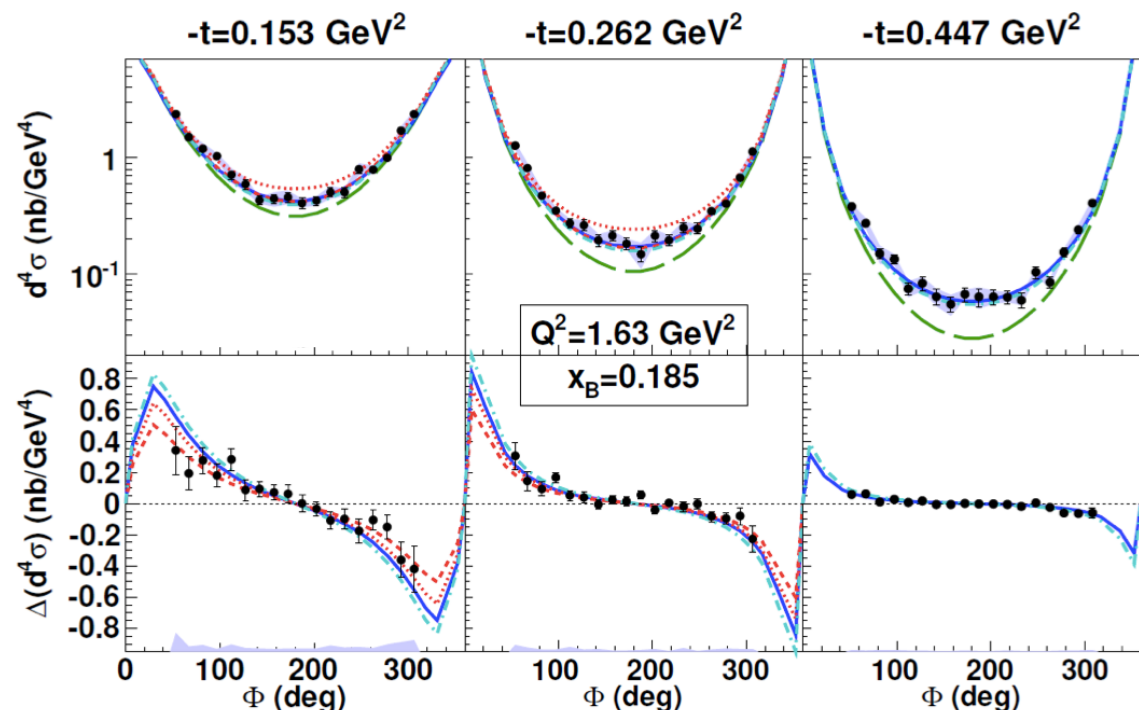
- * Unpolarised DVCS cross-sections and helicity-dependent cross-section differences in a wide kinematic range:



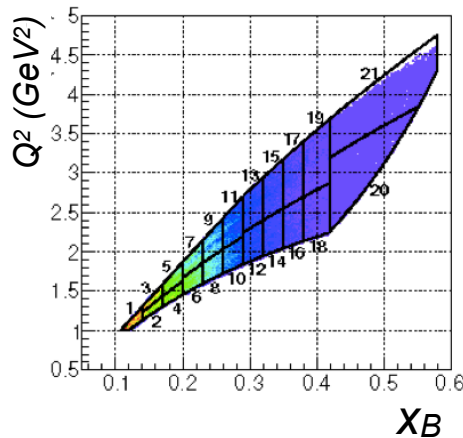
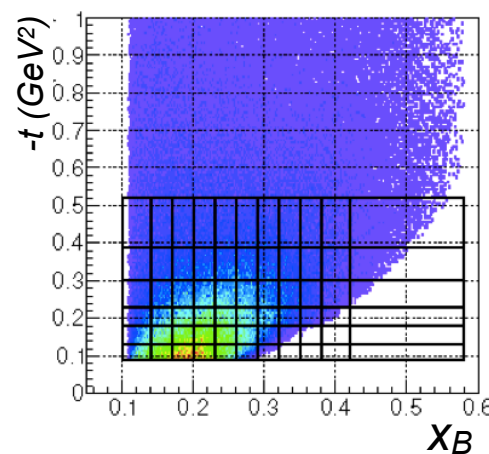
- BH only
- VGG (Vanderhaeghen, Guichon, Guidal) - H only
- KM10 (Kumericki, Mueller) includes strong \tilde{H}
- KM10a (sets \tilde{H} to zero)
- KMS (Kroll, Moutarde, Sabatié, tuned on low x_B meson-production data)

- * Widest phase space coverage in valence quark region: CFF constraints.

- * Dominance of GPD H in unpolarised cross-section.



CLAS unpolarised cross-sections



- BH only
- VGG (Vanderhaeghen, Guichon, Guidal) - H only
- KM10 (Kumericki, Mueller) includes strong \tilde{H}
- - KM10a (sets \tilde{H} to zero)
- - - KMS (Kroll, Moutarde, Sabatié, tuned on low x_B meson-production data)

- * Widest phase space coverage in valence quark region: CFF constraints.
- * Dominance of GPD H in unpolarised cross-section.

$$\frac{d^4\sigma_{ep \rightarrow ep\gamma}}{dQ^2 dx_B dt d\Phi}$$

$$\frac{1}{2} \left(\frac{d^4\vec{\sigma}_{ep \rightarrow ep\gamma}}{dQ^2 dx_B dt d\Phi} - \frac{d^4\overleftarrow{\sigma}_{ep \rightarrow ep\gamma}}{dQ^2 dx_B dt d\Phi} \right)$$

$$d^4\sigma \text{ (nb/GeV}^4\text{)}$$

$$\Delta(d^4\sigma) \text{ (nb/GeV}^4\text{)}$$

$-t=0.153 \text{ GeV}^2$

$-t=0.262 \text{ GeV}^2$

$-t=0.447 \text{ GeV}^2$

$Q^2=1.63 \text{ GeV}^2$
 $x_B=0.185$

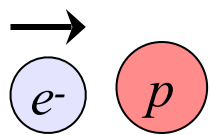
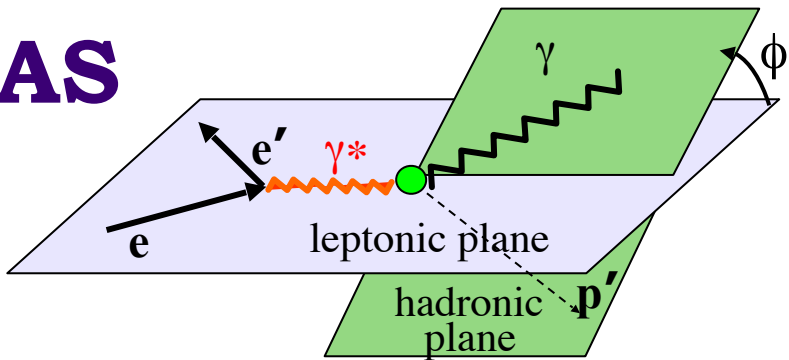
Φ (deg)

Φ (deg)

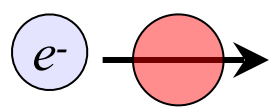
Φ (deg)

DVCS asymmetries @ CLAS

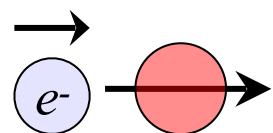
High statistics, large kinematic coverage, strong constraints on fits, simultaneous fit of BSA, TSA and DSA at common kinematics from the same dataset:



Beam-spin asymmetry (BSA): $\Delta\sigma_{LU} \sim \sin\phi \Im(F_1\textcolor{blue}{H} + \xi G_M \tilde{H} - \frac{t}{4M^2} F_2 \textcolor{blue}{E}) d\phi$



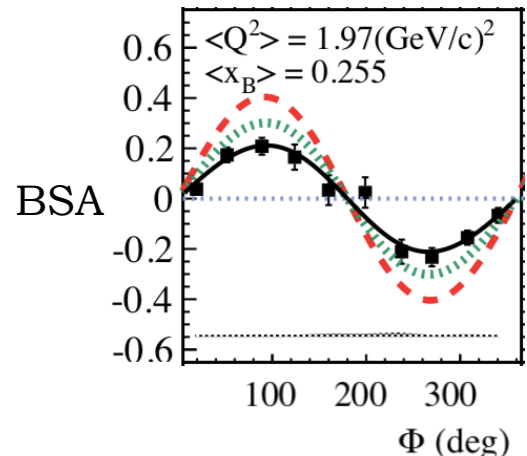
Target-spin asymmetry: $\Delta\sigma_{UL} \sim \sin\phi \Im(F_1\textcolor{blue}{H} + \xi G_M (\textcolor{blue}{H} + \frac{x_B}{2} \textcolor{blue}{E}) - \xi \frac{t}{4M^2} F_2 \tilde{E} + \dots) d\phi$



Double-spin asymmetry: $\Delta\sigma_{LL} \sim (A + B \cos\phi) \Re(F_1\textcolor{blue}{H} + \xi G_M (\textcolor{blue}{H} + \frac{x_B}{2} E) + \dots) d\phi$

F_1, F_2 : Dirac, Pauli form factors

→ Constraints on CFFs H and \tilde{H}

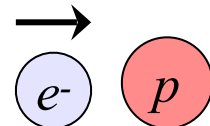
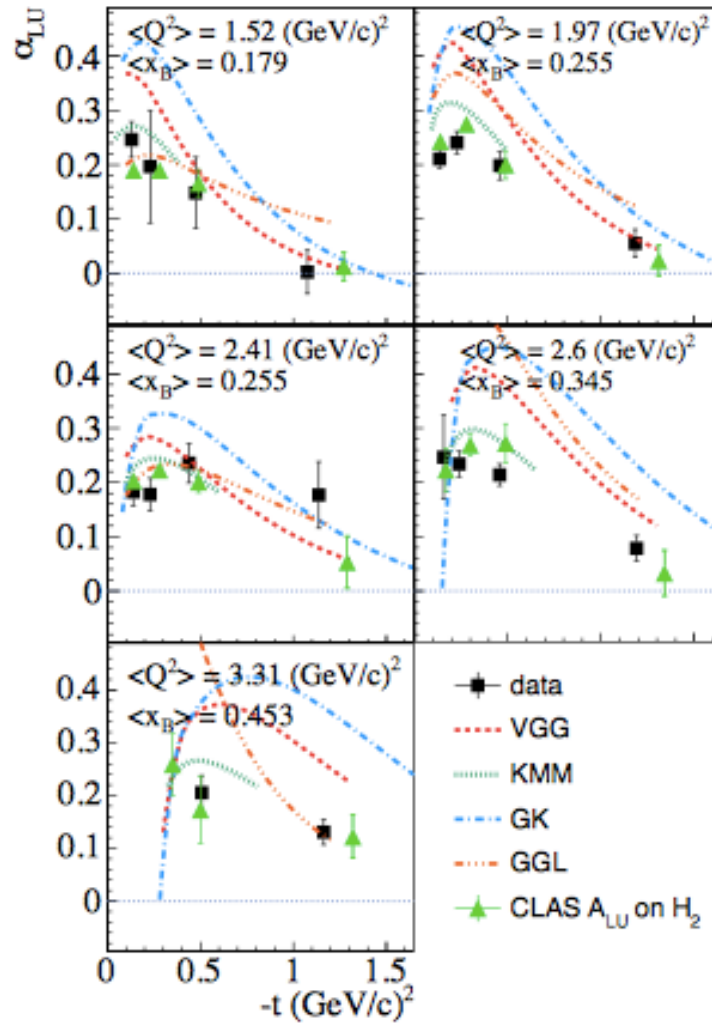


E. Seder *et al* (CLAS), **PRl 114** (2015) 032001

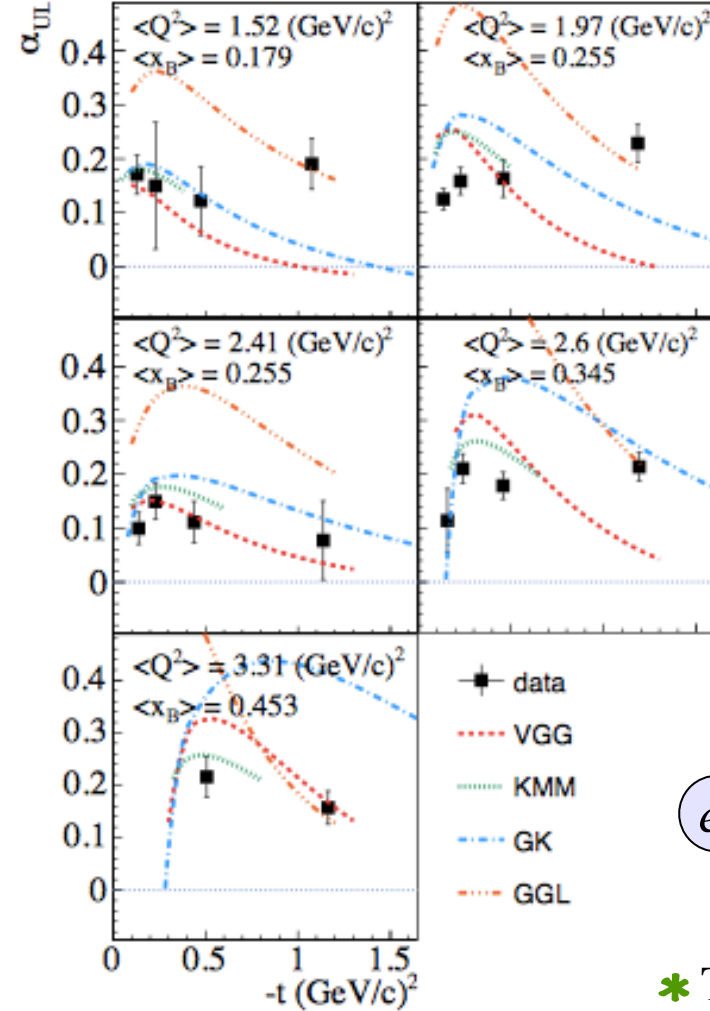
S. Pisano *et al* (CLAS), **PRD 91** (2015) 052014

F.-X. Girod *et al* (CLAS), **PRl 100** (2008) 162002

Beam- and target-spin asymmetries



S. Pisano *et al* (CLAS), **PRD 91** (2015) 052014
 E. Seder *et al* (CLAS), **PRL 114** (2015) 032001



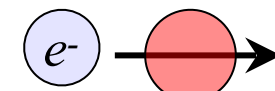
$$A = \frac{\alpha \sin \phi}{1 + \beta \cos \phi}$$

GGL: Goldstein,
Gonzalez, Liuti

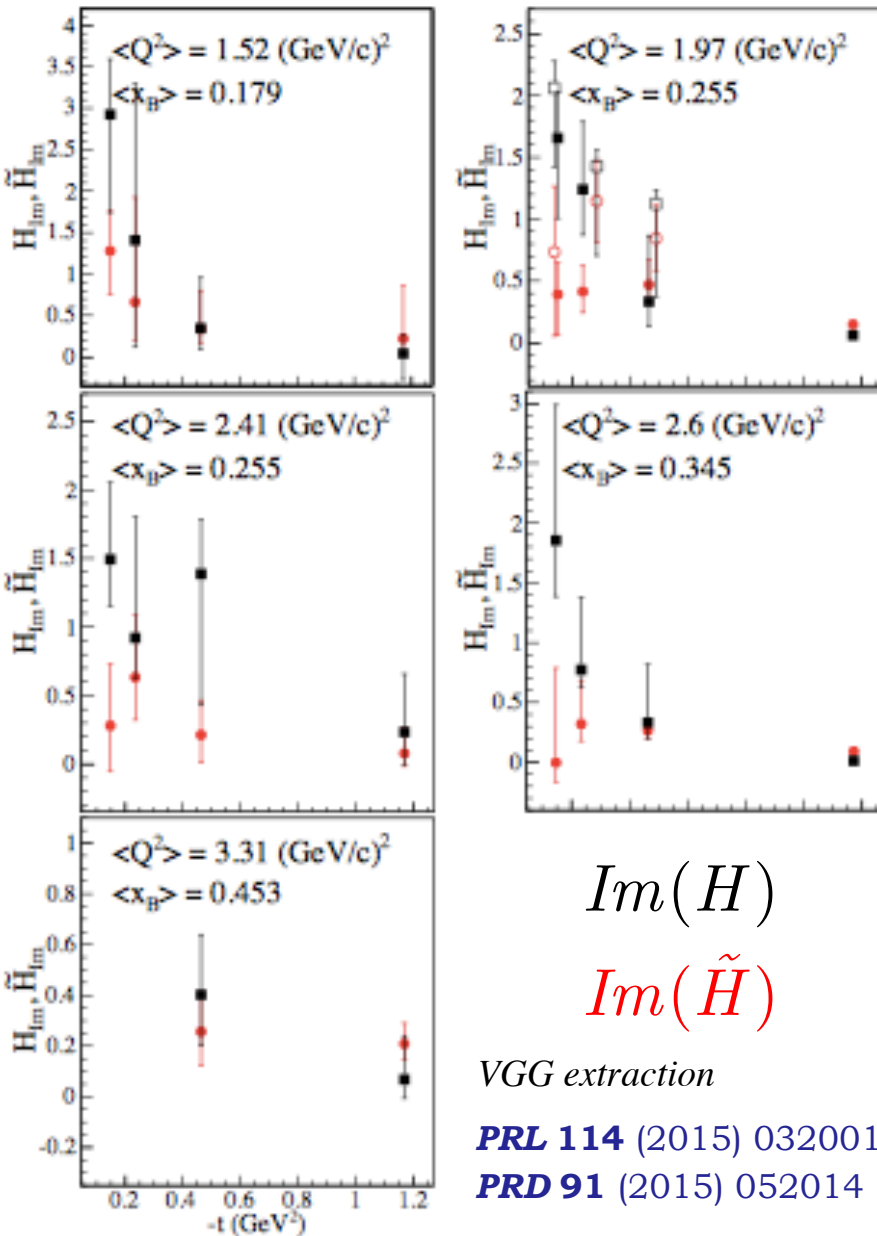
GK: Kroll, Moutarde,
Sabatié

KMM: Kumericki,
Mueller, Murray

VGG: Vanderhaeghen,
Guichon, Guidal



* TSA shows a flatter distribution in t than BSA.



Compton Form Factors from CLAS data

- * Extracted using local fits to cross-sections and asymmetries, constrained by the VGG (Vanderhaeghen, Guichon, Guidal) model.
 - * Information on relative distributions of quark momenta (PDFs) and quark helicity, $\Delta q(x)$

$$H(x, 0, 0) = q(x) \quad \tilde{H}(x, 0, 0) = \Delta q(x)$$
 - * Indications that axial charge is more concentrated than electromagnetic charge.
- $$\int_{-1}^{+1} H dx = F_1 \quad \int_{-1}^{+1} \tilde{H} dx = G_A$$
- * Slope flatter towards higher- x : valence quarks are at centre, lower- x quarks at periphery.

Global analysis of all available data needed.

Towards nucleon tomography

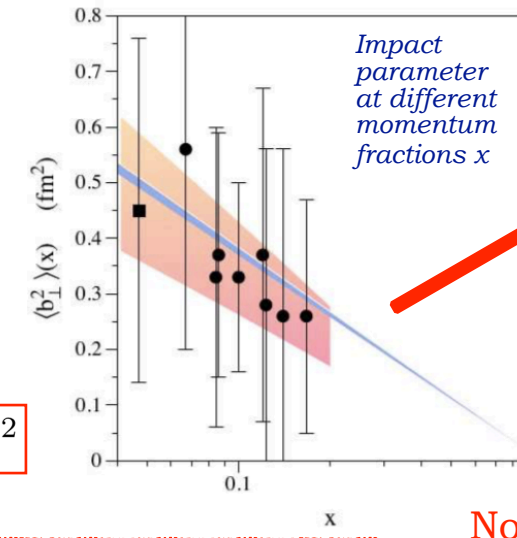
* **Local fit** to extract CFFs: limits based on +/- 5 * the VGG (Vanderhaeghen, Guichon, Guidal) model predictions using leading-twist amplitude based on Double Distributions.

* Assuming leading-twist and exponential dependence of GPD on t , using models to extrapolate to the zero skewness point $\xi = 0$ and assuming similar behaviour for u and d quarks there:

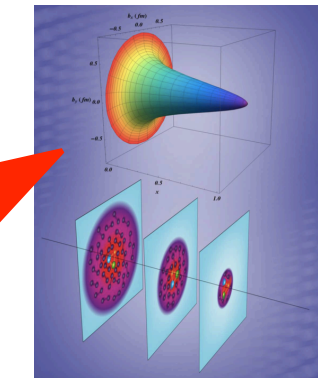
$$\langle b_\perp^2 \rangle^q(x) = -4 \frac{\partial}{\partial \Delta_\perp^2} \ln H_-^q(x, 0, -\Delta_\perp^2) \Big|_{\Delta_\perp=0}$$

$$H_-^q(x, 0, t) \equiv H^q(x, 0, t) + H^q(-x, 0, t)$$

$$t = \Delta^2$$



Impact parameter at different momentum fractions x

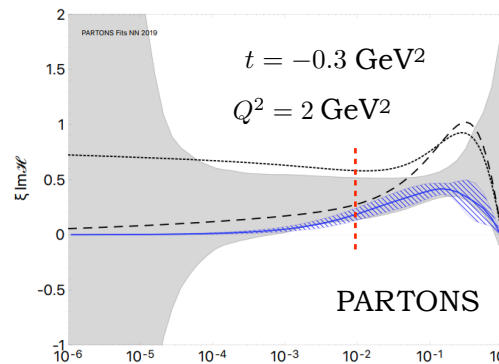


R. Dupré *et al.*, Eur. Phys. J **A 53**, (2017) 171

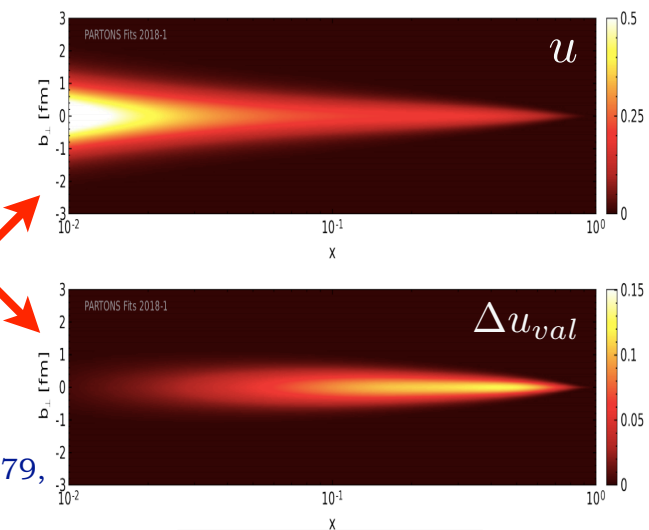
No uncertainties shown!

* **Global fits:** PARTONS framework using neural networks to minimise model-dependence in the extraction of CFFs.

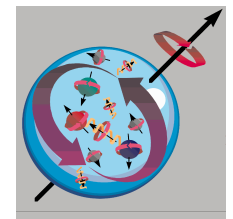
We need more data from multiple channels and across a wide kinematic range!



H. Moutarde *et al.*, Eur. Phys. J **C79**, 614 (2019)



DVCS on the neutron: Hall A



$$J_N = \frac{1}{2} = \frac{1}{2} \sum_q + L_q + J_g$$

* Ji's relation: $J^q = \frac{1}{2} - J^g = \frac{1}{2} \int_{-1}^1 x dx \left\{ H^q(x, \xi, 0) + E^q(x, \xi, 0) \right\}$

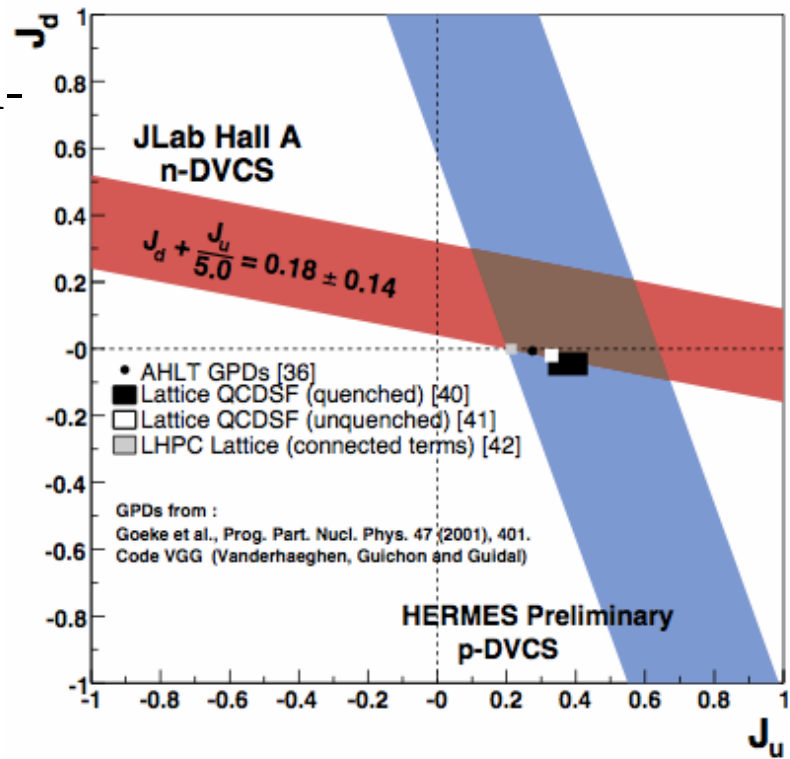
- * H^q in DVCS off the proton, first experimental constraint on E^q from neutron-DVCS beam-spin asymmetry.

M. Mazouz et al, PRL 99 (2007) 242501

- * Gives constraints on orbital angular momentum of quarks: **the spin puzzle**.

- * Rosenbluth separation of interference & DVCS terms underway in neutron-DVCS cross-sections: $E_e = 4.5$ and 5.5 GeV (experiment E08-025).

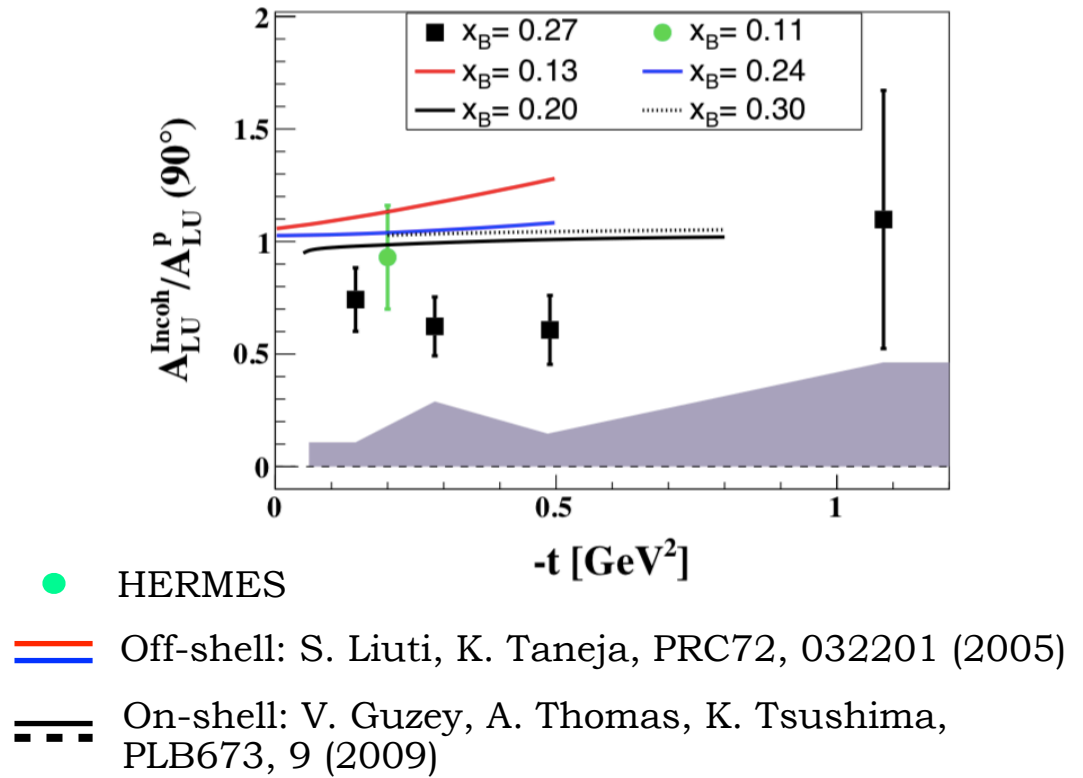
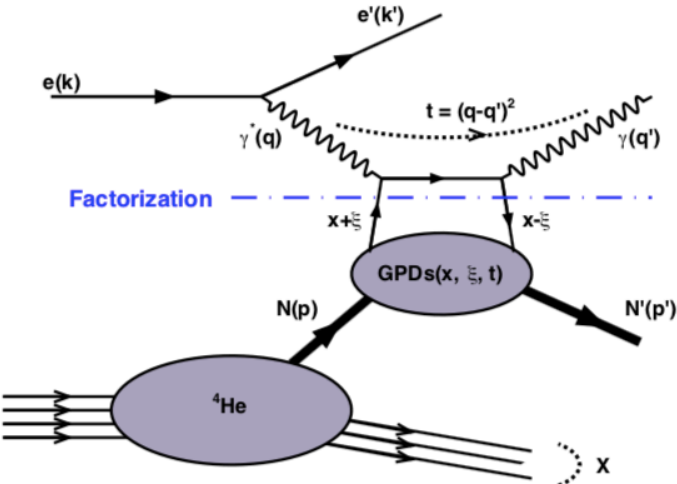
LD_2 target $\langle Q^2 \rangle = 1.75$ GeV 2 $\langle x_B \rangle = 0.36$



DVCS on the bound proton

CLAS

- * Beam spin asymmetry in DVCS from bound protons in ${}^4\text{He}$.



- * 25% - 40% lower asymmetries for bound proton compared to free, no strong dependence on t .
- * Medium-modification effects, initial/final state interactions?

Imaging pressure within the nucleon

- * GPDs provide indirect access to mechanical properties of the nucleon (encoded in the gravitational form factors, GFFs, of the energy-momentum tensor).
X. D. Ji, PRD **55**, 7114-7125 (1997)
M. Polyakov, PLB **555**, 57-62 (2016)

- * Three scalar GFFs, functions of t : encode pressure and shear forces ($d_1(t)$), mass ($M_2(t)$) and angular momentum distributions ($J(t)$).

- * Can be related to GPDs via sum rules:

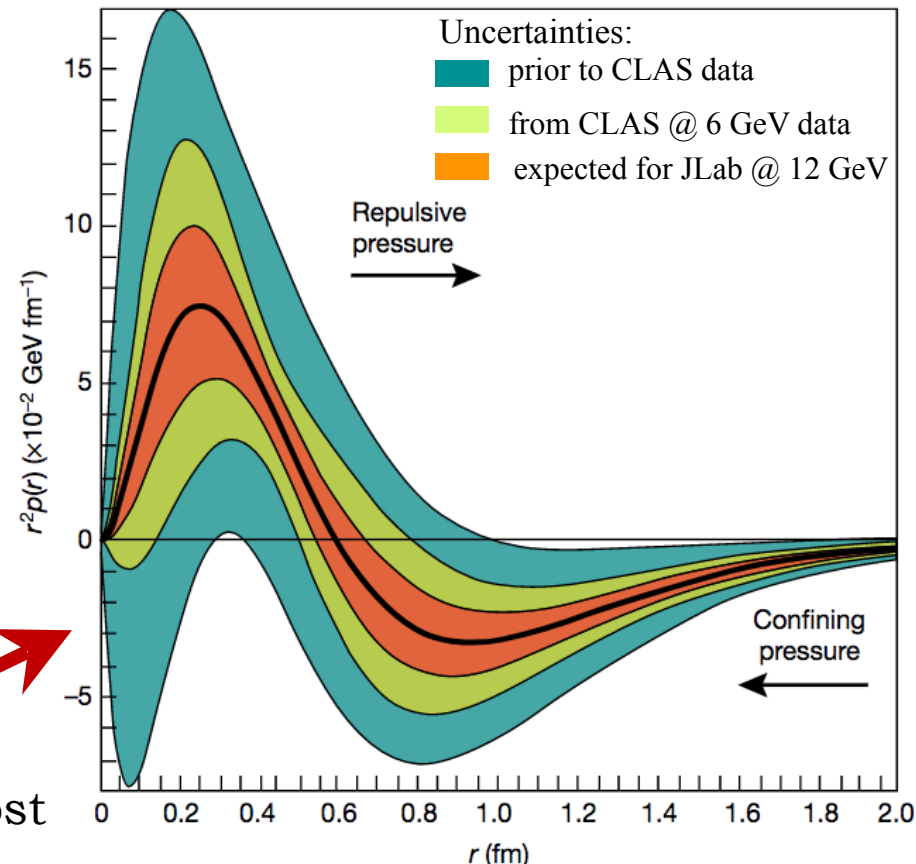
$$\int x [H(x, \xi, t) + E(x, \xi, t)] dx = 2J(t)$$

$$\int x H(x, \xi, t) dx = M_2(t) + \frac{4}{5} \xi^2 d_1(t)$$

- * Severely model-dependent extraction

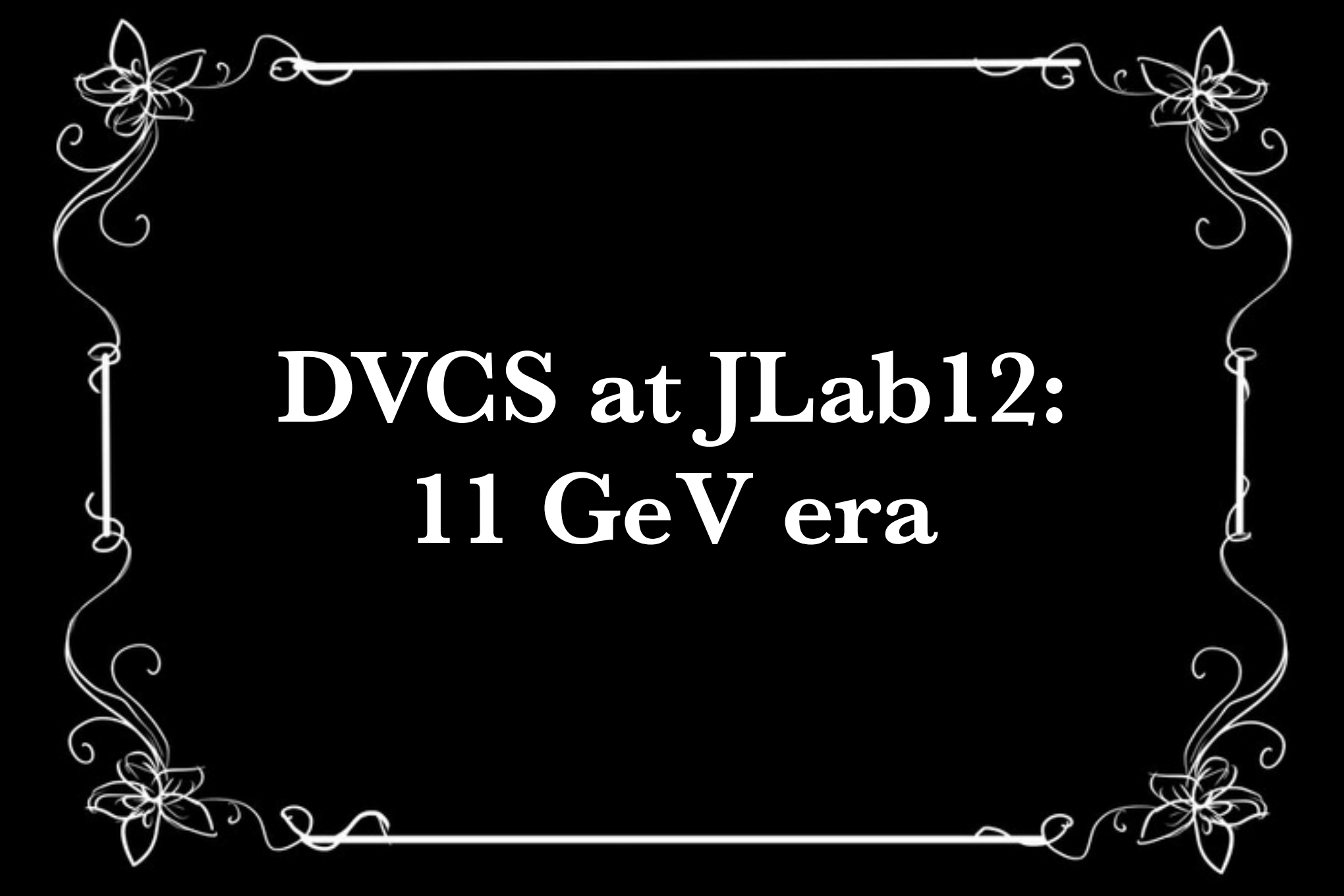
- * Neural net analysis, however: d-term almost unconstrained and consistent with zero

Possibility of extracting pressure distributions! But more data needed.



V. Burkert, L. Elouadrhiri, F.-X. Girod,
Nature **557**, 396-399 (2018)

K. Kumerički, Nature **570**, E1-E2 (2019)



DVCS at JLab12: 11 GeV era

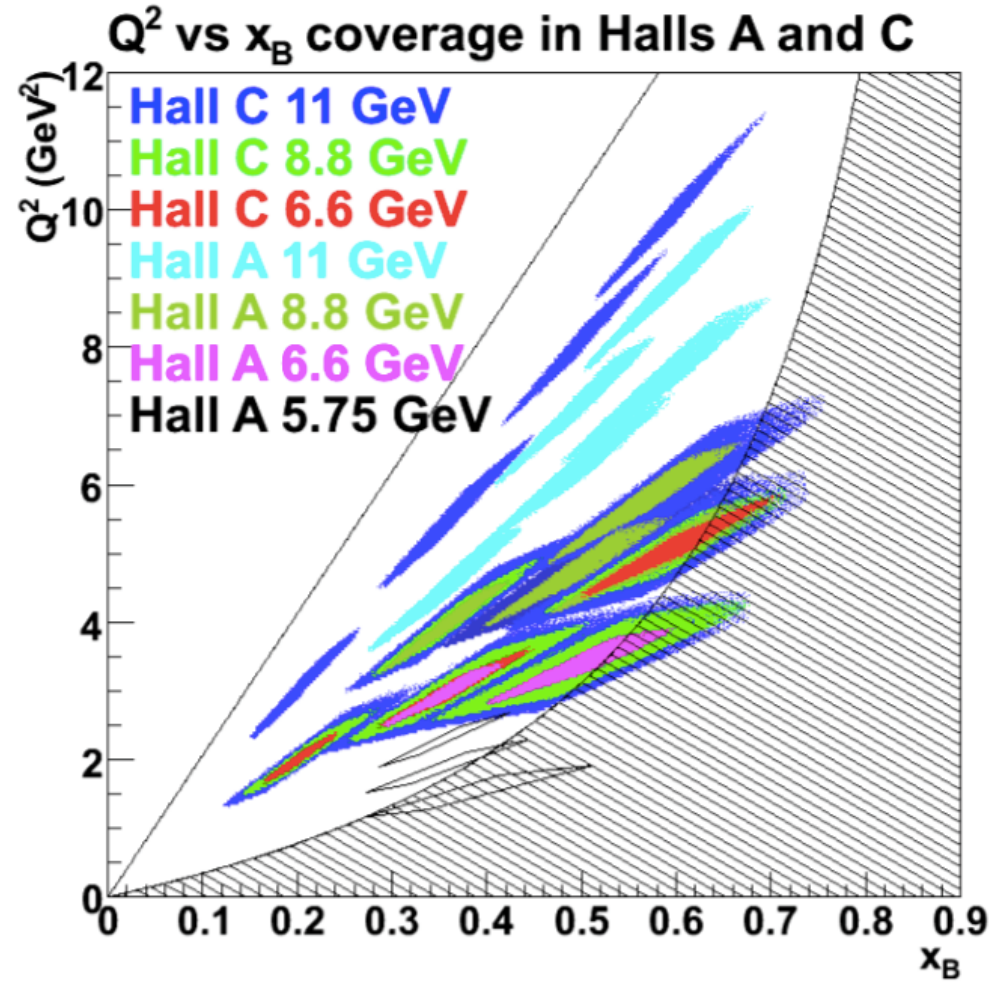
11 GeV era DVCS Cross-sections: Halls A and C

Experiments:

E12-06-114 (Hall A, 100 days),
E12-13-010 (Hall C, 53 days)

Unpolarised liquid H₂ target:

- Beam energies: 6.6, 8.8, 11 GeV
 - Scans of Q^2 at fixed x_B .
 - Hall A: aim for absolute cross-sections with 4% relative precision.
-



* Azimuthal, energy and helicity dependencies of cross-section to separate $|T_{DVCS}|^2$ and interference contributions in a wide kinematic coverage.

* Separate *Re* and *Im* parts of the DVCS amplitude.

11 GeV era: DVCS with CLAS12

E12-06-119: Unpolarised liquid H₂ target

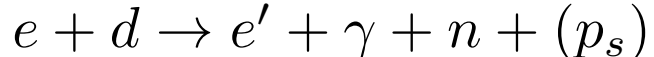
Beam-spin asymmetry $\rightarrow \text{Im}(\mathbf{H}_p)$

First experiment with CLAS12! ~50% done

E12-16-010: Unpolarised liquid H₂ target

Beam energy: 6.6 GeV, 8.8 GeV **Almost complete**

E12-11-003: Unpolarised liquid D₂ target



Beam-spin asymmetry
in neutron-DVCS $\rightarrow \text{Im}(\mathbf{E}_n)$

Running this year!

E12-06-109: Longitudinally polarised NH₃ and ND₃ targets

- Dynamic Nuclear Polarisation (DNP) of target material, cooled in a He evaporation cryostat.
- P_{proton} = 80%, P_{deuteron} up to 50%

P_{beam} = 85%

L = 10³⁵ cm⁻²s⁻¹

1 < Q² < 10 GeV²

0.1 < x_B < 0.65

-t_{min} < -t < 2.5 GeV²

E12-12-010: Transversely polarised HD target.

Target-spin asymmetries
~2023? $\rightarrow \text{Im}(\mathbf{E}_p)$

Target-spin asymmetry
in proton- and neutron- DVCS

~ 2021

$\rightarrow \text{Im}(\tilde{\mathbf{H}}_p),$
 $\text{Im}(\mathbf{H}_n)$

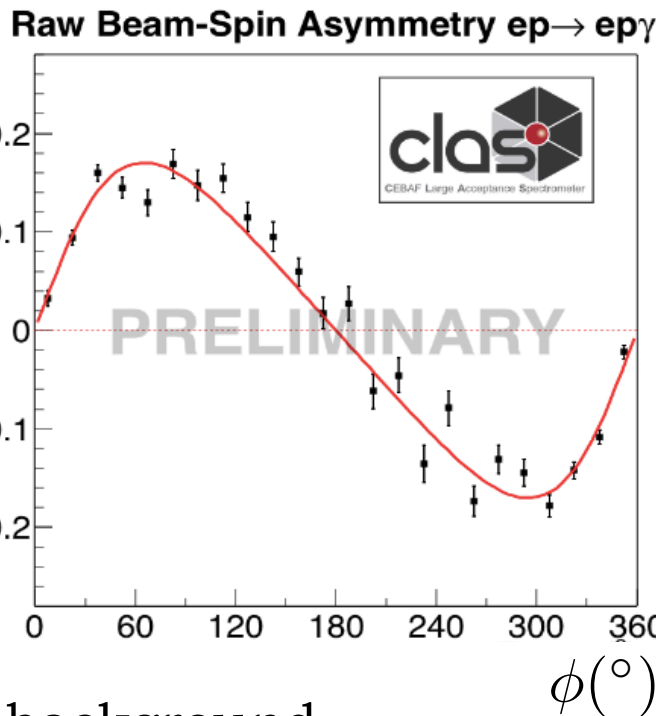
DVCS with CLAS12

E12-06-119: Unpolarised liquid H₂ target

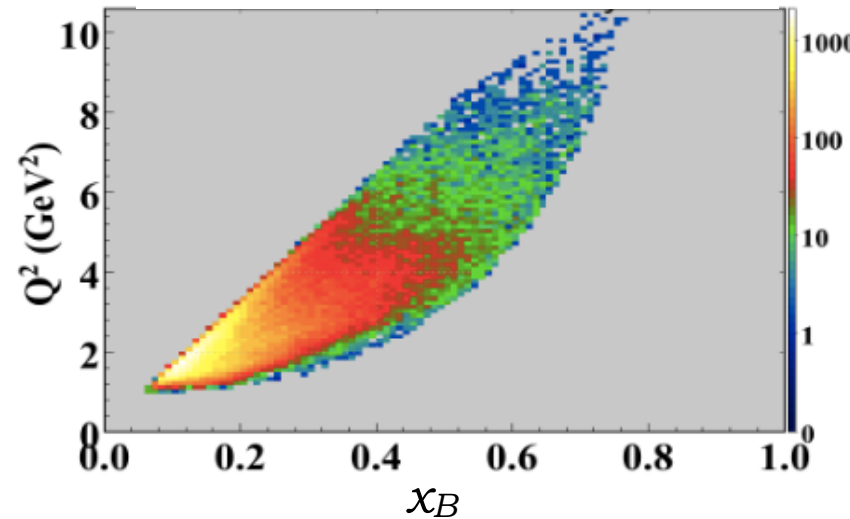
Beam-spin asymmetry → $Im(\mathbf{H}_p)$

First experiment with CLAS12! ~50% done

$P_{beam} = 85\%$
 $L = 10^{35} \text{ cm}^{-2}\text{s}^{-1}$
 $1 < Q^2 < 10 \text{ GeV}^2$
 $0.1 < x_B < 0.65$
 $-t_{min} < -t < 2.5 \text{ GeV}^2$

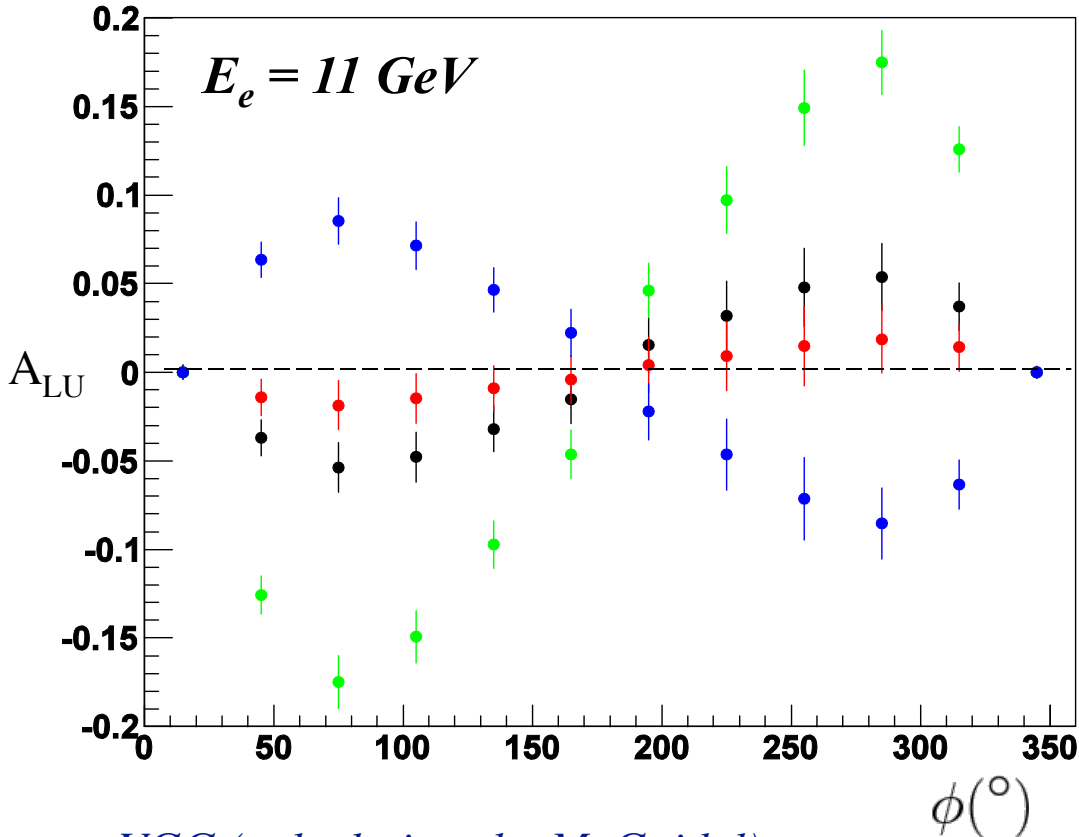


No background subtraction



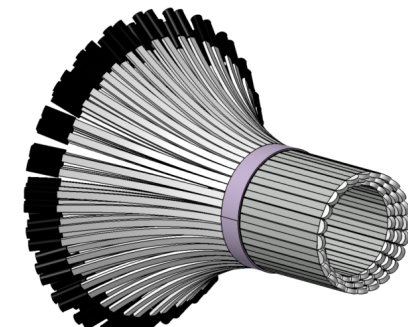
Guillaume Christiaens

Neutron DVCS @ 11 GeV: sensitivity to J_q



$J_u = 0.3, J_d = -0.1 \quad J_u = 0.3, J_d = 0.1$
 $J_u = 0.1, J_d = 0.1 \quad J_u = 0.3, J_d = 0.3$

- * At 11 GeV, beam spin asymmetry (A_{LU}) in neutron DVCS is very sensitive to J_u, J_d
- * Dedicated neutron detector added to CLAS12: Central Neutron Detector



Measurement currently in process...

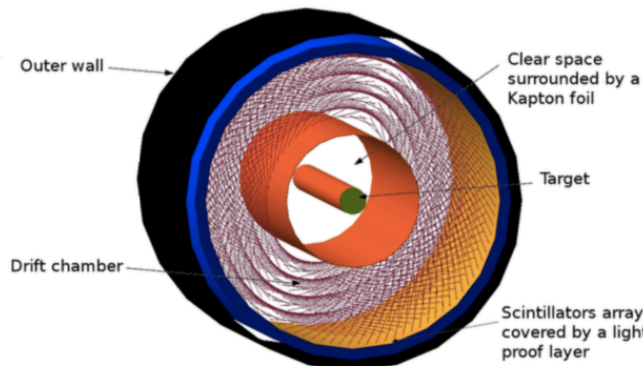
DVCS on ${}^4\text{He}$: CLAS12 with ALERT

Experiment E12-17-012:

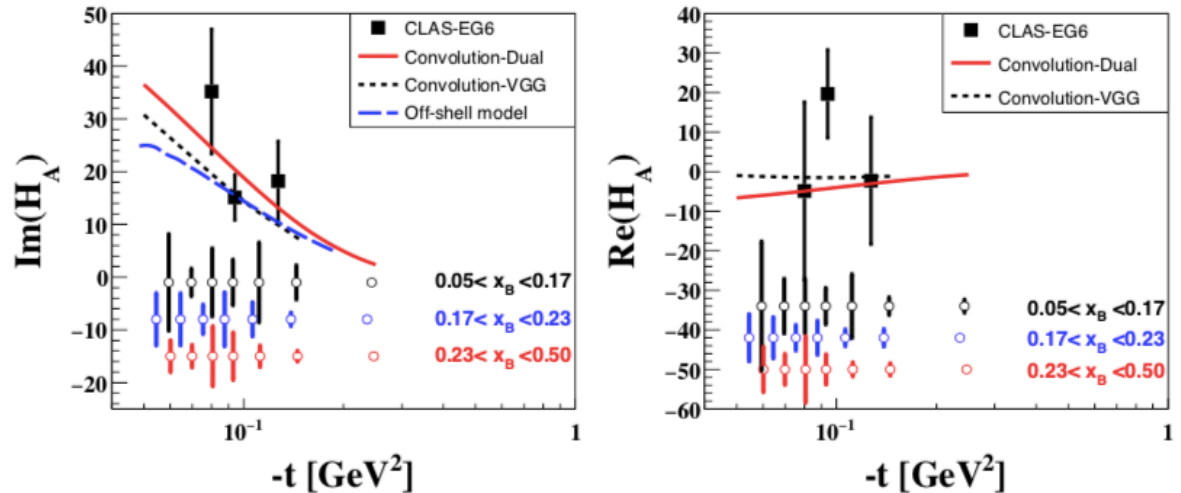
Measurement of BSA in coherent DVCS from a ${}^4\text{He}$ target: partonic structure of nuclei.

- * Builds on 6 GeV measurement: M. Hattawy *et al*, PRL 119 (2017) 202004.
- * Spin 0 target, so at leading twist only one chiral-even GPD: \mathbf{H}_A .

11 GeV beam, 80% polarised.
Gas target straw @ 3 atm
 $L = 6 \times 10^{34}$ nucleon $\text{cm}^{-2}\text{s}^{-1}$
with 1000 nA beam.



CLAS12 + ALERT: central recoil detector

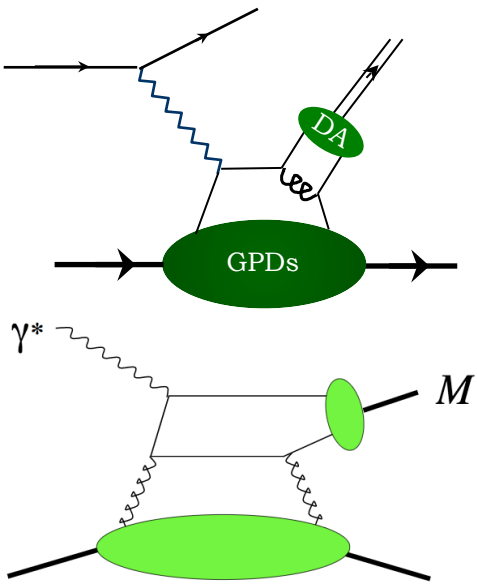


Experiment E12-17-012B

Incoherent, spectator-tagged DVCS
on ${}^4\text{He}$ and d .

Hard Exclusive Meson Production

Hard Exclusive Meson Production



* Amplitude depends on convolution of GPDs and meson Distribution Amplitudes (DA).

* At leading order & twist, access to the four chiral-even (parton helicity-conserving) GPDs:

- Pseudo-scalar mesons: $\tilde{H}^q, \tilde{E}^q(x, \xi, t)$
- Vector mesons: $H^q, E^q, H^g, E^g(x, \xi, t)$

Gluon
GPDs!

HEMP enables flavour decomposition of quark GPDs and gives access to gluon GPDs

Caveats:

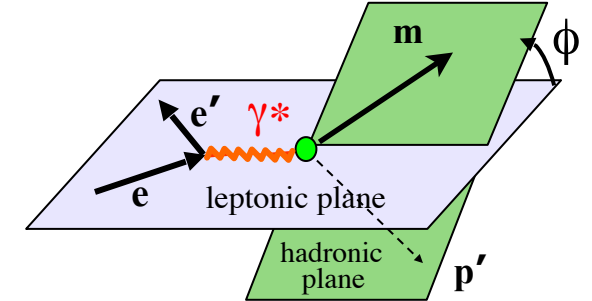
- factorisation established only for longitudinal photons,
- factorisation sets in at a higher scale than in DVCS,
- DA not entirely understood

*Extracting GPDs from
HEMP is hard!*

HEMP Cross-section

Virtual
photon flux

unpolarised



$$\frac{2\pi}{\Gamma} \frac{d^4\sigma}{dQ^2 dx_B dt d\phi_{meson}} = \boxed{\sigma_T + \epsilon\sigma_L + \epsilon\sigma_{TT} \cos 2\phi + \sqrt{\epsilon(1+\epsilon)}\sigma_{LT} \cos \phi}$$

polarised beam \longrightarrow $+P_b \sqrt{\epsilon(1-\epsilon)}\sigma_{LT} \sin \phi$

longitudinally polarised target \longrightarrow $+P_{tg} (\sqrt{\epsilon(1+\epsilon)}\sigma_{UL}^{\sin \phi} \sin \phi + \epsilon\sigma_{UL}^{\sin 2\phi} \sin 2\phi)$

Target and beam longitudinally polarised \longrightarrow $+P_b P_{tg} (\sqrt{1-\epsilon^2}\sigma_{LL} + \sqrt{\epsilon(1-\epsilon)}\sigma_{LL}^{\cos \phi} \cos \phi)$

ϵ : ratio of the fluxes of longitudinally (L) and transversely (T) polarised virtual photons.

σ_i : structure functions, related to scattering amplitudes ($i = L, T, LT, \dots$), eg:

$$\frac{d\sigma_L}{dt} = \frac{4\pi\alpha}{k'} \frac{1}{Q^6} \left\{ (1 - \xi^2) |\langle \tilde{H} \rangle|^2 - 2\xi^2 \text{Re}[\langle \tilde{H} \rangle^* \langle \tilde{E} \rangle] - \frac{t'}{4m^2} \xi^2 |\langle \tilde{E} \rangle|^2 \right\}$$

where $\langle F \rangle \equiv \sum_\lambda \int_{-1}^1 dx \mathcal{H}_{\mu'\lambda'\mu\lambda} F$

hard-scattering kernel

GPD

Transversity GPDs

- * For pseudo-scalar mesons, access four chiral-odd (parton helicity-flipping) transversity GPDs (via convolutions of leading-twist GPDs with twist-3 meson DA): $E_T^q, \tilde{E}_T^q, H_T^q, \tilde{H}_T^q(x, \xi, t)$

Appear in DVMP amplitude when virtual photon has transverse polarisation — not accessible at LT in DVCS.

- * \tilde{E}_T can be related to the transverse anomalous magnetic moment:

$$\kappa_T = \int_{-1}^{+1} \tilde{E}_T(x, \xi, t=0) dx$$

- * and H_T to the transversity distribution: $H_T(x, 0, 0) = h_1(x)$

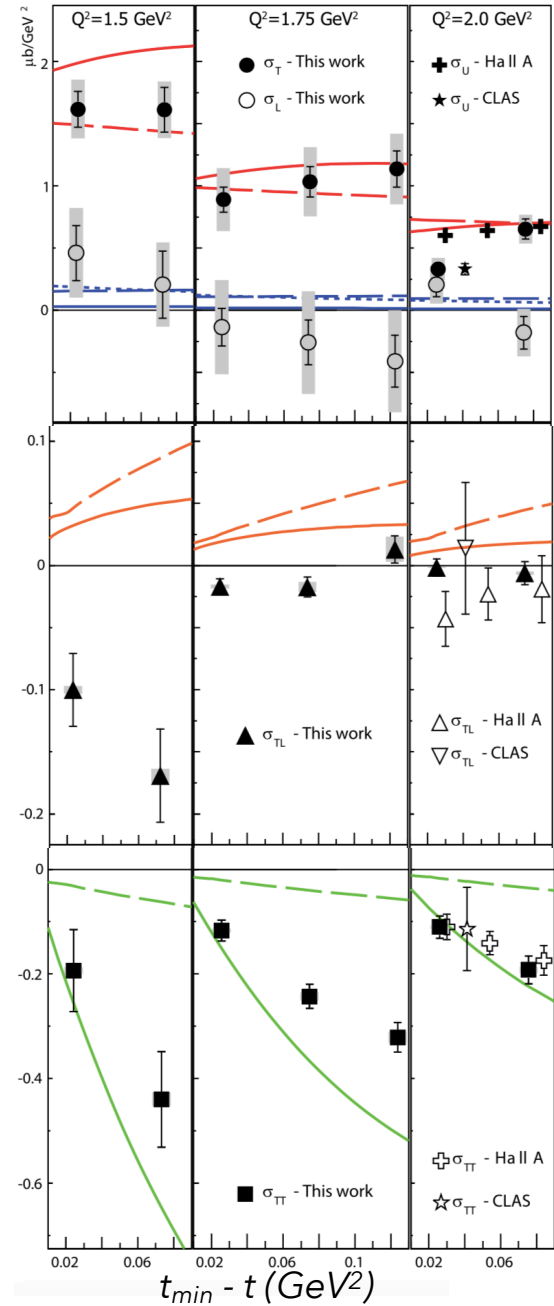
which describes distribution of transverse partons in a transverse nucleon

$$h_1 = \text{circle with black dot and red arrow} - \text{circle with black dot and red arrow pointing down}$$

- * The combination $\bar{E}_T = 2\tilde{H}_T + E_T$ is related to spatial density of **transversely polarised quarks** in an **unpolarised nucleon**.

$$e + p \rightarrow p\pi^0$$

$$x_B = 0.36$$



HEMP @ JLab

Pseudo-scalar mesons:

- * Separation of L/T contributions to cross-sections through Rosenbluth-like techniques / simultaneous fits at different kinematics.
- * Strong transverse contribution observed in charged and neutral pion / K+ cross-sections: possible access to transversity GPDs.

— Goloskokov Kroll (EPJ A47, 112 (2011))
- - - Goldstein, Hernandez, Liuti
 (PRD 84, 034007 (2011))

M. Defurne *et al*, **PRL 117** (2016) 262001

- * Attempt at GPD flavour-separation using π^0 and η BSA.

Vector mesons:

- * L/T contributions to cross-sections separated by using helicity conservation between virtual photon and meson: strong deviations from leading-twist GPD formalism (higher-twist? evolution effects? meson-size corrections?)
- * Gluonic GPD Hg dominates at small x : gluonic radius.
→ GPD extraction much cleaner for heavier quarks: J/Ψ

Too close to threshold @ JLab12, ideal for the Electron-Ion Collider!

Meson production at JLab 12 GeV

Cross-sections and spin asymmetries in the 11 GeV kinematics:

- * Hard exclusive electroproduction of η and π^0 (E12-06-108, CLAS12)
- * Exclusive ϕ meson electroproduction (E12-12-007, CLAS12)
- * DVCS and neutral pion cross-sections (E12-13-010, Hall C)
- * Scaling study of the L-T separated pion electroproduction cross-section (E12-07-105, Hall C)
- * Studies of the L-T separated kaon electroproduction cross-section from 5-11 GeV (E12-09-011, Hall C)
- * Near-threshold electroproduction of J/Ψ (E12-12-006, Hall A)
- * Time-like Compton scattering and J/Ψ electroproduction (E12-12-001, CLAS12). *Analysis under-way!*

Summary

JLab 6 GeV programme:

- * Indications of higher-twist or higher-orders at play in DVCS: hint of gluons?
- * Constraints for GPD models: most info on Re and Im parts of \mathbf{H}_p CFF, a little on $\tilde{\mathbf{H}}_p, \mathbf{E}_n$.
- * First attempt at tomography with the limited data.
- * DVCS on a bound protons and a nuclear target (helium).
- * Significant contributions from transverse photon polarisation: possible access to transversity GPDs in pseudo-scalar meson production.
- * Vector mesons: GPD interpretation tricky, strong deviations from leading-twist formalism.

JLab 12 GeV programme:

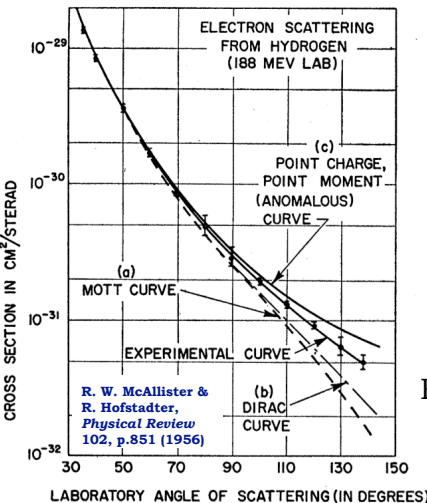
- * High precision — separation of DVCS and interference terms: sensitivity to higher twist / higher orders, gluons.
- * Extensive mapping of a wider kinematic region — strides towards tomography.
- * Extraction of Re and Im parts of \mathbf{H} CFF, $\tilde{\mathbf{H}}$, \mathbf{E} , flavour-separation: u/d .
- * Access to transversity GPDs.
- * Many more channels to be measured: meson-production, time-like Compton scattering, double DVCS, photon-meson-pair production: significant constraints on GPDs in the valence region.

Stay tuned!

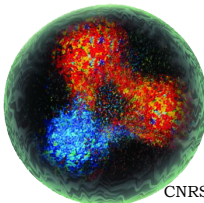
Thank you!

Back-up

An abridged history of nucleon structure



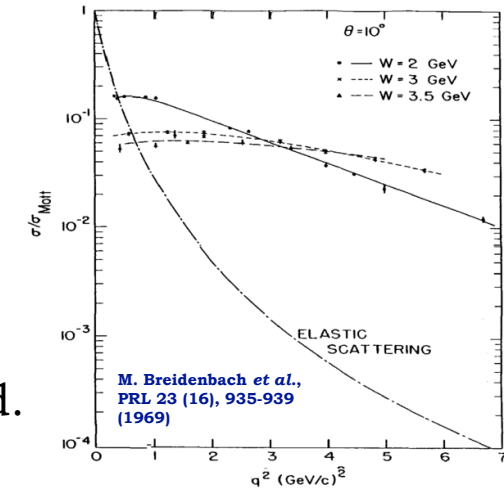
Robert Hofstadter
1915 - 1990
(Wikipedia)



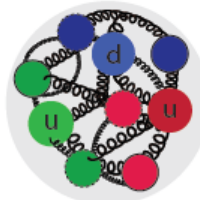
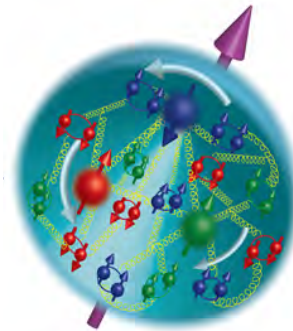
1960s: the Quark Model. Nucleons are composed of three valence quarks! Gell-Mann (Nobel Prize 1969), Zweig.

1968: Deep Inelastic scattering at SLAC: scaling observed. The proton consists of point-like charges: partons!

Friedman, Kendall, Taylor:
Nobel Prize 1990

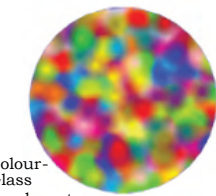
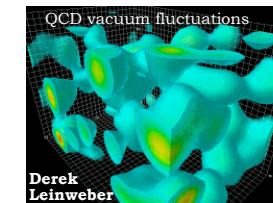
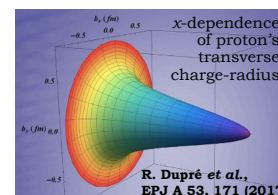


1956: Elastic scattering at Stanford: the proton has internal structure! Hofstadter: Nobel Prize 1961.



1970s-1990s: Deep Inelastic Scattering reveals a rich structure: quark-gluon sea, flavour distributions, puzzles of spin and mass... what you see depends on how closely you look!

21st Century: High-precision imaging of quarks and gluons. 3D tomography of the nucleon: spatial and momentum distributions inside it, mechanical properties of the nucleon, ...



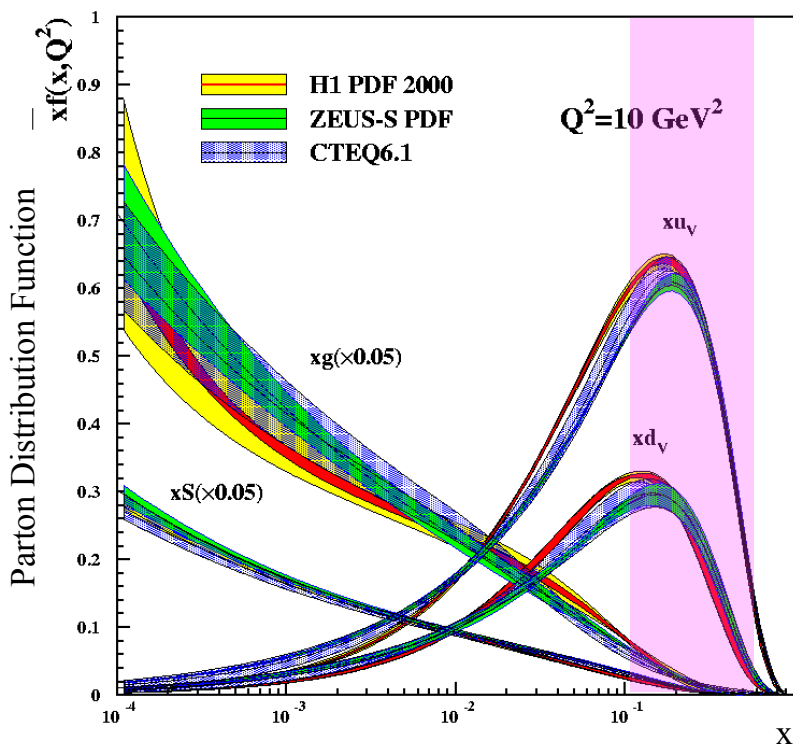
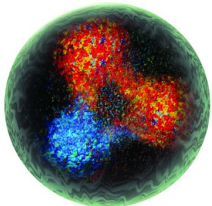
Colour-Glass Condensate

Nucleon at different scales

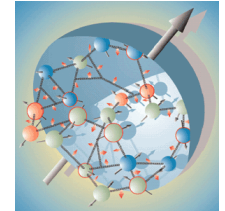
Valence quarks

Jefferson Lab: fixed-target
electron scattering

$$0.1 < x_B < 0.7$$



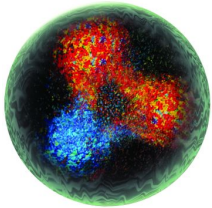
Nucleon at different scales



Valence quarks

Jefferson Lab: fixed-target electron scattering

$$0.1 < x_B < 0.7$$

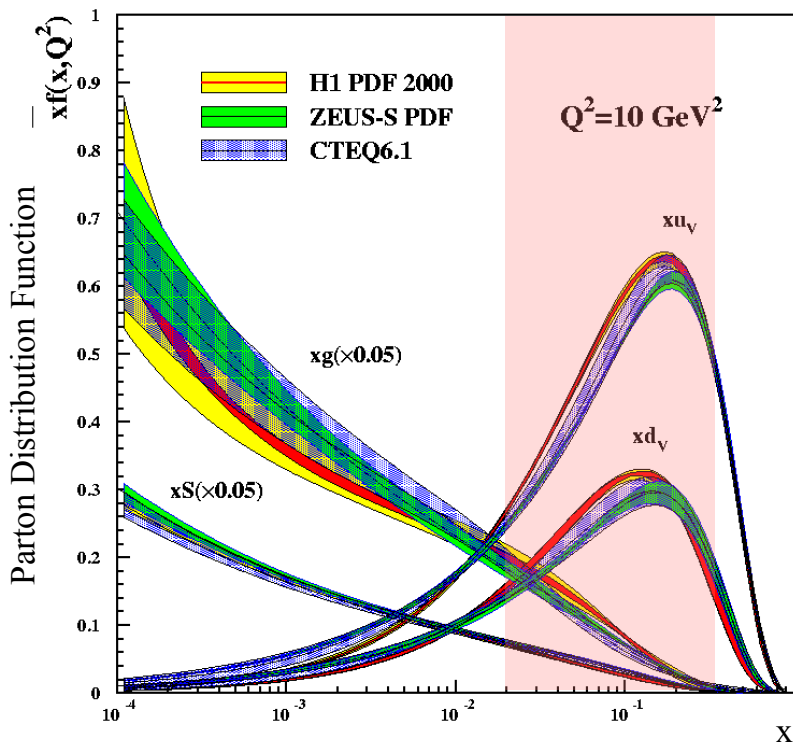


Sea quarks

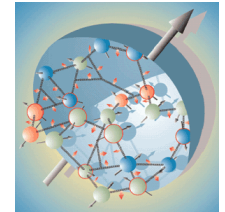


HERMES: fixed gas-target electron/positron scattering

$$0.02 < x_B < 0.3$$



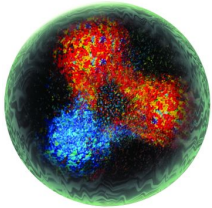
Nucleon at different scales



Valence quarks

Jefferson Lab: fixed-target electron scattering

$$0.1 < x_B < 0.7$$



Sea quarks



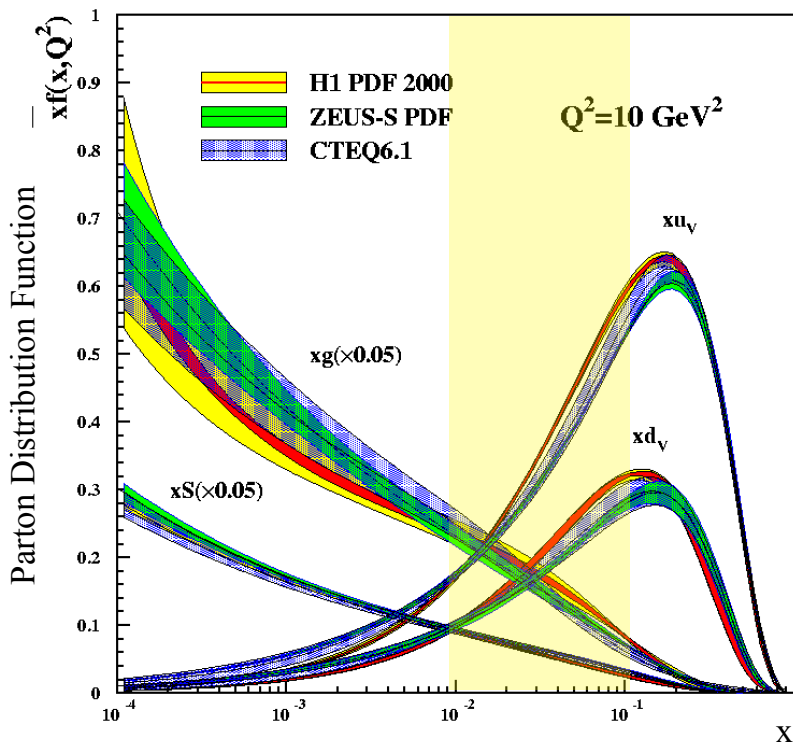
HERMES: fixed gas-target electron/positron scattering

$$0.02 < x_B < 0.3$$

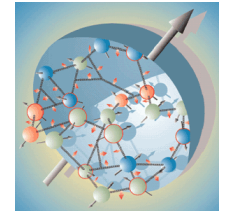


COMPASS: fixed-target muon scattering

$$0.01 < x_B < 0.1$$



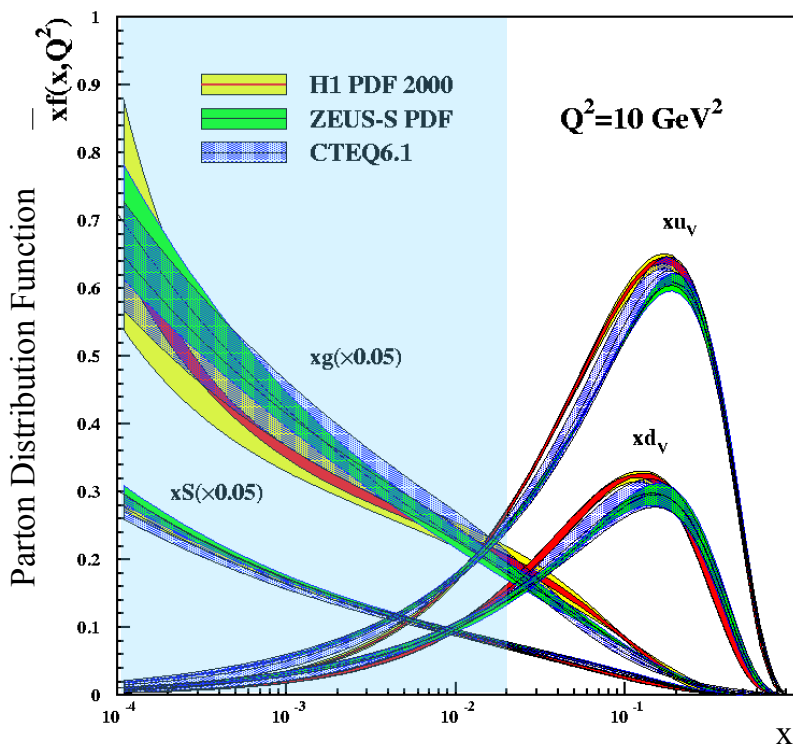
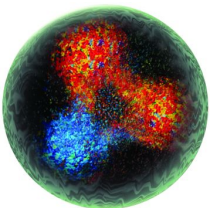
Nucleon at different scales



Valence quarks

Jefferson Lab: fixed-target electron scattering

$$0.1 < x_B < 0.7$$



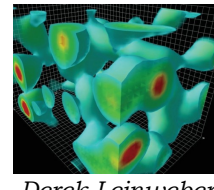
Sea quarks

HERMES: fixed gas-target electron/positron scattering

$$0.02 < x_B < 0.3$$



COMPASS: fixed-target muon scattering

$$0.01 < x_B < 0.1$$


Derek Leinweber

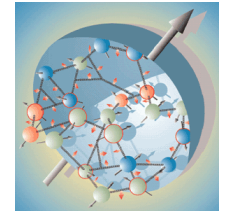
The glue

ZEUS/H1: electron/positron-proton collider

$$10^{-4} < x_B < 0.02$$



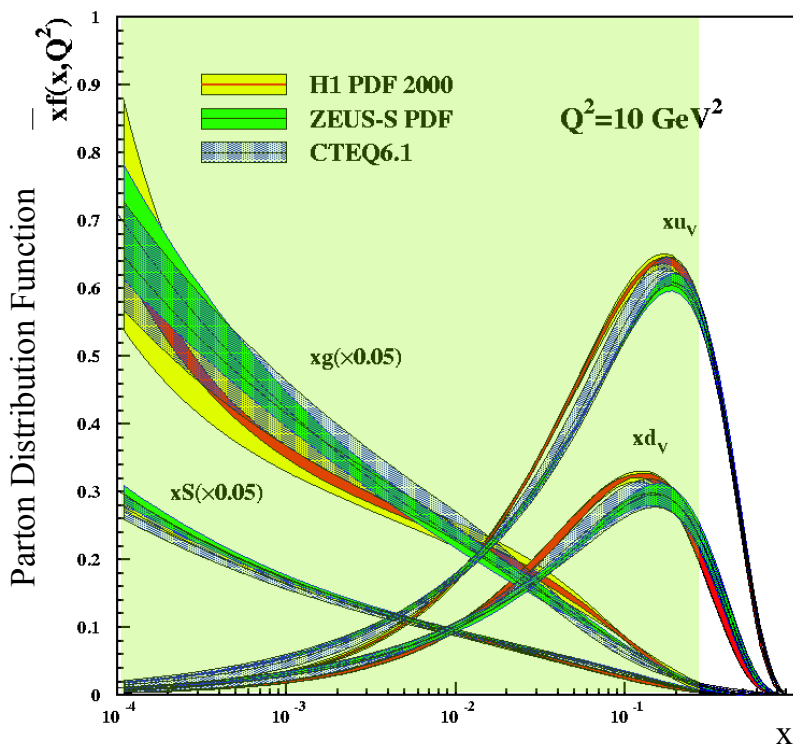
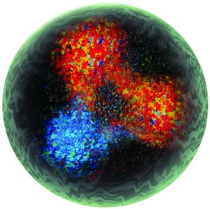
Nucleon at different scales



Valence quarks

Jefferson Lab: fixed-target electron scattering

$$0.1 < x_B < 0.7$$



Sea quarks



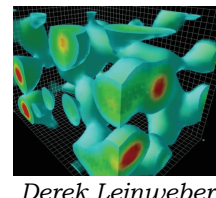
HERMES: fixed gas-target electron/positron scattering

$$0.02 < x_B < 0.3$$



COMPASS: fixed-target muon scattering

$$0.01 < x_B < 0.1$$



Derek Leinweber

The glue

ZEUS/H1: electron/positron-proton collider

$$10^{-4} < x_B < 0.02$$



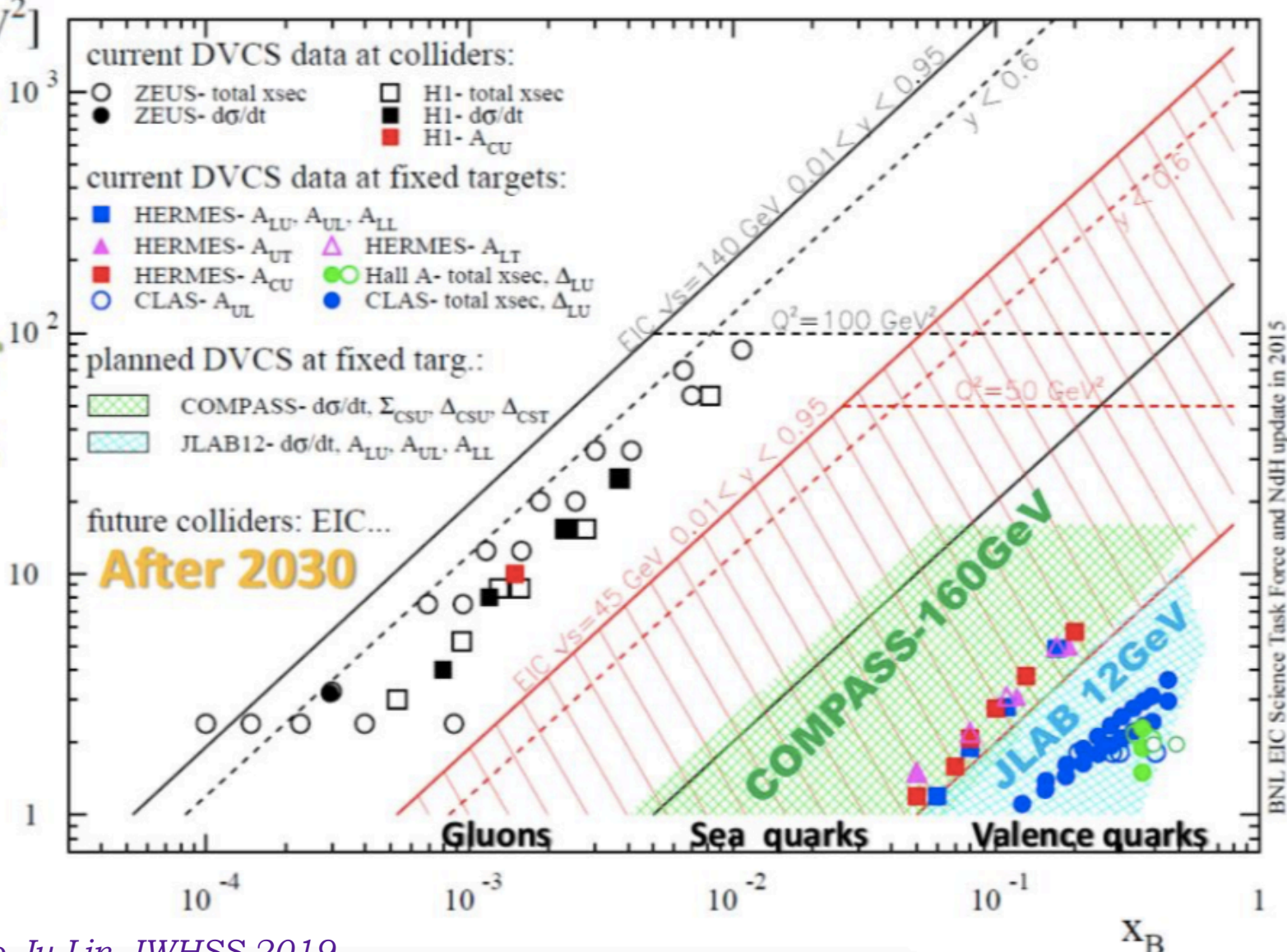
Electron-ion collider: $10^{-4} < x_B < 10^{-1}$
Luminosity 100 - 1000 times that of HERA

Kinematic landscape

Start
 Q^2 [GeV 2]

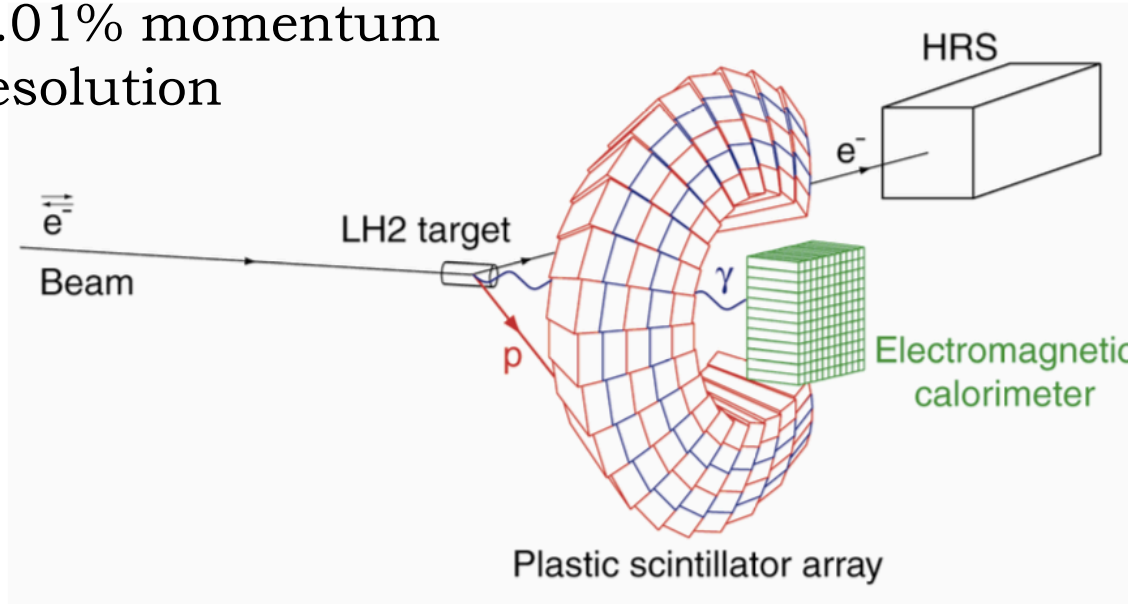
2001

After
2016



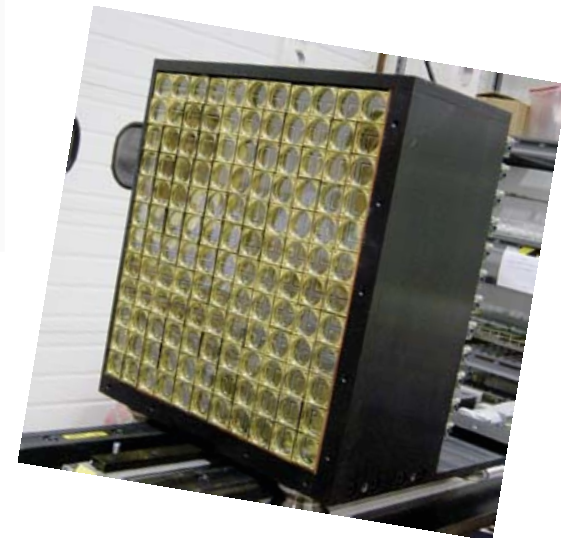
DVCS in Hall A

Detect electron in the Left
High Resolution
Spectrometer (HRS-L):
0.01% momentum
resolution



Plastic scintillator array built for
proton detection, but not used
in most recent measurements /
re-analyses.

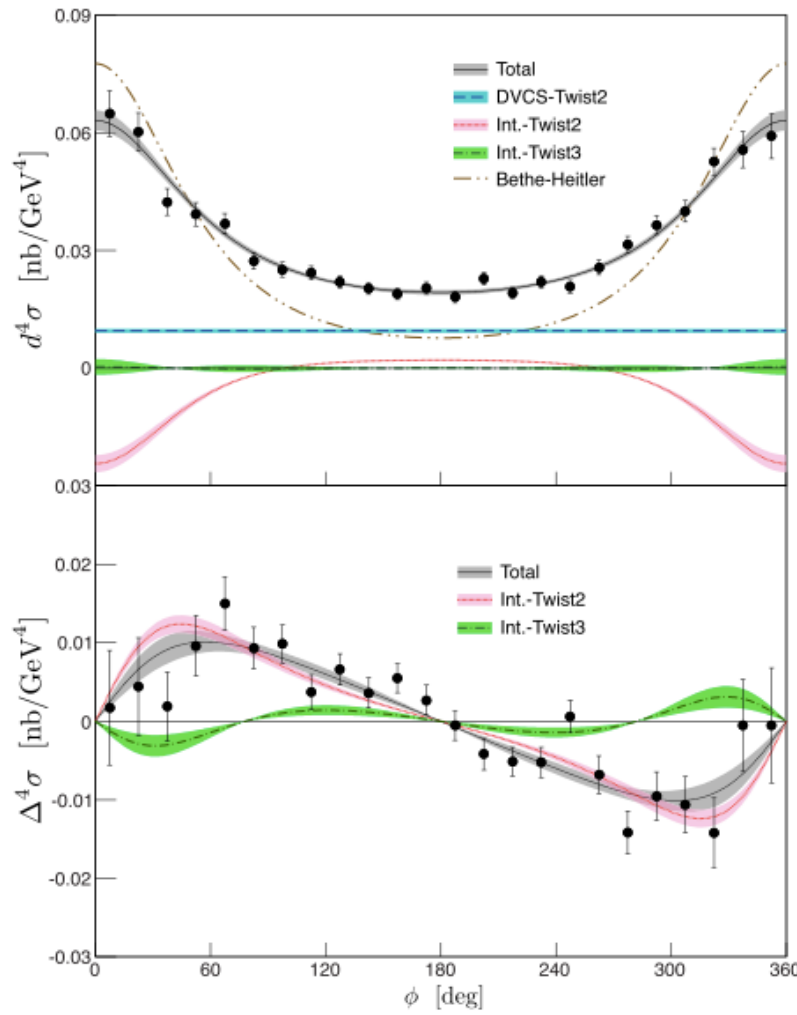
Detect photon in
PbF₂ calorimeter:
< 3% energy
resolution



First DVCS cross-sections in valence region

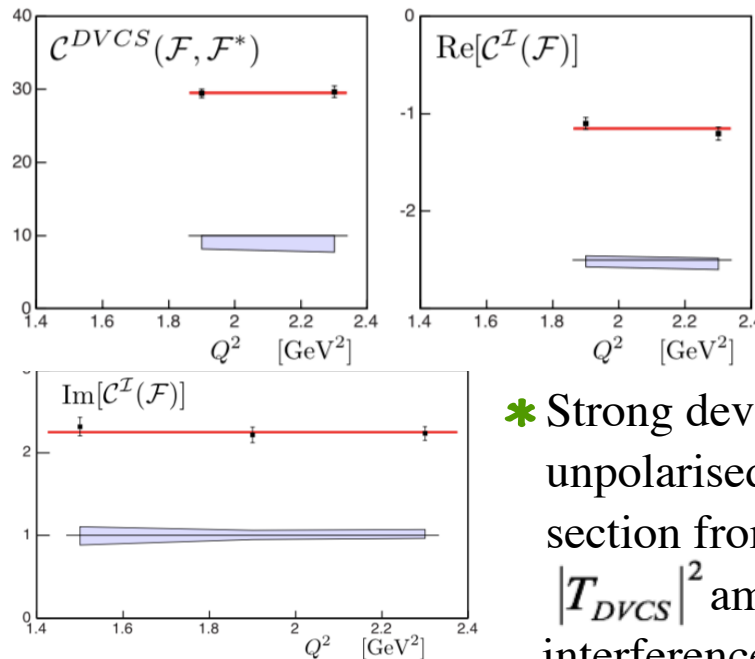
Hall A

- * E00-110: Hall A, ran in 2004, high precision, narrow kinematic range.



$$x_B = 0.36, Q^2 = 2.3 \text{ GeV}^2, -t = 0.32 \text{ GeV}^2$$

- * Luminosity = $10^{37} \text{ cm}^{-2}\text{s}^{-1}$.
- * Measure Q^2 -dependence (Q^2 : 1.5, 1.9, 2.3 GeV^2) of DVCS-BH cross-sections at fixed x_B (0.36).
- * Also x_B dependence at constant Q^2 .
- * CFFs show scaling in DVCS: leading twist (twist-2) dominance at this moderate Q^2 .

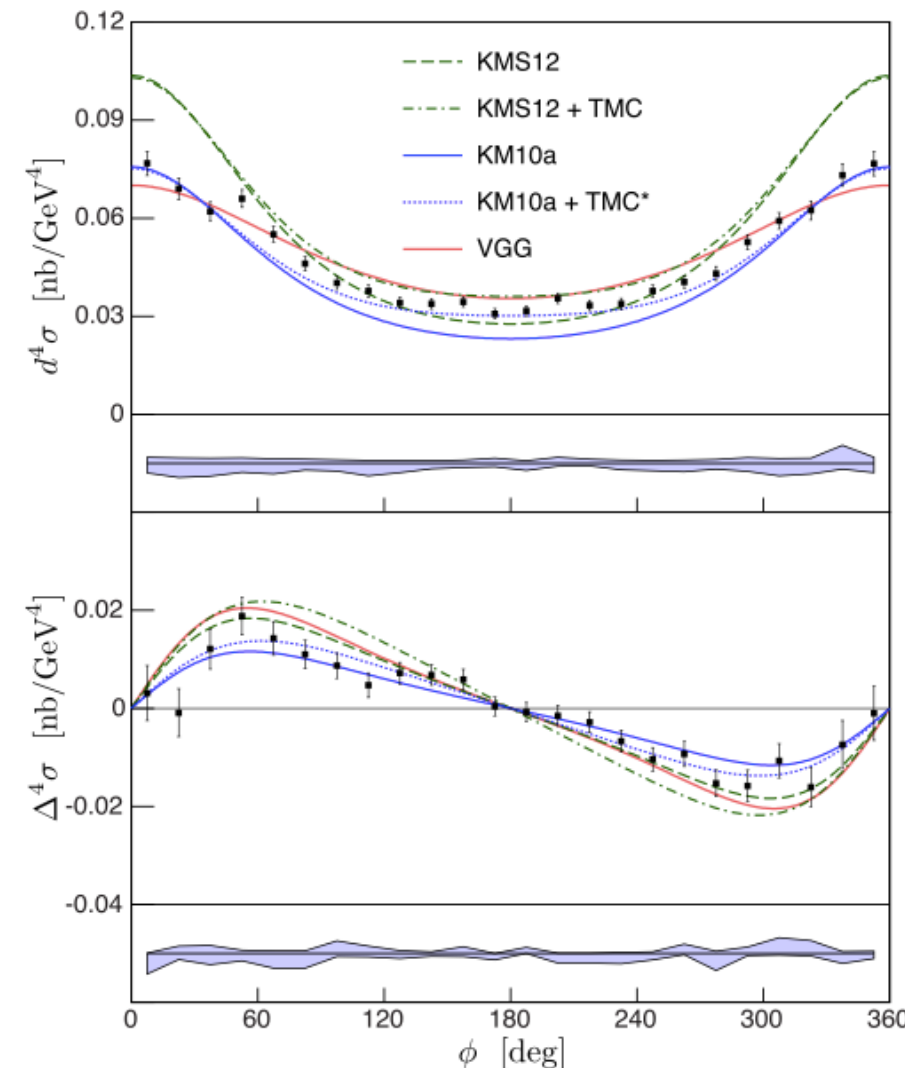


M. Defurne *et al*,
PRC 92 (2015)
055202.

- * Strong deviation of unpolarised DVCS cross-section from BH: extraction of $|T_{DVCS}|^2$ amplitude as well as interference terms.

First DVCS cross-sections in valence region

Hall A



$$x_B = 0.36, Q^2 = 1.9 \text{ GeV}^2, -t = 0.32 \text{ GeV}^2$$

- * High precision of the data: sensitivity to subtle differences in model predictions.

VGG model: Vanderhaeghen, Guichon, Guidal

KMS model: Kroll, Moutarde, Sabatié

KM model: Kumericki, Mueller

TMC: kinematic twist-4 target-mass and finite- t corrections, calculated for proton DVCS and estimated for KMS12.

- * KMS parameters tuned on very low x_B meson-production data: not adapted to valence quarks.

→ TMC*: TMC extracted from the KMS12 model and applied to KM10a.

- * TMC improve agreement for KM10a model, especially at $\phi = 180^\circ$. Higher-twist effects?

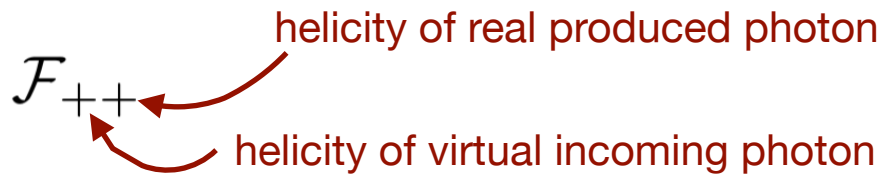
The devil is in the detail...

Here comes the twist...

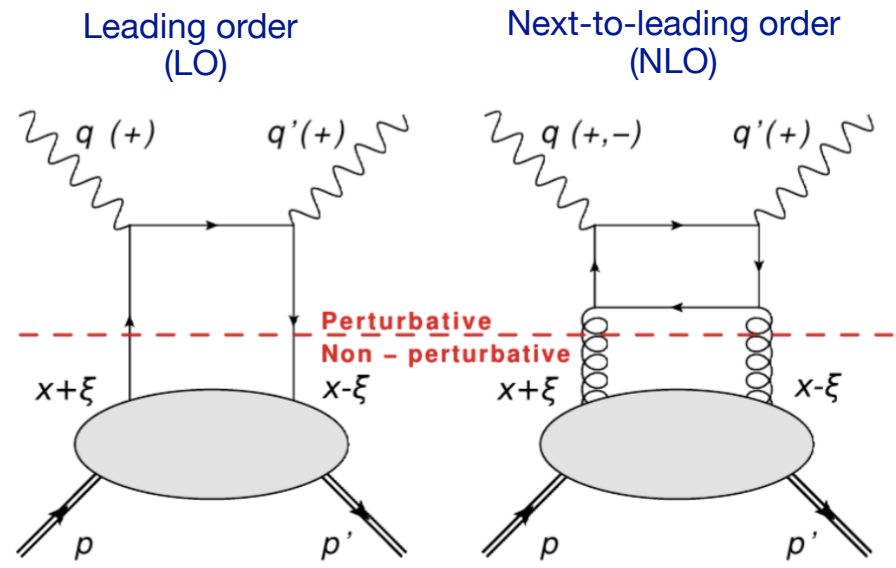
- * Twist: powers of $\frac{1}{\sqrt{Q^2}}$ in the DVCS amplitude. Leading-twist (LT) is twist-2.
- * Order: introduces powers of α_s
- * LO requires $Q^2 \gg M^2$ (M : target mass)

Bold assumption for JLab 6 GeV kinematics!

- * CFFs can be classified according to real and virtual photon helicity:



- Helicity-conserved CFFs – \mathcal{F}_{++}
- Helicity-flip (transverse) – \mathcal{F}_{-+}
- Longitudinal to transverse flip – \mathcal{F}_{0+}



- * CFFs contributing to the scattering amplitude:
 - LT in LO: only \mathcal{F}_{++}
 - LT in NLO: both \mathcal{F}_{++} and \mathcal{F}_{-+}
 - Twist-3: \mathcal{F}_{0+}

Here comes the twist...

- * At finite Q^2 and non-zero t there's ambiguity in defining the light-cone axis:

- Traditional GPD phenomenology uses the Belitsky convention, in plane of q and P :
A. Belitsky *et al*, **Nucl. Phys. B878** (2014), 214

- New, Braun definition using q and q' : more natural.
V. Braun *et al*, **Phys. Rev. D89** (2014), 074022

Reformulating CFFs in this frame absorbs most kinematic power corrections (TMC):

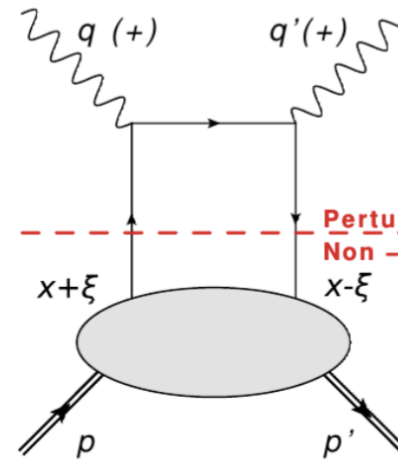
$$\mathcal{F}_{++} = \mathbb{F}_{++} + \frac{\chi}{2} [\mathbb{F}_{++} + \mathbb{F}_{-+}] - \chi_0 \mathbb{F}_{0+}$$

$$\mathcal{F}_{-+} = \mathbb{F}_{-+} + \frac{\chi}{2} [\mathbb{F}_{++} + \mathbb{F}_{-+}] - \chi_0 \mathbb{F}_{0+}$$

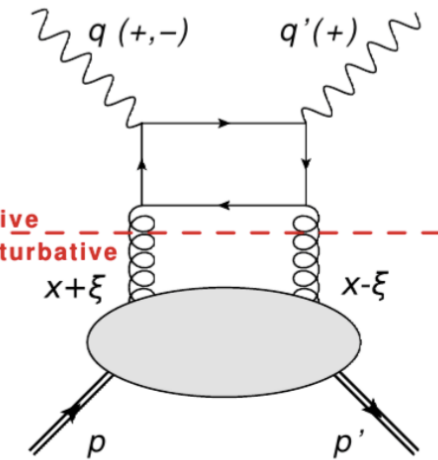
$$\mathcal{F}_{0+} = -(1 + \chi) \mathbb{F}_{0+} + \chi_0 [\mathbb{F}_{++} + \mathbb{F}_{-+}]$$



Leading order
(LO)



Next-to-leading order
(NLO)



Assuming LO and LT in the Braun frame:

$$\mathcal{F}_{++} = (1 + \frac{\chi}{2}) \mathbb{F}_{++}$$

$$\mathcal{F}_{-+} = \frac{\chi}{2} \mathbb{F}_{++}$$

$$\mathcal{F}_{0+} = \chi_0 \mathbb{F}_{++}$$

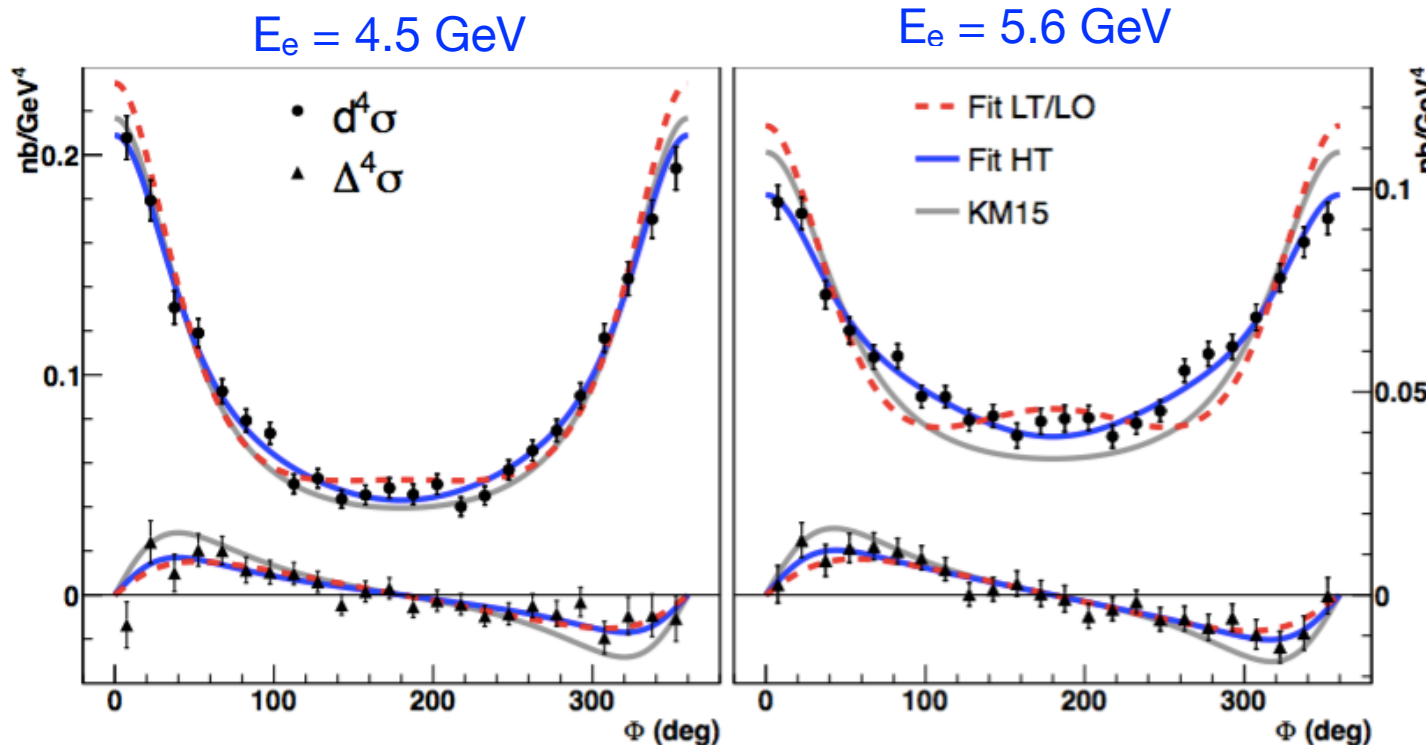
HT/HO contributions in the Belitsky frame, scaled by kinematic factors χ and χ_0 .

Non-negligible at the Q^2 and x_B of the Hall A cross-section measurement:

$$\chi_0 = 0.25, \chi = 0.06 \text{ for } Q^2 = 2 \text{ GeV}^2, x_B = 0.36, t = -0.24 \text{ GeV}^2$$

Hints of higher twist or higher orders

- * Including either higher order or higher twist effects (HT) improves the match with data:



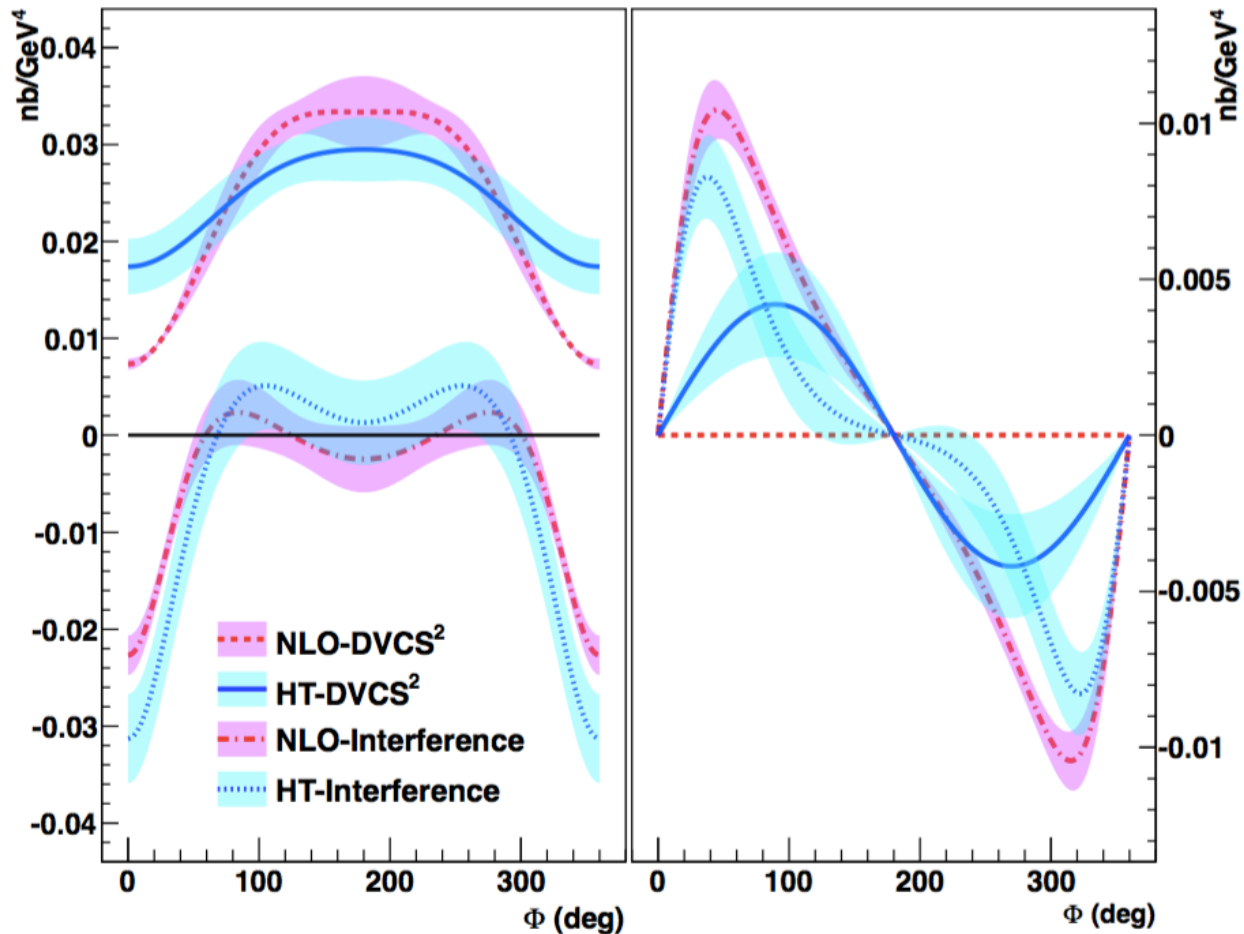
Higher-order and / or higher-twist terms are important! A glimpse of gluons.

Wider range of beam energy needed to identify the dominant effect → **JLab at 11 GeV.**

Rosenbluth separation of DVCS² and BH-DVCS terms

Hall A

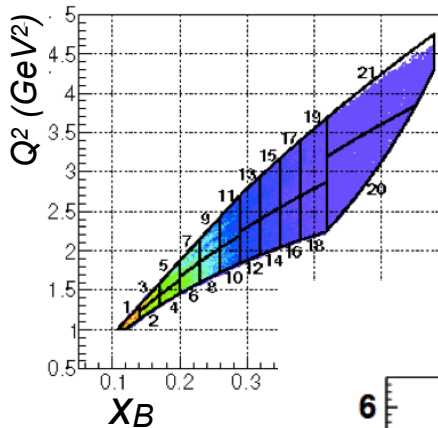
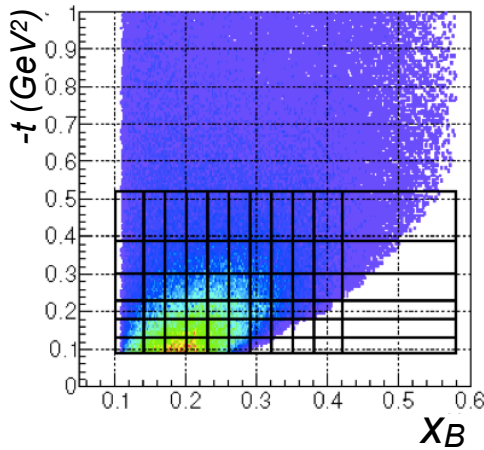
- * Generalised Rosenbluth separation of the DVCS² (scales as E_e^2) and the BH-DVCS interference (scales as E_e^3) terms in the cross-section is possible but NLO and/or higher-twist required: experiment E07-007 @ two beam energies: 4.5 and 5.6 GeV.



- * Significant differences between pure DVCS and interference contributions.
- * Helicity-dependent cross-section has a sizeable DVCS² contribution in the higher-twist scenario.
- * Separation of HT and NLO effects requires scans across wider ranges of Q^2 and beam energy: JLab12!

Large kinematic coverage: CLAS

- * Unpolarised DVCS cross-sections and helicity-dependent cross-section differences in a wide kinematic range:



- * CFFs extracted in a VGG fit.

$$F_{Im}(\xi, t) = F(\xi, \xi, t) \mp F(-\xi, \xi, t)$$

— VGG (Vanderhaeghen, Guichon, Guidal)
- - - Ae^{bt}
prediction

$$Q^2=1.11 \text{ GeV}^2$$

$$x_B=0.126$$

$$Q^2=1.63 \text{ GeV}^2$$

$$x_B=0.185$$

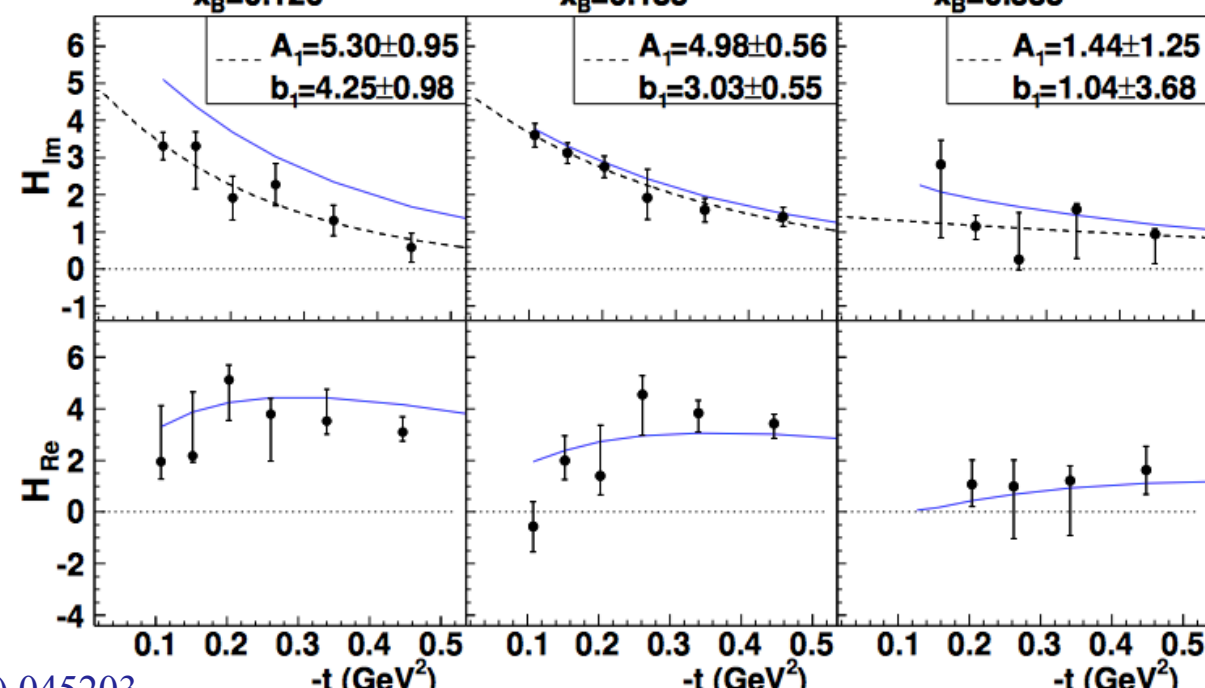
$$Q^2=2.23 \text{ GeV}^2$$

$$x_B=0.335$$

- * Dominance of GPD H in unpolarised cross-section.

- * H_{Im} slope in t becomes flatter at higher x_B

Valence quarks at centre, sea quarks spread out towards the periphery.

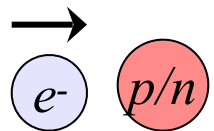


Which DVCS experiment?

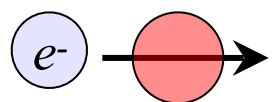
Real parts of CFFs accessible in cross-sections, beam-charge and double polarisation asymmetries,

imaginary parts of CFFs in single-spin asymmetries.

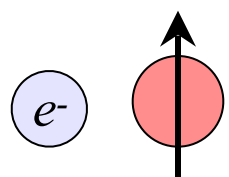
Beam, target
polarisation



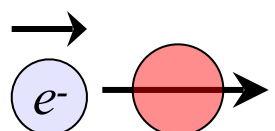
$$\Delta\sigma_{LU} \sim \sin \phi \Im(F_1 \mathbf{H} + \xi G_M \tilde{\mathbf{H}} - \frac{t}{4M^2} F_2 \mathbf{E}) d\phi \rightarrow$$



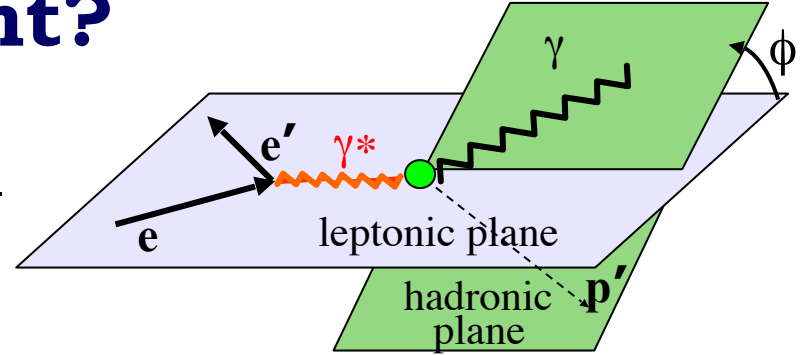
$$\Delta\sigma_{UL} \sim \sin \phi \Im(F_1 \tilde{\mathbf{H}} + \xi G_M (\mathbf{H} + \frac{x_B}{2} \mathbf{E}) - \xi \frac{t}{4M^2} F_2 \tilde{\mathbf{E}} + \dots) d\phi \rightarrow$$



$$\Delta\sigma_{UT} \sim \cos \phi \Im(\frac{t}{4M^2} (F_2 \mathbf{H} - F_1 \mathbf{E}) + \dots) d\phi \rightarrow$$

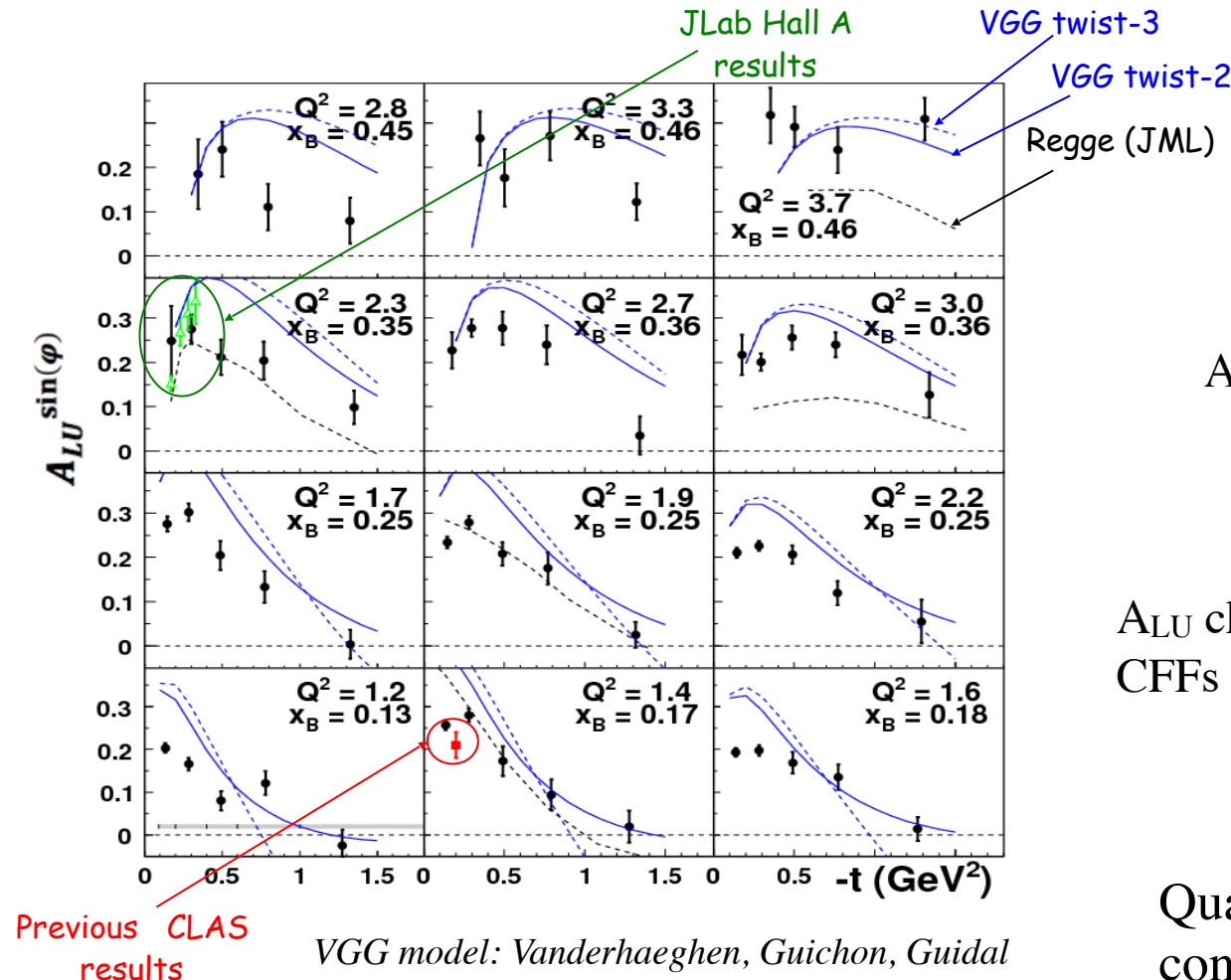


$$\Delta\sigma_{LL} \sim (A + B \cos \phi) \Re(F_1 \tilde{\mathbf{H}} + \xi G_M (\mathbf{H} + \frac{x_B}{2} \mathbf{E}) + \dots) d\phi \rightarrow$$



Proton	Neutron
$\text{Im}\{\mathbf{H}_p, \tilde{\mathbf{H}}_p, E_p\}$	$\tilde{\text{Im}}\{\mathbf{H}_p, \tilde{\mathbf{H}}_p, E_p\}$
$\text{Im}\{H_n, H_n, E_n\}$	$\text{Im}\{H_n, E_n, \tilde{E}_n\}$
$\text{Im}\{\mathbf{H}_p, \tilde{\mathbf{H}}_p\}$	$\text{Im}\{\mathbf{H}_n, E_n, \tilde{E}_n\}$
$\text{Im}\{\mathbf{H}_p, E_p\}$	$\text{Im}\{\mathbf{H}_n\}$
$\text{Re}\{\mathbf{H}_p, \tilde{\mathbf{H}}_p\}$	$\text{Re}\{H_n, E_n, \tilde{E}_n\}$

Beam-spin Asymmetry (A_{LU})



Follows first CLAS measurement:
S. Stepanyan *et al* (CLAS), **PRL 87**
(2001) 182002

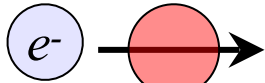
A_{LU} from fit to asymmetry:

$$A_i = \frac{\alpha_i \sin \phi}{1 + \beta_i \cos \phi}$$

A_{LU} characterised by imaginary parts of
CFFs via: $F_1 \mathbf{H} + \xi G_M \tilde{\mathbf{H}} - \frac{t}{4M^2} \mathbf{E}$

Qualitative agreement with models,
constraints on fit parameters.

Target-spin Asymmetry (A_{UL})



Follows first CLAS measurement:
 S. Chen *et al* (CLAS),
PRL 97 (2006) 072002

A_{UL} from fit to asymmetry:

$$A_i = \frac{\alpha_i \sin \phi}{1 + \beta_i \cos \phi}$$

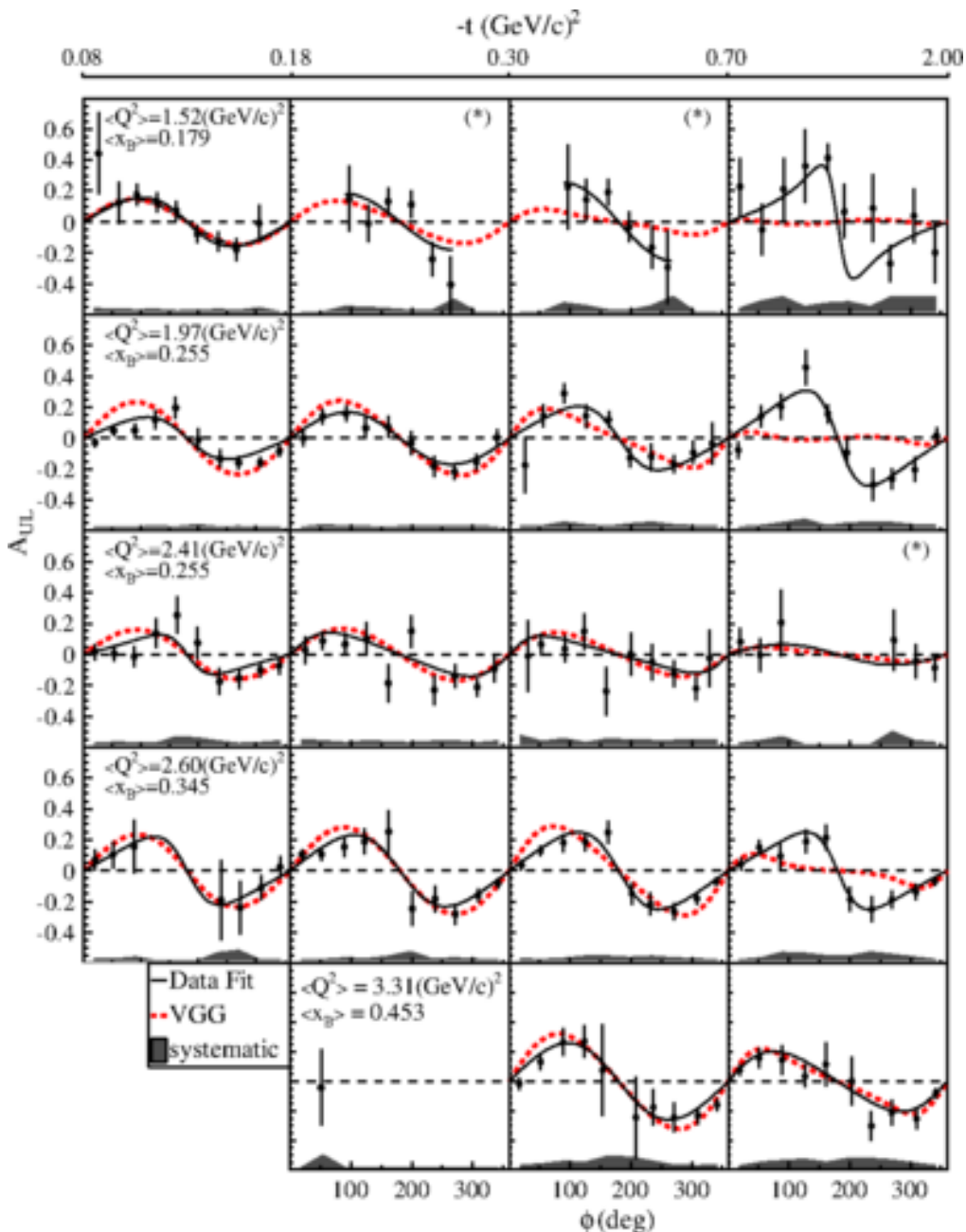
A_{UL} characterised by imaginary parts of CFFs
 via:

$$F_1 \tilde{H} + \xi G_M (\textcolor{red}{H} + \frac{x_B}{2} \textcolor{blue}{E}) - \frac{\xi t}{4M^2} F_2 \tilde{E} + \dots$$

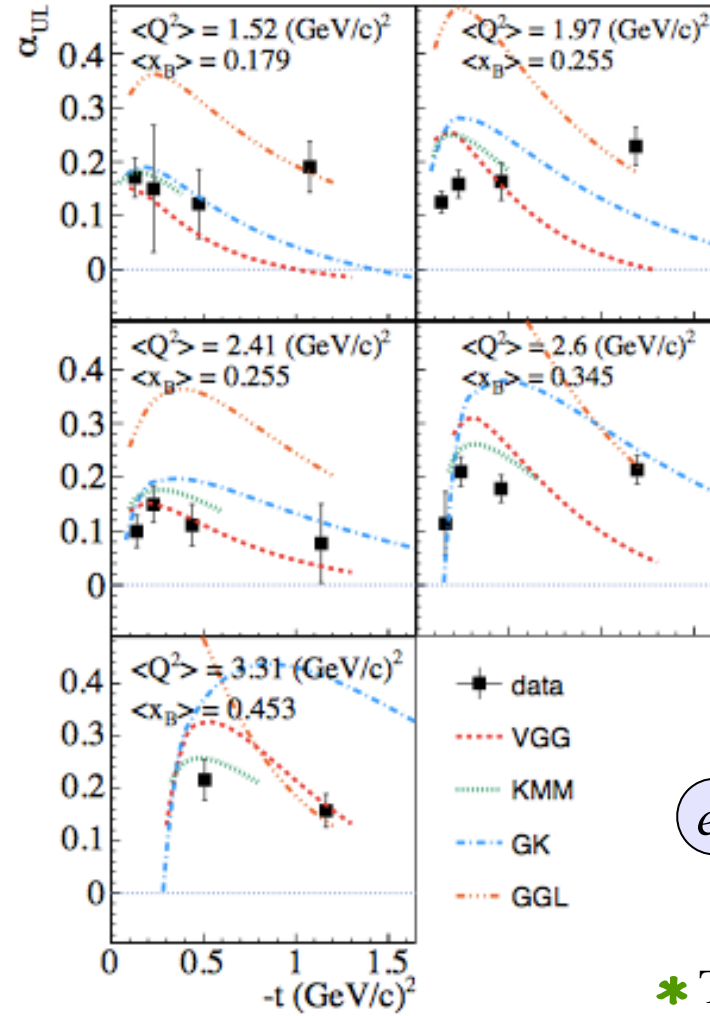
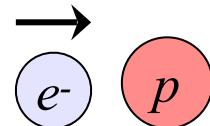
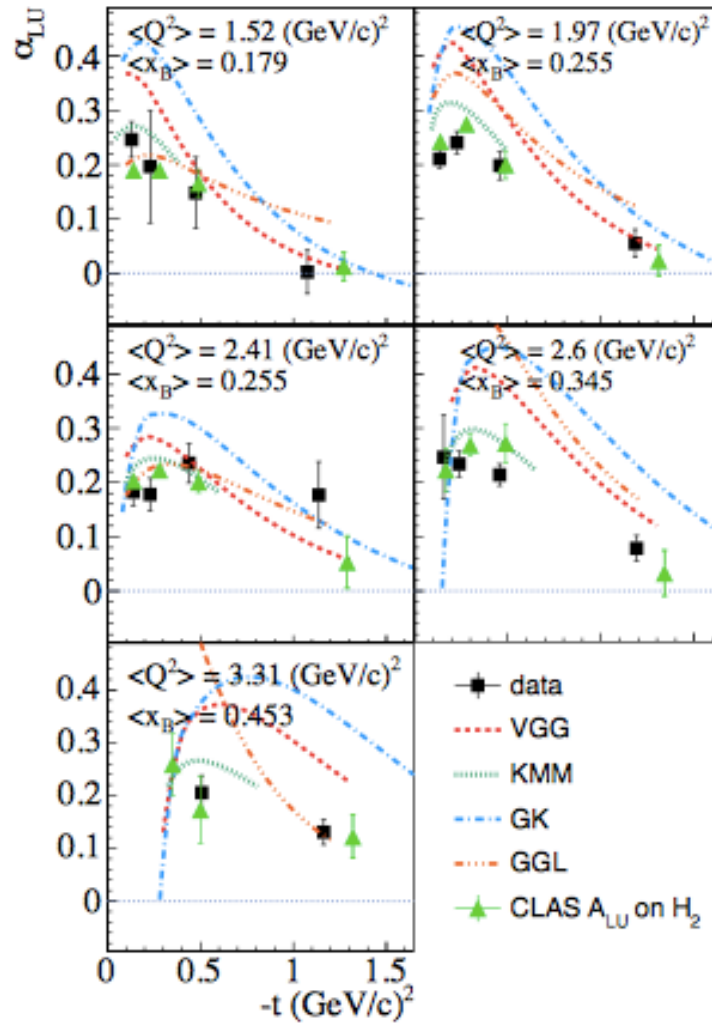
High statistics, large kinematic coverage,
 strong constraints on fits, simultaneous fit
 with BSA and DSA from the same dataset.

E. Seder *et al* (CLAS), **PRL 114** (2015) 032001

S. Pisano *et al* (CLAS), **PRD 91** (2015) 052014



Beam- and target-spin asymmetries



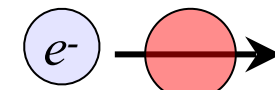
$$A = \frac{\alpha \sin \phi}{1 + \beta \cos \phi}$$

GGL: Goldstein,
Gonzalez, Liuti

GK: Kroll, Moutarde,
Sabatié

KMM: Kumericki,
Mueller, Murray

VGG: Vanderhaeghen,
Guichon, Guidal



* TSA shows a flatter distribution in t than BSA.

S. Pisano *et al* (CLAS), **PRD 91** (2015) 052014
E. Seder *et al* (CLAS), **PRL 114** (2015) 032001

Double-spin asymmetry

At leading twist, double-spin asymmetry (DSA) can be expressed as:

$$A_{LL}(\phi) \sim \frac{c_{0,Lp}^{BH} + c_{0,Lp}^{\mathcal{I}} + (c_{1,Lp}^{BH} + c_{1,Lp}^{\mathcal{I}}) \cos \phi}{c_{0,unp}^{BH} + (c_{1,unp}^{BH} + c_{1,unp}^{\mathcal{I}} + \dots) \cos \phi \dots}$$

$$c_{0,Lp}^{\mathcal{I}}, c_{1,Lp}^{\mathcal{I}} \propto \Re e[F_1 \hat{\mathcal{H}} + \xi(F_1 + F_2)(\mathcal{H} + \frac{x_B}{2}\mathcal{E}) - \xi(\frac{x_B}{2}F_1 + \frac{t}{4M^2}F_2)\tilde{\mathcal{E}}]$$

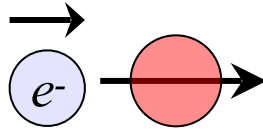
At CLAS kinematics, leading-twist dominance of these CFFs

- * Fit function for the phi-dependence of the asymmetry:

$$\frac{\kappa_{LL} + \lambda_{LL} \cos \phi}{1 + \beta \cos \phi}$$

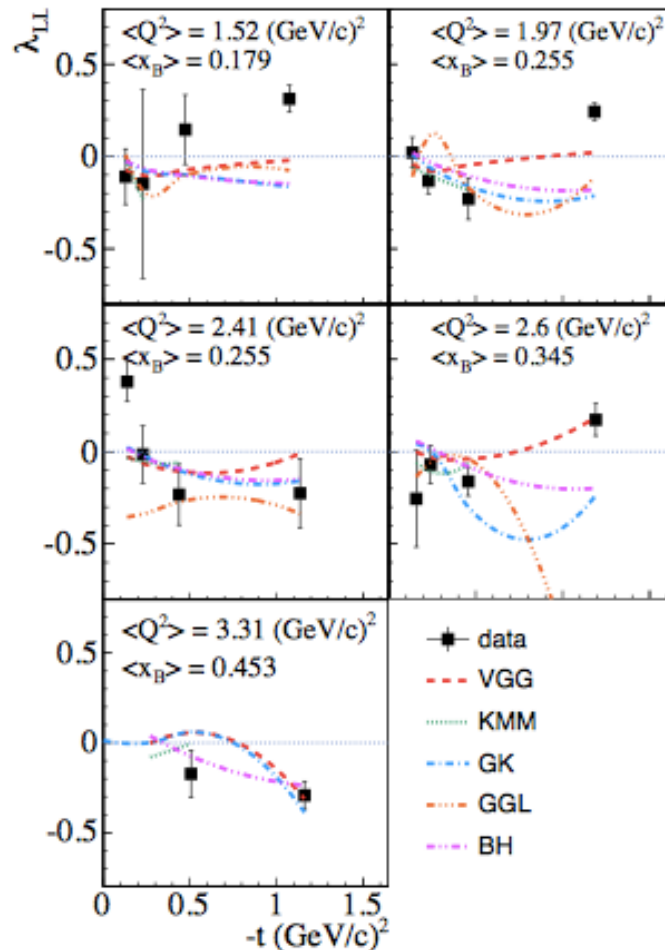
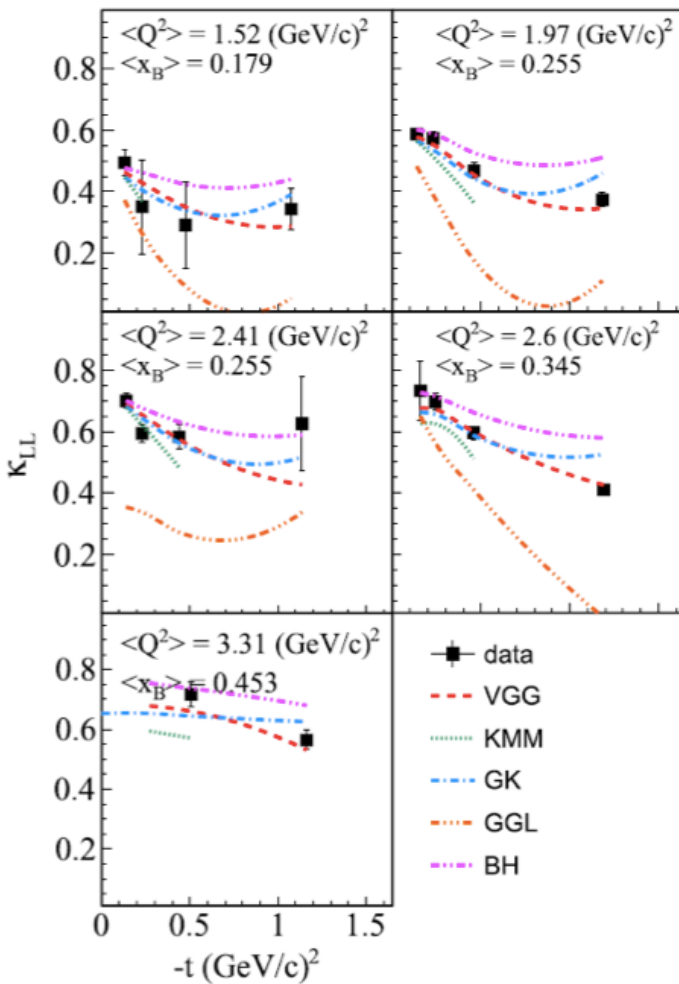
Shares denominator with BSA and TSA!

If measurements at same kinematics, can do a simultaneous fit.



Double-spin Asymmetry (A_{LL})

~~CLAS~~



A_{LL} from fit to asymmetry:

$$\frac{\kappa_{LL} + \lambda_{LL} \cos \phi}{1 + \beta \cos \phi}$$

ALL characterised by real parts of CFFs via:

$$F_1 \tilde{H} + \xi G_M (H + \frac{x_B}{2} E) + \dots$$

- * Fit parameters extracted from a simultaneous fit to BSA, TSA and DSA.
- * Constant term dominates and is almost entirely BH.

CFF extraction from three spin asymmetries at common kinematics.

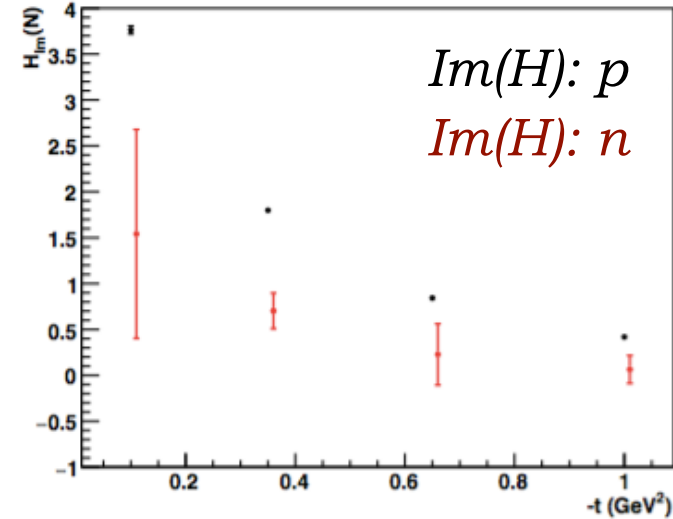
E. Seder *et al* (CLAS), **PRL 114** (2015) 032001

S. Pisano *et al* (CLAS), **PRD 91** (2015) 052014

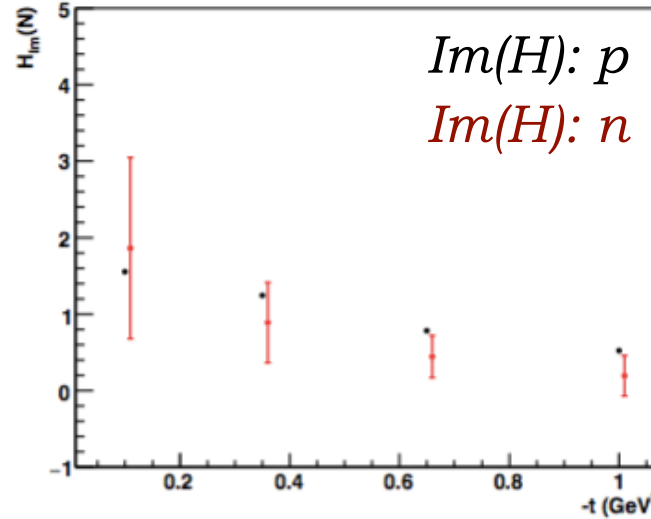
Projected sensitivities to $Im(H)$ CFF



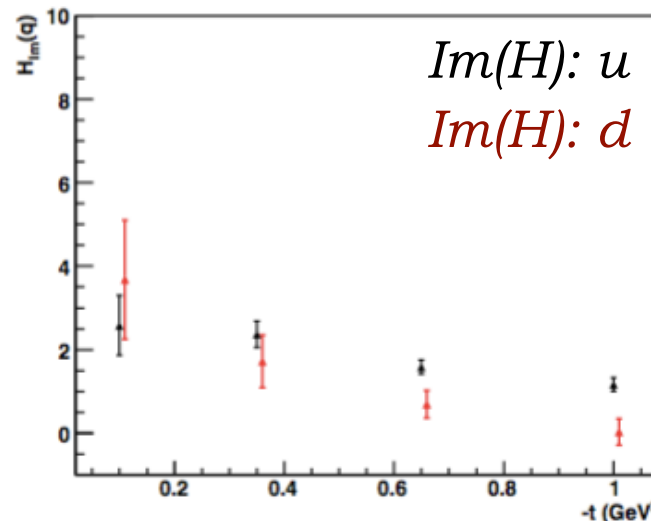
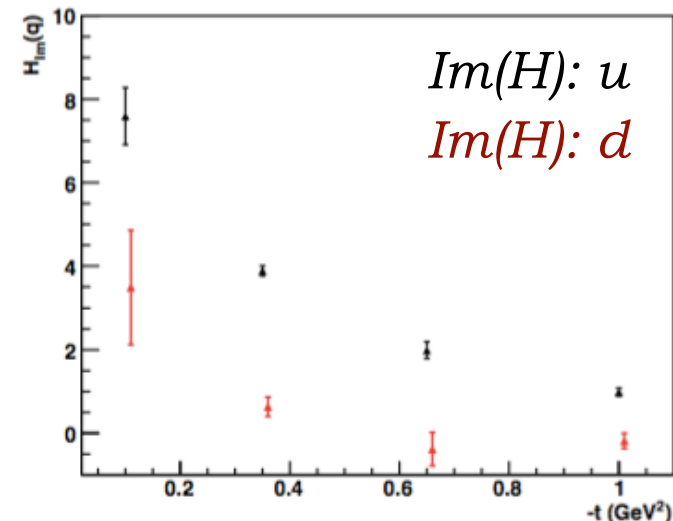
$Q^2 = 2.6 \text{ GeV}^2, x_B = 0.23$



$Q^2 = 5.9 \text{ GeV}^2, x_B = 0.35$



Projections for $Im(H)$ neutron and proton and up and down CFFs extracted from approved CLAS12 experiments.

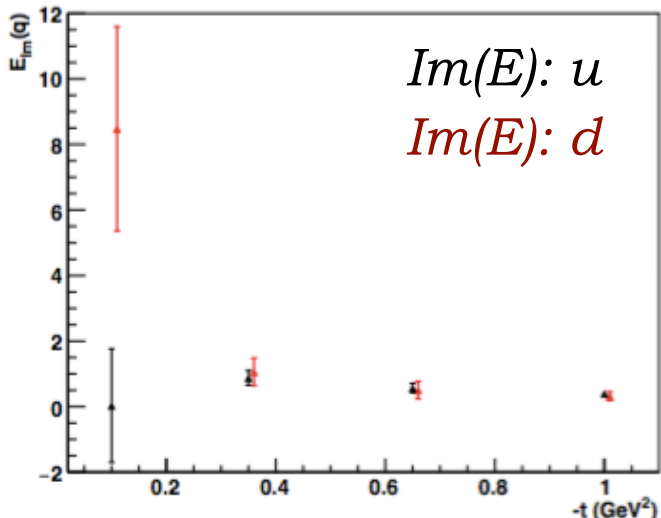
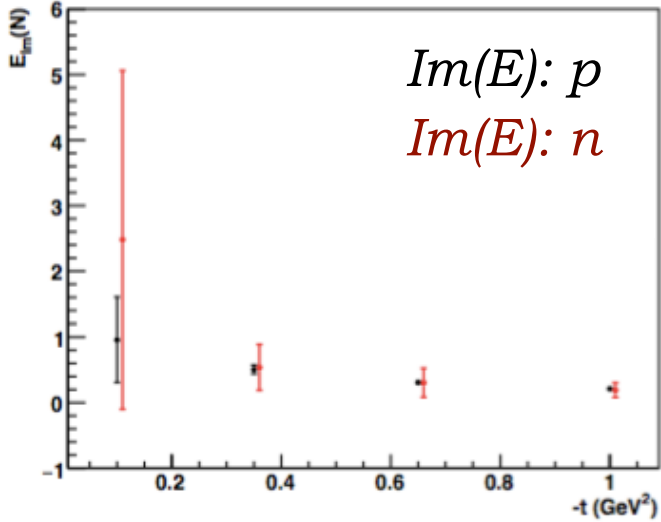


VGG fit (M. Guidal)

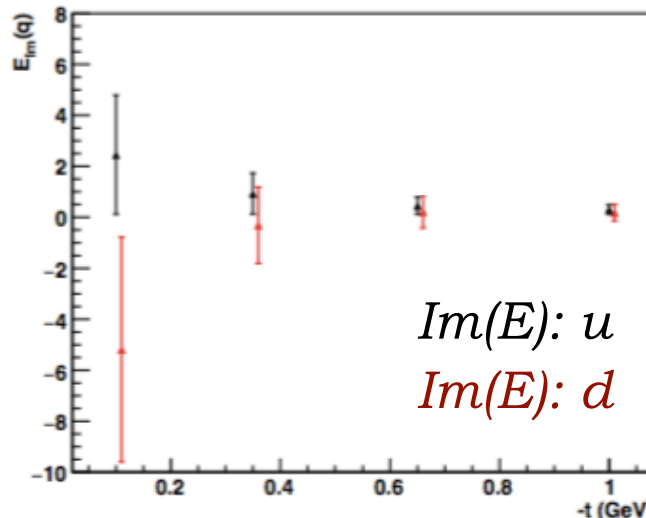
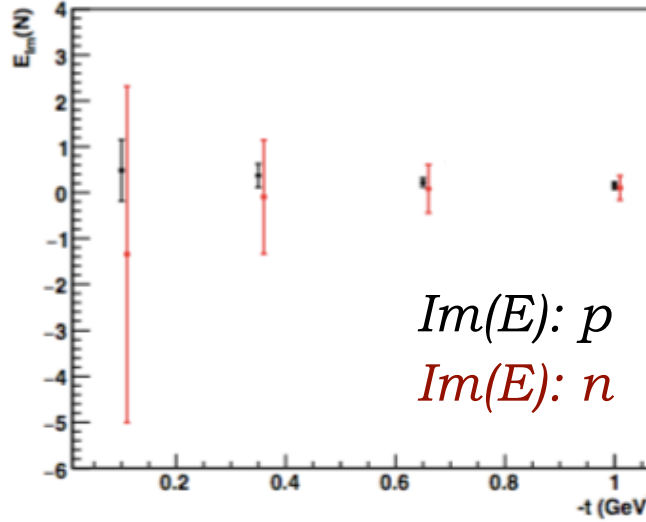
Projected sensitivities to $Im(E)$ CFF



$Q^2 = 2.6 \text{ GeV}^2, x_B = 0.23$



$Q^2 = 5.9 \text{ GeV}^2, x_B = 0.35$



Projections for $Im(E)$ neutron and proton and up and down CFFs extracted from approved and conditionally-approved CLAS12 experiments.

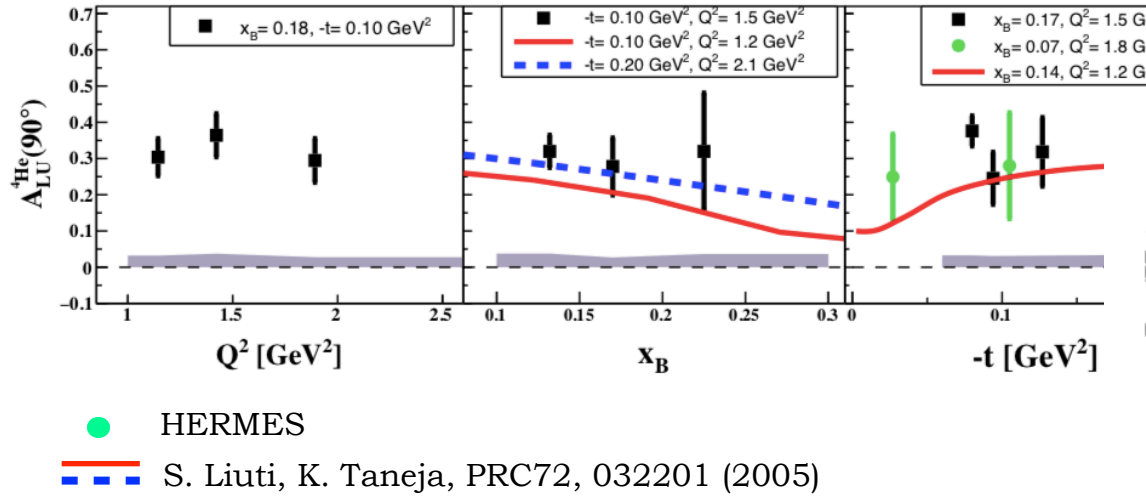
VGG fit (M. Guidal)

Nuclear GPDs: coherent DVCS on ${}^4\text{He}$

~~CLAS~~

- * ${}^4\text{He}$ is spin-0, so only one GPD at leading twist, \mathbf{H}_A .

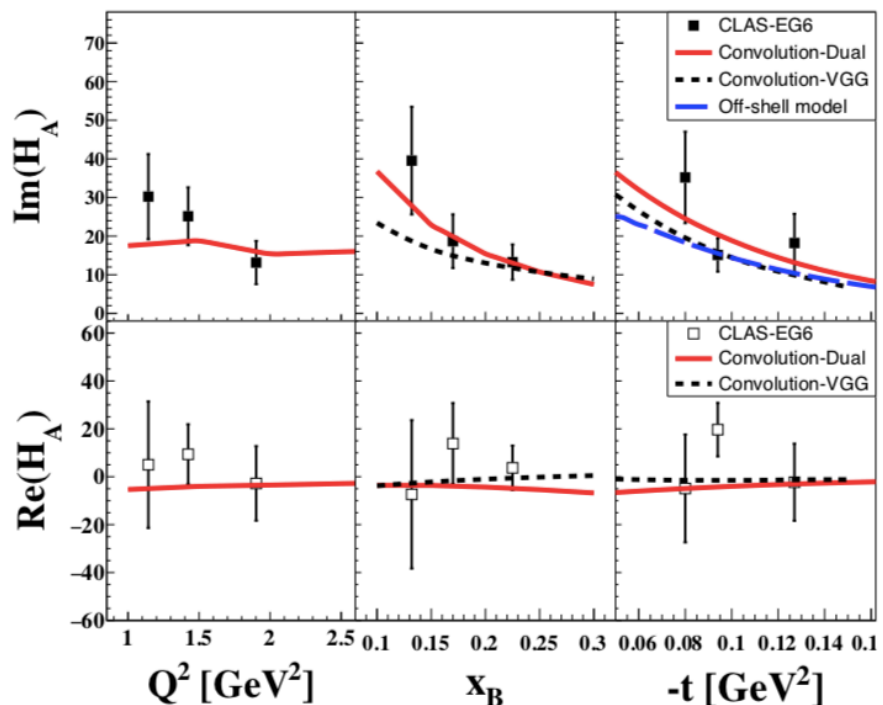
$$\begin{aligned}\Re e(\mathcal{H}_A) &= \mathcal{P} \int_0^1 dx [H_A(x, \xi, t) - H_A(-x, \xi, t)] C^+(x, \xi) \\ \Im m(\mathcal{H}_A) &= -\pi(H_A(\xi, \xi, t) - H_A(-\xi, \xi, t))\end{aligned}$$



- * Beam spin asymmetry in coherent DVCS from ${}^4\text{He}$: CLAS and a radial time projection chamber (RTPC) for detection of recoiling helium, data taken in 2009.

- * Paves the way for measurements at 11 GeV.

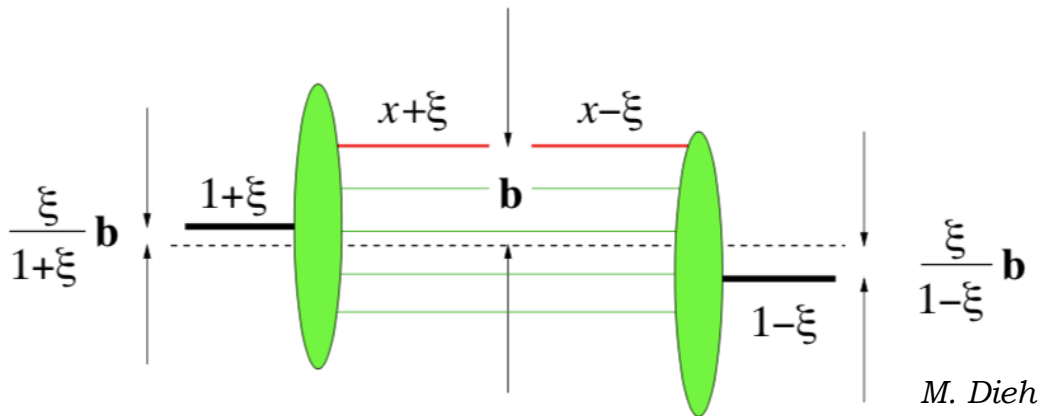
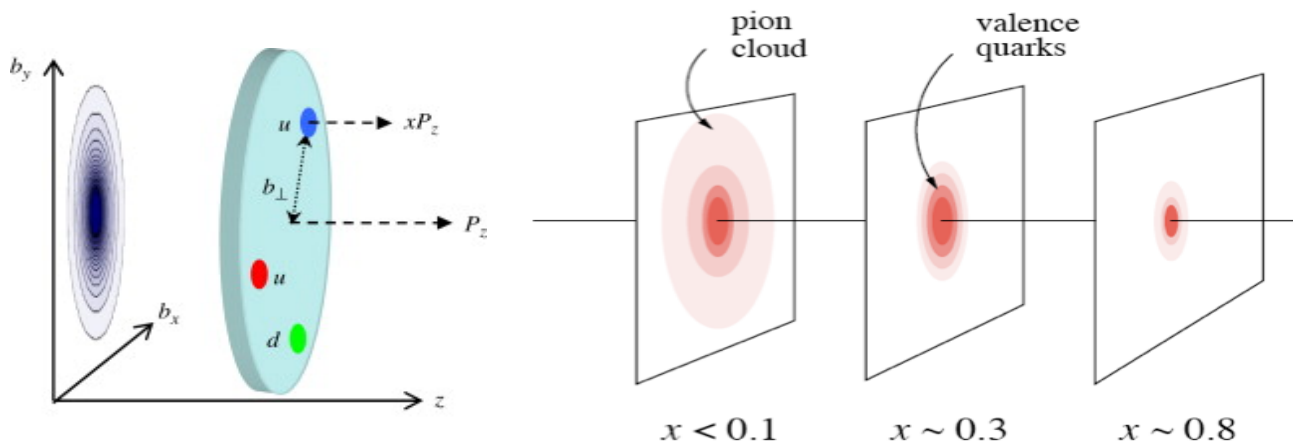
M. Hattawy *et al*, PRL 119 (2017) 202004.



- V. Guzey, PRC78, 025211 (2008)
 - - M. Guidal *et al*, PRD72, 054013 (2005)
 — J. Gonzalez-Hernandez *et al*, PRC88, 065206 (2013)

Nucleon Tomography from GPDs

- * At a fixed Q^2 , x_B , slope of GPD with t is related, via a Fourier Transform, to the transverse spatial spread.



Formally, the radial separation, \mathbf{b} , between the struck parton and the centre of momentum of the remaining spectators.

- * Experimentally, fit the t -dependence of structure functions or CFFs with an exponential.

$$\text{eg: } \frac{d\sigma_U}{dt} = Ae^{Bt}$$

GPDs and nucleon spin

$$J_N = \frac{1}{2} = \frac{1}{2} \Sigma_q + L_q + J_g$$

* Ji's relation: $J^q = \frac{1}{2} - J^g = \frac{1}{2} \int_{-1}^1 x dx \left\{ H^q(x, \xi, 0) + E^q(x, \xi, 0) \right\}$

Second Mellin moments of the GPDs contain information on the total angular momentum carried by quarks.

Note that the contribution from GPD H is given by the quark momentum, already known from PDFs:

$$2J^q = \int_0^1 dx x[q(x) + \bar{q}(x)] + \int_{-1}^{+1} dx x E^q(x, 0, 0)$$

Compton Form Factors in DVCS

Experimentally, DVCS amplitude is proportional to Compton Form Factors (CFFs) — sums of GPD integrals over x :

$$\int_{-1}^1 dx F(\mp x, \xi, t) \left[\frac{1}{x - \xi + i\epsilon} \pm \frac{1}{x + \xi - i\epsilon} \right]$$

↗ *GPD* ↓ *Plus sign for unpolarised GPDs, minus for polarised.*

Can be decomposed into real and imaginary parts:

Cauchy's principal value integral

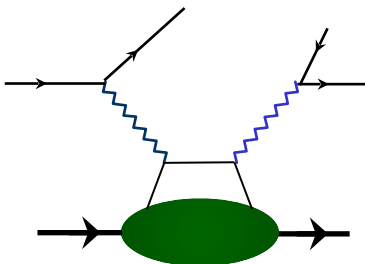
$$\Re e \mathcal{F} = \mathcal{P} \int_{-1}^1 dx \left[\frac{1}{x - \xi} \mp \frac{1}{x + \xi} \right] F(x, \xi, t)$$

$$\Im m \mathcal{F}(\xi, t) = -\pi [F(\xi, \xi, t) \mp F(-\xi, \xi, t)]$$

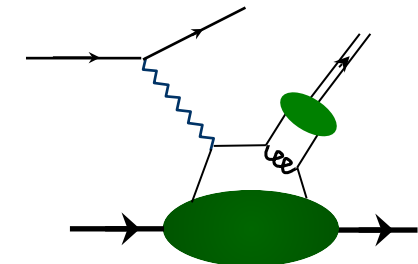
- * Both parts are accessible in different experimental observables

Other reactions to get at GPDs

- * **Time-like Compton scattering:** virtual photon is time-like. At leading order, access same integrals of GPDs. At higher orders, they differ.

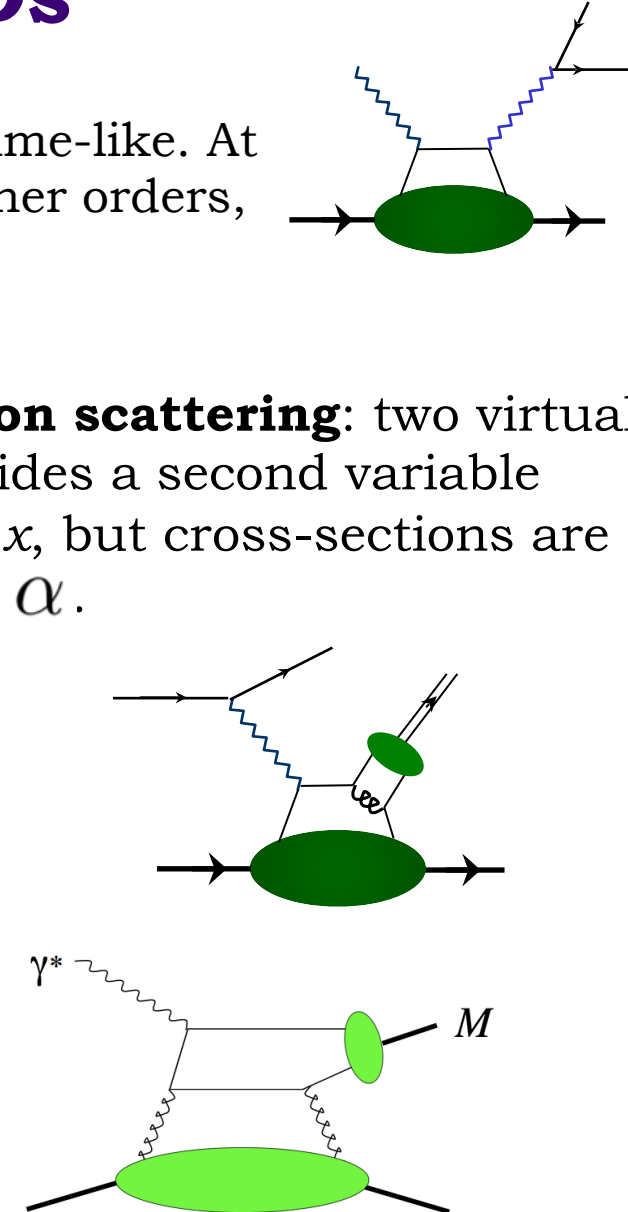


- * **Double Deeply Virtual Compton scattering:** two virtual photons: the second vertex provides a second variable Q'^2 . This allows direct access to x , but cross-sections are suppressed by another factor of α .



- * **Deeply Virtual Meson Production:** the meson vertex provides flavour information. Amplitude now depends on GPDs and the meson Distribution Amplitudes. In light mesons, more sensitive to higher order and higher twist.

In vector mesons, gluon GPDs appear at lowest order!



Nucleon Tomography from GPDs

- * Flavour separation is possible in DVCS using different targets (proton and neutron), and in DVMP with different mesons.

For example, compare measurements of π^0 and η DVMP:

$$H_T^{\pi^0} = (e_u H_T^u - e_d H_T^d) / \sqrt{2}, \quad H_T^\eta = (e_u H_T^u + e_d H_T^d) / \sqrt{6},$$
$$\bar{E}_T^{\pi^0} = (e_u \bar{E}_T^u - e_d \bar{E}_T^d) / \sqrt{2}, \quad \bar{E}_T^\eta = (e_u \bar{E}_T^u + e_d \bar{E}_T^d) / \sqrt{6}.$$

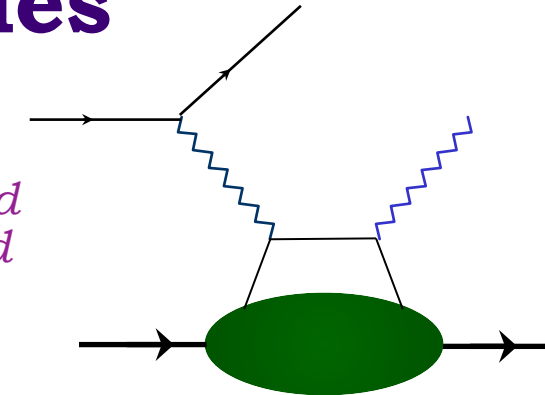
Up-quark charge (Goloskokov-Kroll model)

- * Different GPDs represent different aspects of the parton distributions: EM charge, axial charge, transversity, etc....
- * Sensitivity to gluon distributions through gluon GPDs.

Particularly cleanly accessible for heavier q : J/Ψ

Extracting asymmetries

Number of DVCS/BH events for each kinematic bin:



$$N^{bt} = (1 - B_{\pi^0}^{bt}) \cdot \frac{N_{ep\gamma}^{bt}}{FC^{bt}}$$

Polarisation state of beam, target
 Background due to π^0 contamination
 Number of detected events in identified reaction
 Normalisation by beam current (in Faraday Cup)

* Beam-spin asymmetry: $A_{LU} = \frac{P_t^- (N^{++} - N^{-+}) + P_t^+ (N^{+-} - N^{--})}{P_b (P_t^- (N^{++} + N^{-+}) + P_t^+ (N^{+-} + N^{--}))}$

* Target-spin asymmetry:

$$A_{UL} = A_{UL}^{\text{lab}} + c_{A_{UT}}$$

Correction for electron / virtual photon axes

$$A_{UL}^{\text{lab}} = \frac{N^{++} + N^{-+} - N^{+-} - N^{--}}{D_f (P_t^- (N^{++} + N^{-+}) + P_t^+ (N^{+-} + N^{--}))}$$

Dilution factor due to unpolarised background

* Double-spin asymmetry:

$$A_{LL} = A_{LL}^{\text{lab}} + c_{A_{LT}}$$

$$A_{LL}^{\text{lab}} = \frac{N^{++} + N^{--} - N^{+-} - N^{-+}}{P_b \cdot D_f (P_t^- (N^{++} + N^{-+}) + P_t^+ (N^{+-} + N^{--}))}$$

The DVCS/BH amplitude

$$\mathcal{T}^2 = |\mathcal{T}_{\text{BH}}|^2 + |\mathcal{T}_{\text{DVCS}}|^2 + \mathcal{I} \quad \xleftarrow{\text{Interference term for DVCS/BH}}$$

$$|\mathcal{T}_{\text{BH}}|^2 = \frac{e^6}{x_B^2 y^2 (1 + \epsilon^2)^2 t \mathcal{P}_1(\phi) \mathcal{P}_2(\phi)} [c_0^{\text{BH}} + \sum_{n=1}^2 c_n^{\text{BH}} \cos n\phi + s_1^{\text{BH}} \sin \phi]$$

$$|\mathcal{T}_{\text{DVCS}}|^2 = \frac{e^6}{y^2 Q^2} \{c_0^{\text{DVCS}} + \sum_{n=1}^2 [c_n^{\text{DVCS}} \cos n\phi + s_n^{\text{DVCS}} \sin n\phi]\}$$

$$\mathcal{I} = \frac{e^6}{x_B y^3 t \mathcal{P}_1(\phi) \mathcal{P}_2(\phi)} \{c_0^{\mathcal{I}} + \sum_{n=1}^3 [c_n^{\mathcal{I}} \cos n\phi + s_n^{\mathcal{I}} \sin n\phi]\}$$

Intermediate lepton propagators

*Coefficients depending on
Compton Form Factors*

From asymmetries to CFFs

At leading twist, beam-spin asymmetry (BSA) can be expressed as:

$$A_{\text{LU}}(\phi) \sim \frac{s_{1,\text{unp}}^{\mathcal{I}} \sin \phi}{c_{0,\text{unp}}^{\text{BH}} + (c_{1,\text{unp}}^{\text{BH}} + c_{1,\text{unp}}^{\mathcal{I}} + \dots) \cos \phi \dots} \quad \text{higher-twist terms...}$$

The leading coefficient is related to the imaginary part of the Compton Form Factors:

$$s_{1,\text{unp}}^{\mathcal{I}} \propto \Im[\bar{F}_1 \mathcal{H} + \xi(F_1 + F_2)\tilde{\mathcal{H}} - \frac{t}{4M^2} F_2 \mathcal{E}]$$

At CLAS kinematics, this dominates

*F₁, F₂: Dirac,
Pauli form factors*

Likewise, for the target-spin asymmetry (TSA):

$$A_{\text{UL}}(\phi) \sim \frac{s_{1,\text{LP}}^{\mathcal{I}} \sin \phi}{c_{0,\text{unp}}^{\text{BH}} + (c_{1,\text{unp}}^{\text{BH}} + c_{1,\text{unp}}^{\mathcal{I}} + \dots) \cos \phi + \dots}$$

$$s_{1,\text{LP}}^{\mathcal{I}} \propto \Im[\bar{F}_1 \tilde{\mathcal{H}} + \xi(F_1 + F_2)(\mathcal{H} + \frac{x_B}{2} \mathcal{E}) - \xi(\frac{x_B}{2} F_1 + \frac{t}{4M^2} F_2) \tilde{\mathcal{E}}]$$

At CLAS kinematics, these CFFs dominate

- * Obtain coefficients from fitting the phi-dependence of the asymmetry:

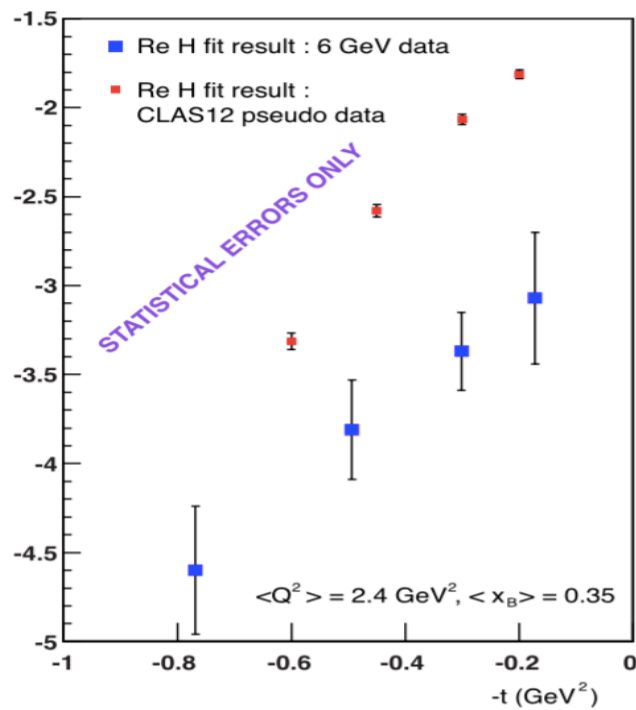
$$A_i = \frac{\alpha_i \sin \phi}{1 + \beta_i \cos \phi}$$

Proton DVCS @ 11 GeV

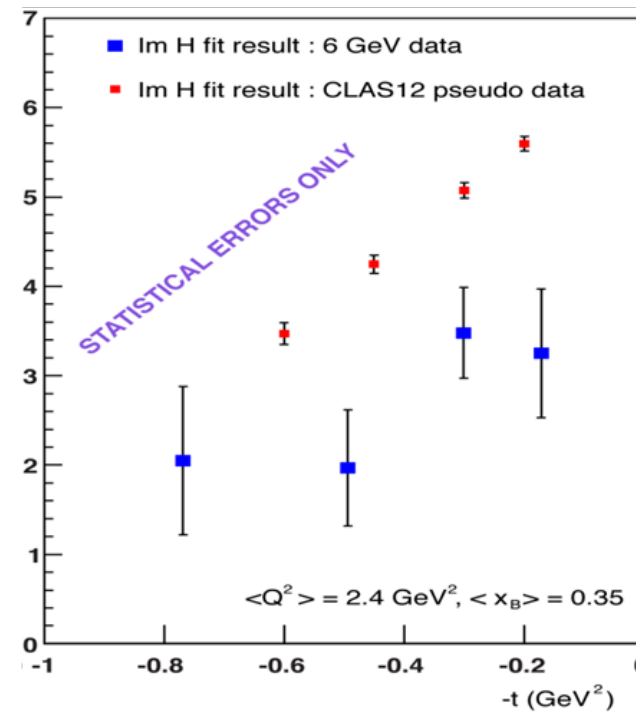


Impact of CLAS12 unpolarised target proton-DVCS data on the extraction of $\text{Re}(H)$ and $\text{Im}(H)$.

$\text{Re}(H)$



$\text{Im}(H)$

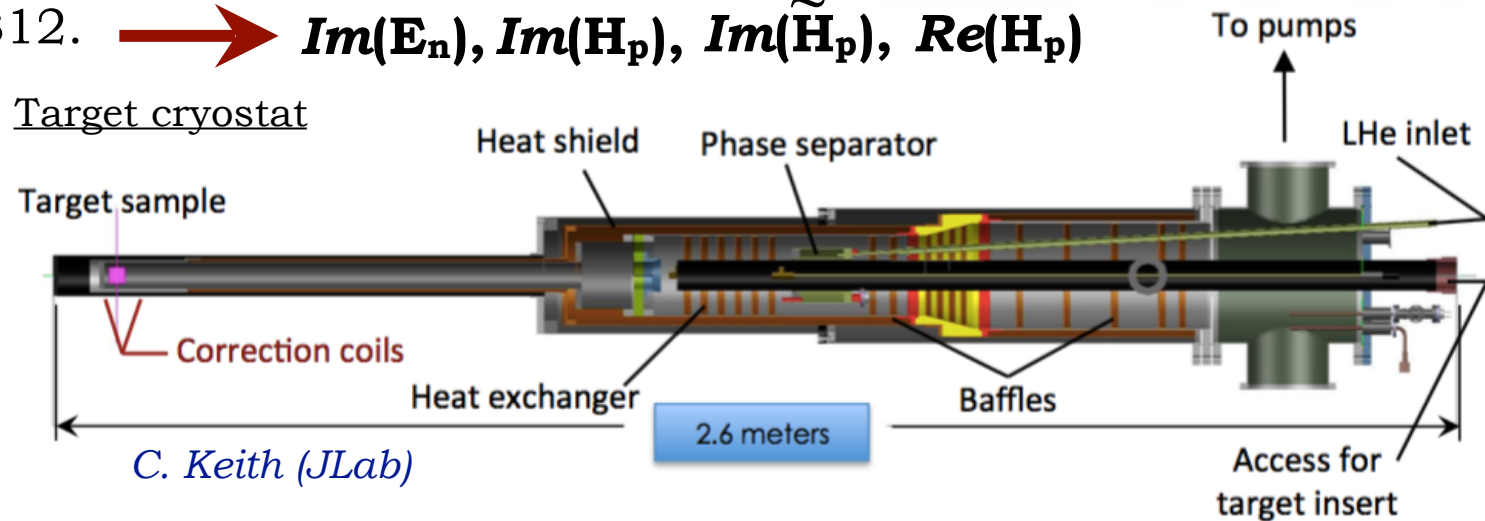


(CLAS 6 GeV extraction H. Moutarde)

DVCS @ JLab12

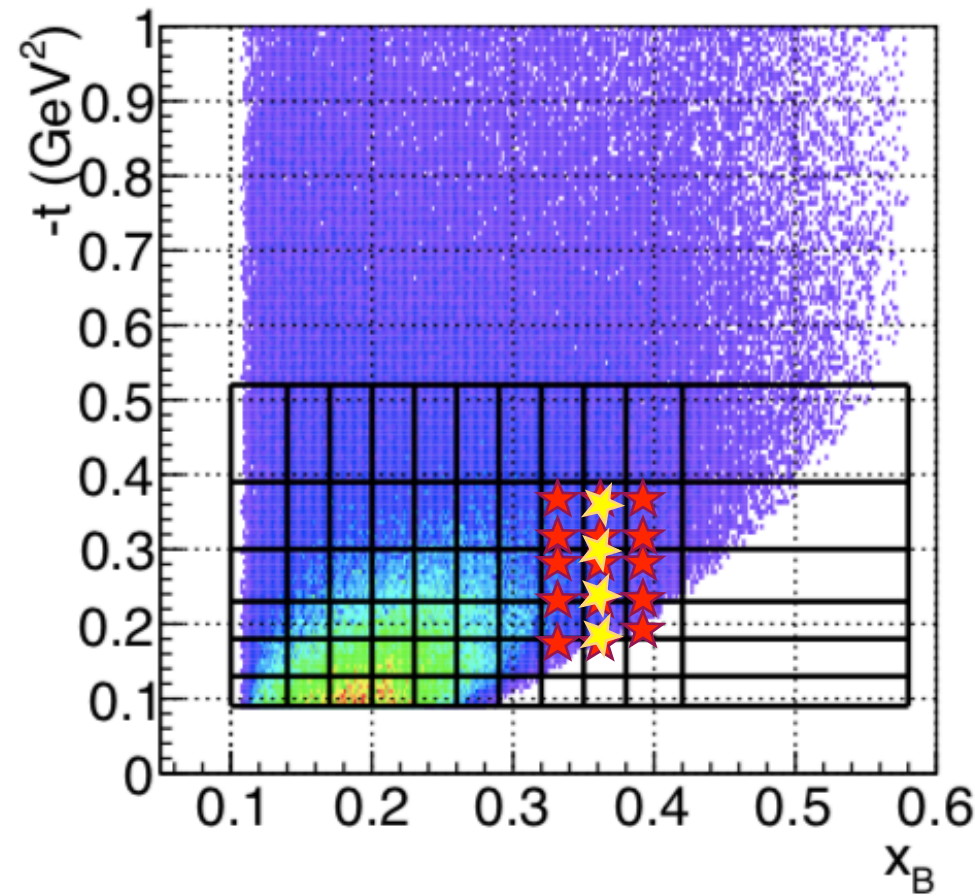
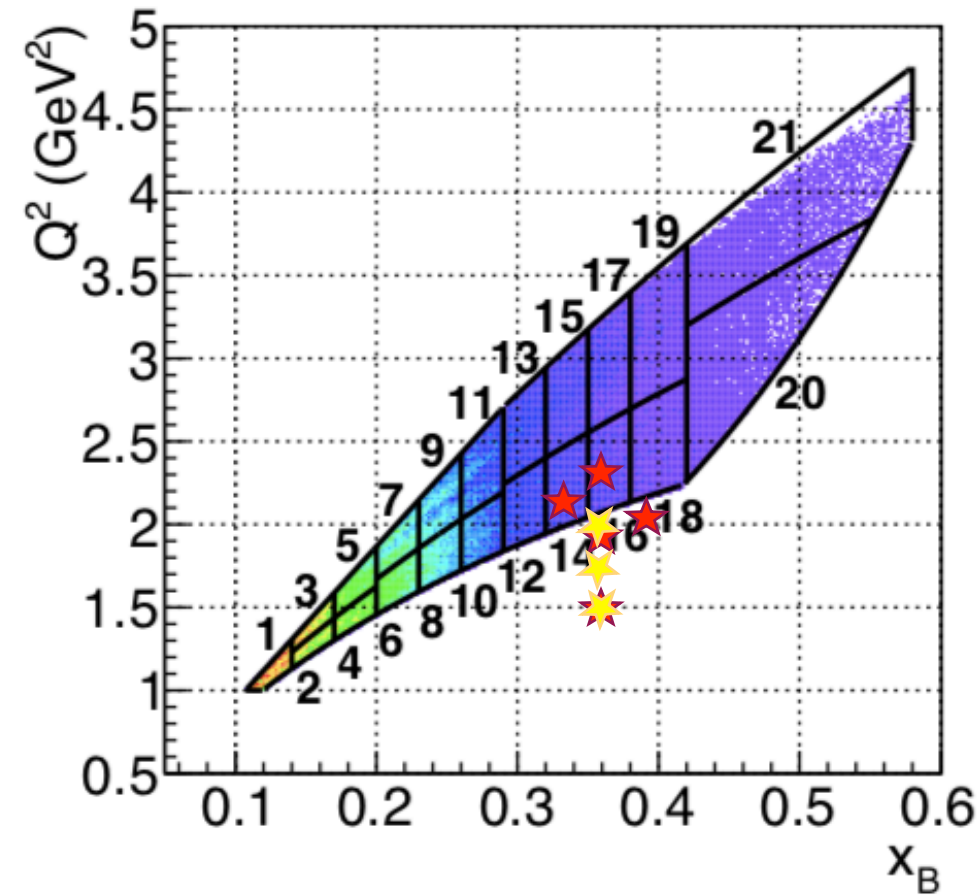
- * Scheduled experiments to measure cross-sections and spin asymmetries with unpolarised and longitudinally polarised liquid H_2 and D_2 targets using CLAS12. → $Im(E_n)$, $Im(H_p)$, $Im(\tilde{H}_p)$, $Re(H_p)$

- Dynamic Nuclear Polarisation (DNP) of target material, cooled in a He evaporation cryostat.
- $P_{\text{proton}} = 80\%$,
- P_{deuteron} up to 50%



- * Measurements of cross-sections at 10.6, 8.8 and 6.6 GeV (allows separation of pure DVCS amplitude and the DVCS/Bethe-Heitler interference terms) in Halls A, B and C.
- * Transversely-polarised target (HD) for use with electron beams is under development (Hall B). → $Im(E_p)$
- * Measurement of beam-spin asymmetry in coherent DVCS from a 4He target (CLAS12 + recoil detector ALERT): partonic structure of nuclei. → $Im(H_A)$

JLab 6 GeV era DVCS X-sections: kinematics



CLAS 2D distributions: H.-S. Jo *et al* (CLAS), **PRL 115** (2015) 212003

Hall A

★ M. Defurne *et al*, **PRC 92** (2015) 055202

★ M. Defurne *et al*, **Nature Communications 8** (2017) 1408

Proton DVCS @ 11 GeV



Experiment E12-06-119

F. Sabatié et al.

$P_{\text{beam}} = 85\%$

$L = 10^{35} \text{ cm}^{-2}\text{s}^{-1}$

$1 < Q^2 < 10 \text{ GeV}^2$

$0.1 < x_B < 0.65$

$-t_{\min} < -t < 2.5 \text{ GeV}^2$

*Kinematics similar for all proton DVCS
@ 11 GeV with CLAS12 experiments*

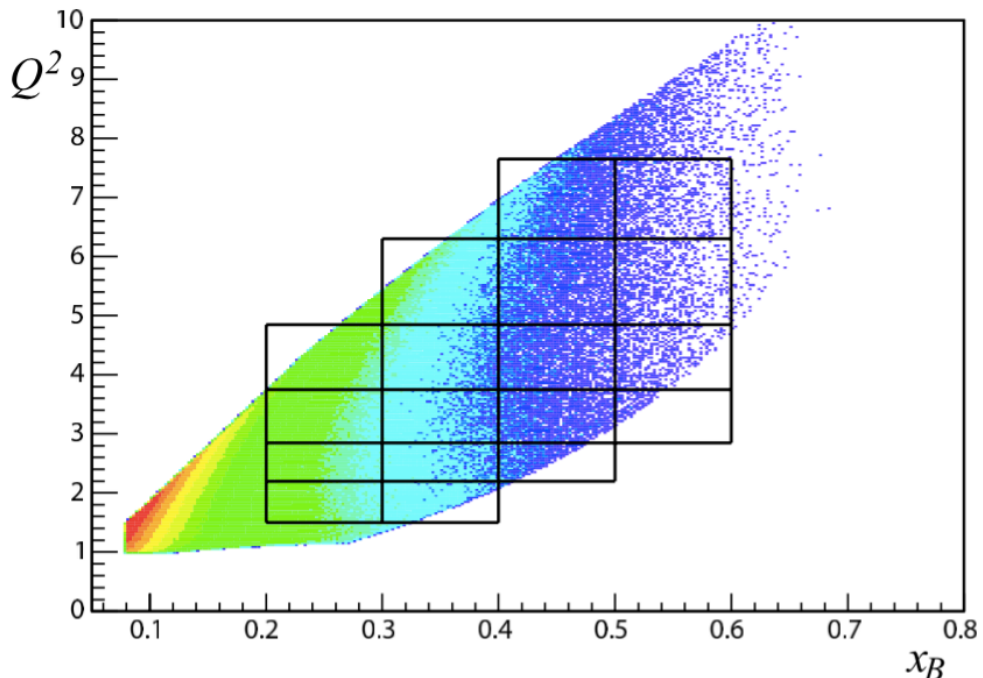
Unpolarised liquid H₂ target:

- Statistical error: 1% - 10% on $\sin\varphi$ moments
- Systematic uncertainties: ~ 6 - 8%

ALU characterised by imaginary parts of

CFFs via:

$$F_1 \mathbf{H} + \xi G_M \tilde{\mathbf{H}} - \frac{t}{4M^2} \mathbf{E} \longrightarrow \mathbf{Im}(\mathbf{H}_p)$$



First experiment with CLAS12

Started this February!

DVCS at lower energies with CLAS12

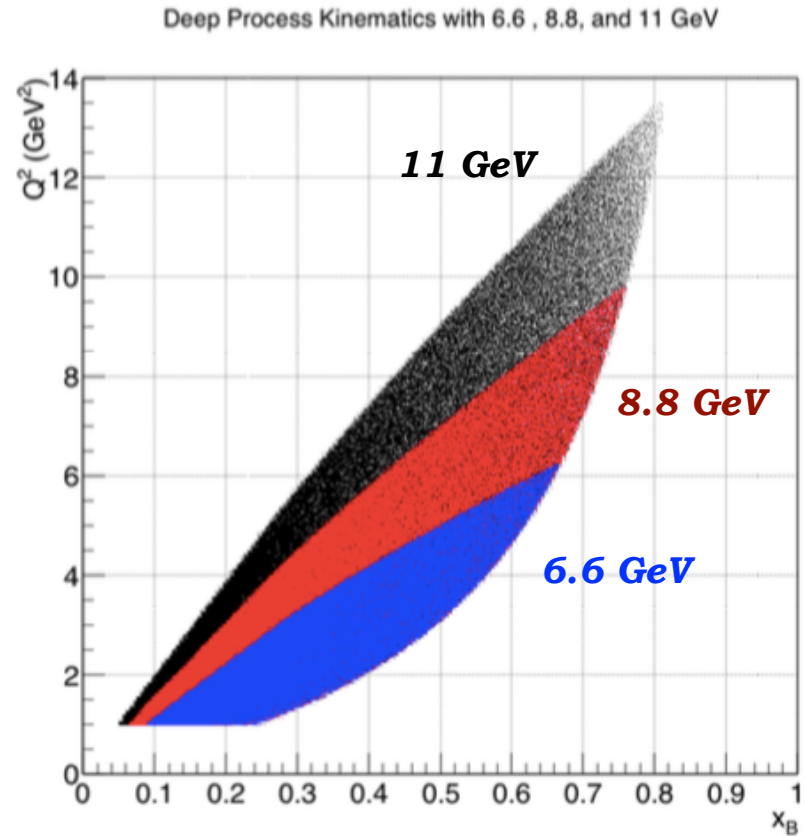


Experiment E12-16-010B

F.-X. Girod *et al.*

Unpolarised liquid H₂ target:

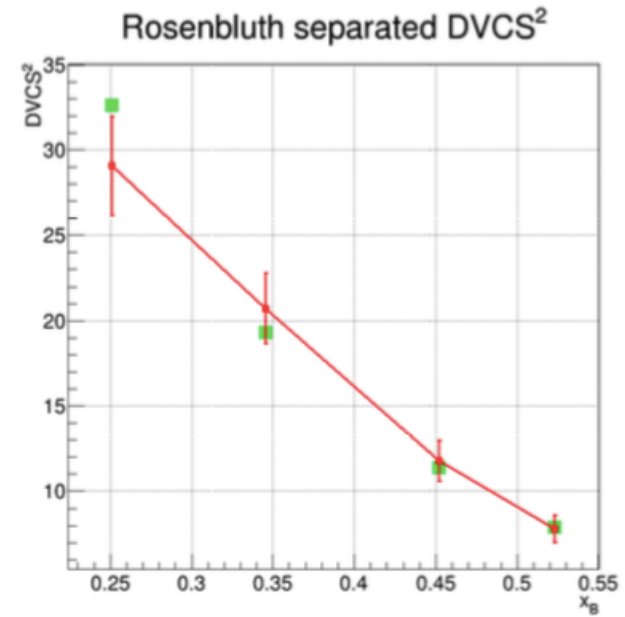
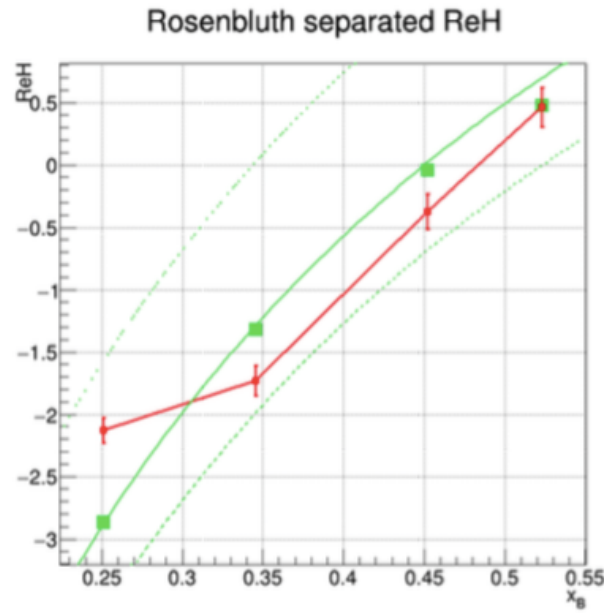
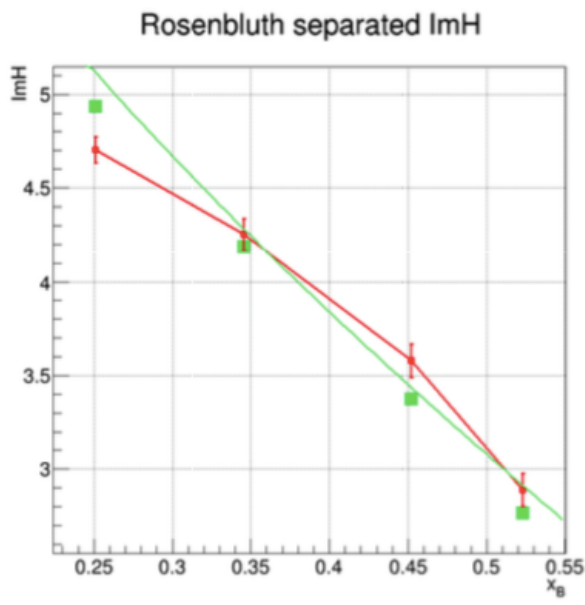
- Beam energies: 6.6, 8.8 GeV
 - Simultaneous fit to beam-spin and total cross-sections.
- * Rosenbluth separation of interference and $|T_{DVCS}|^2$ terms in the cross-section
- * Scaling tests of the extracted CFFs
- * Model-dependent determination of the D-term in the Dispersion Relation between *Re* and *Im* parts of CFFs: sensitivity to Gravitational Form Factors.



Compare with measurements from Halls A and C: cross-check model and systematic uncertainties.

DVCS at lower energies with CLAS12

Projected extraction of CFFs (red) compared to generated values (green). Three curves on the $Re(H)$ show three different scenarios for the D-term.

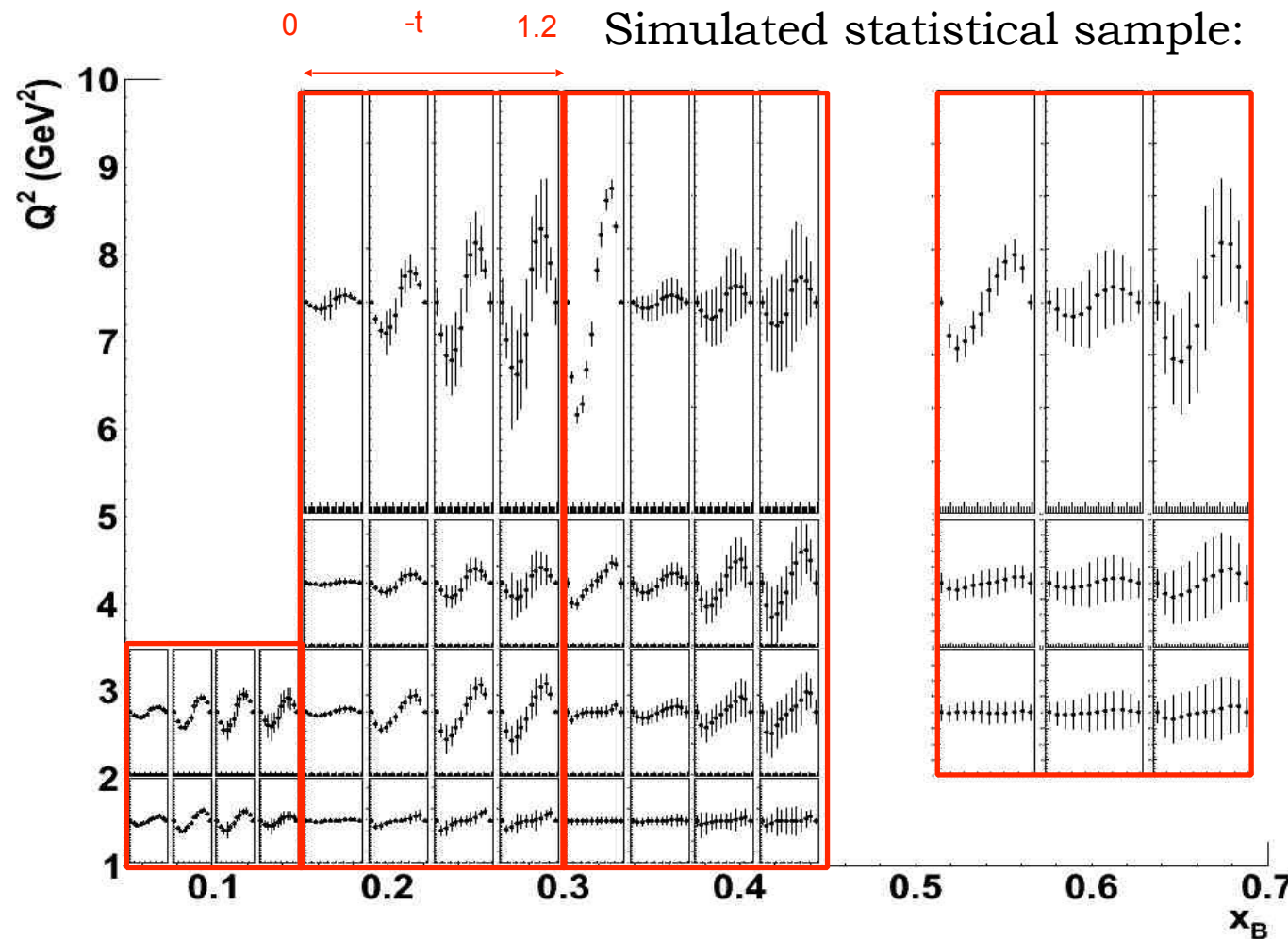




Neutron DVCS @ 11 GeV

Experiment E12-11-003
S. Niccolai, D. Sokhan et al.

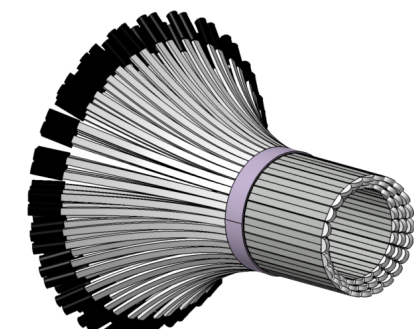
$$\Delta\sigma_{LU} \sim \sin\phi \operatorname{Im}\{F_1 H + \xi(F_1 + F_2) \tilde{H} - k F_2 E\} d\phi$$



$\operatorname{Im}(E_n)$ dominates.

$L = 10^{35} \text{ cm}^{-2}\text{s}^{-1}/\text{nucleon}$
 $e + d \rightarrow e' + \gamma + n + (p_s)$

CLAS12 +
Forward Tagger +
Neutron Detector



Scheduled: 2019



Neutron DVCS with a longitudinally polarised target

Experiment E12-06-109A.

S. Niccolai, D. Sokhan et al.

Longitudinally polarised ND₃ target:

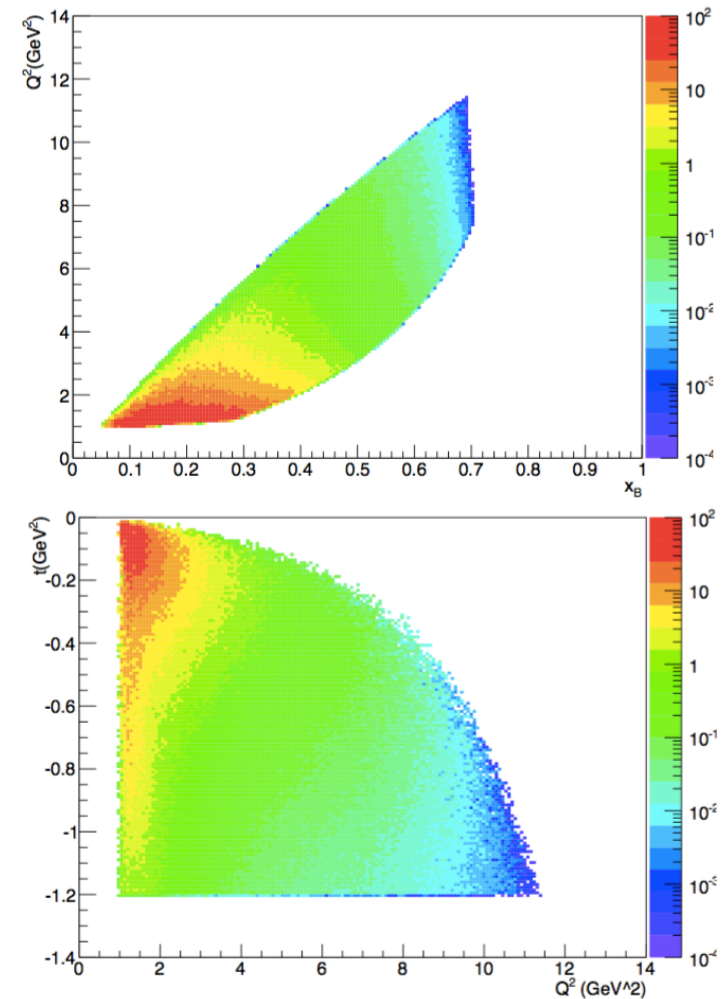
- Dynamic Nuclear Polarisation (DNP) of target material in a cryostat shared with the NH₃ target.
- P_{deuteron} up to 50%
- Systematic uncertainties: ~ 12%

AUL characterised by imaginary parts of CFFs via:

$$F_1 \tilde{H} + \xi G_M (\textcolor{red}{H} + \frac{x_B}{2} \textcolor{blue}{E}) - \frac{\xi t}{4M^2} F_2 \tilde{E} + \dots$$

$$\rightarrow \textcolor{red}{Im}(\mathbf{H}_n)$$

In combination with pDVCS, will allow flavour-separation of the H_q CFFs.



Tentative schedule: 2020



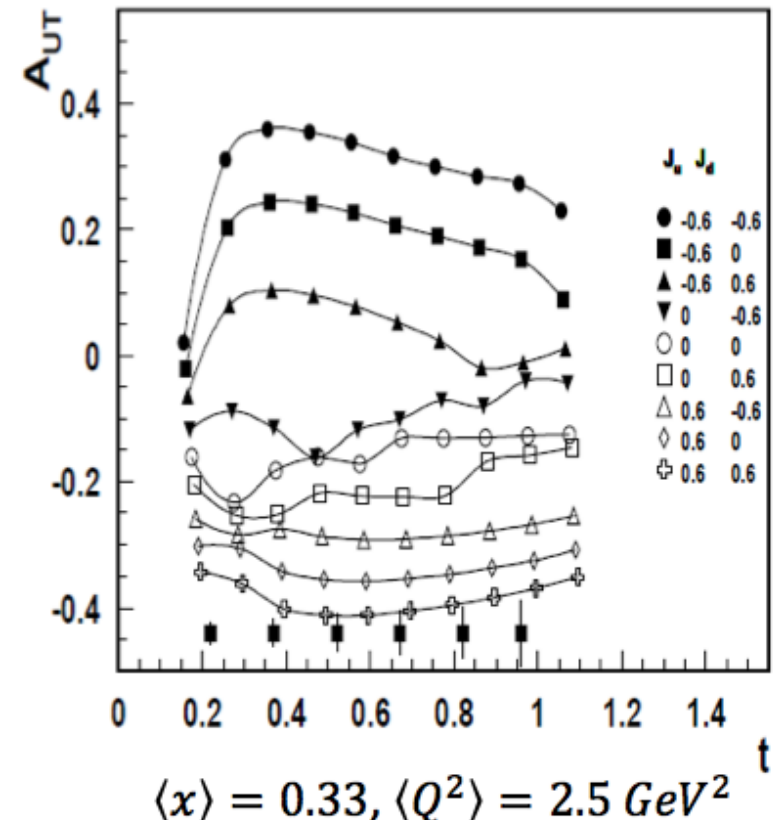
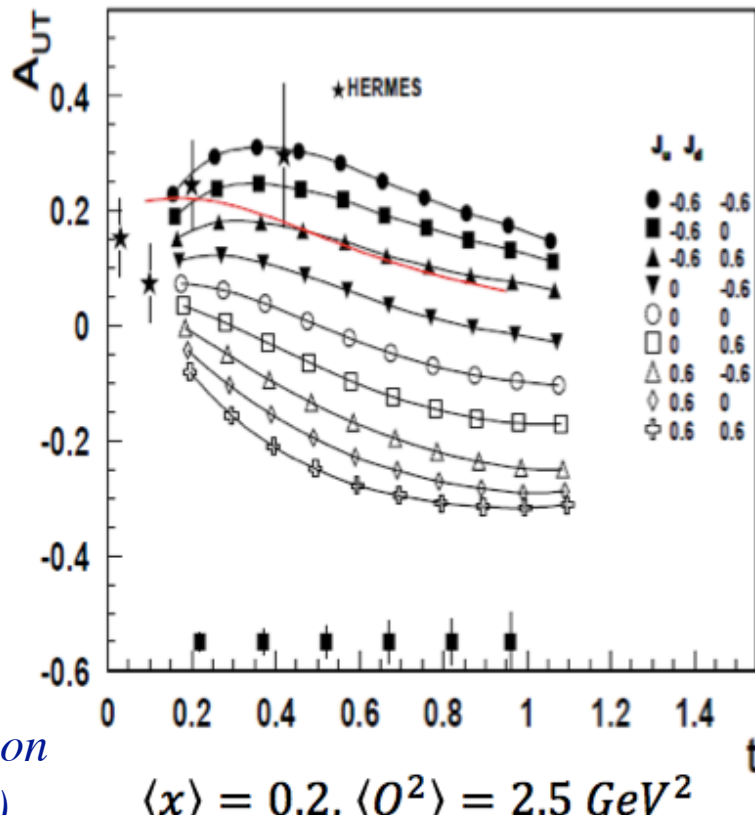
Proton DVCS with transversely polarised target at CLAS12

C12-12-010: with transversely polarised HD target (conditionally approved).

L. Elouardhiri et al.

$$\Delta\sigma_{UT} \sim \cos\phi \operatorname{Im}\{k(F_2 H - F_1 E) + \dots\} d\phi$$

Sensitivity to **Im(E)** for the proton.



Towards nucleon tomography: local fits

Quasi model-independent extraction of CFFs based on a local fit:

- * Set 8 CFFs as free parameters to fit, at each (x_B, t) point, the available observables.
- * Limits imposed within $+/- 5$ times the VGG model predictions (Vanderhaeghen-Guichon-Guidal).
- * Leading-twist DVCS amplitude parametrisation based on Double Distributions.

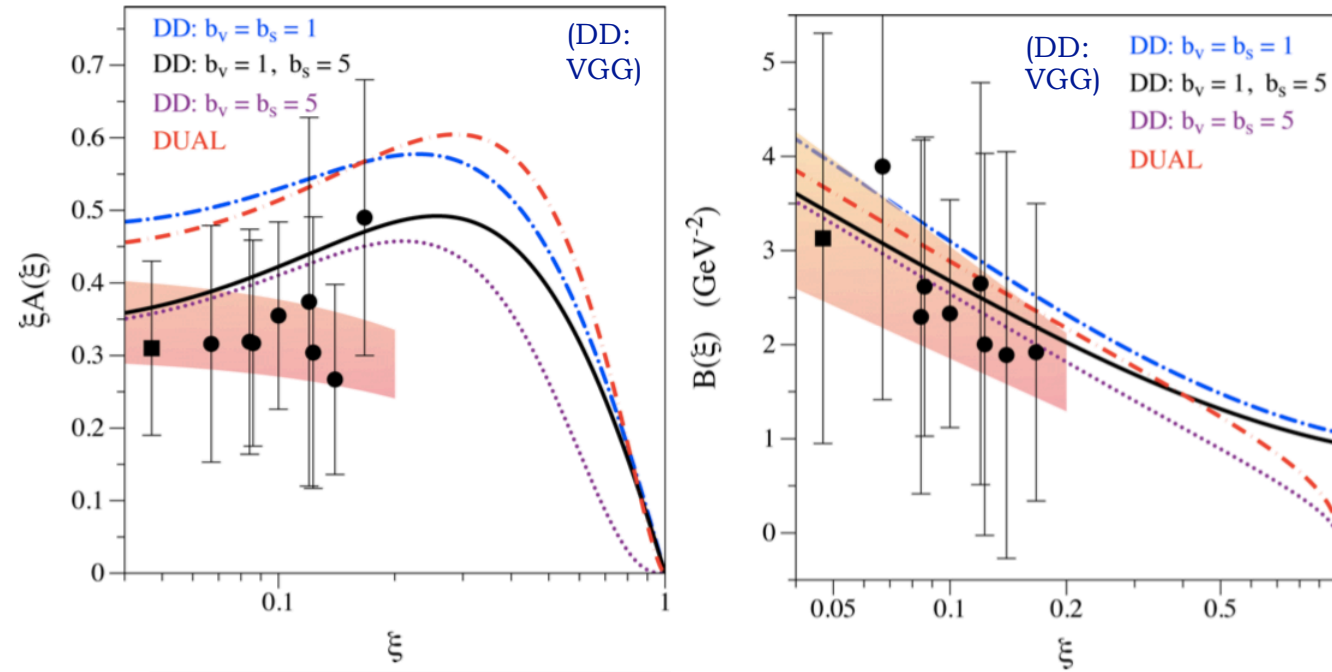
The best constraints in fits to CLAS data were obtained on H_{Im} .

Parametrise its dependence on t :

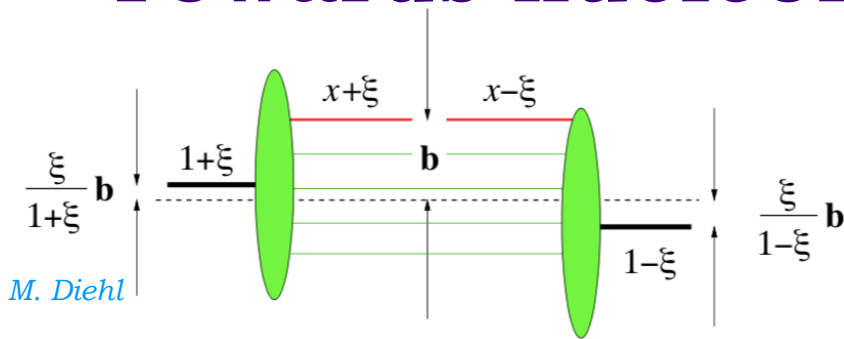
$$H_{Im}(\xi, t) = A(\xi)e^{B(\xi)t}$$

Relates to quark density

Inverse relation to spatial distribution



Towards nucleon tomography: local fits



Transverse parton position interpretation only at $\xi = 0$.

Assuming leading-twist and exponential dependence of GPD on t , using models to extrapolate to the zero skewness point $\xi = 0$ and assuming similar behaviour for u and d quarks there:

$$\langle b_\perp^2 \rangle^q(x) = -4 \frac{\partial}{\partial \Delta_\perp^2} \ln H_-^q(x, 0, -\Delta_\perp^2) \Big|_{\Delta_\perp=0}$$

Tentative hints of 3D distributions are emerging.

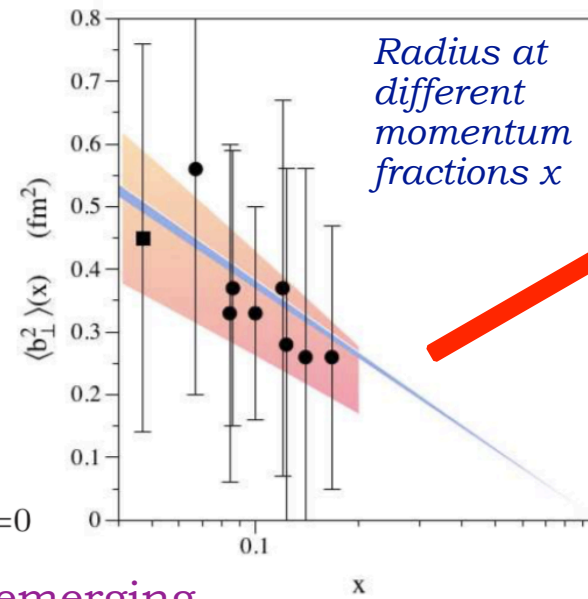
We need more data from JLab @ 11 GeV!

Relating the impact parameter to helicity-averaged transverse distribution:

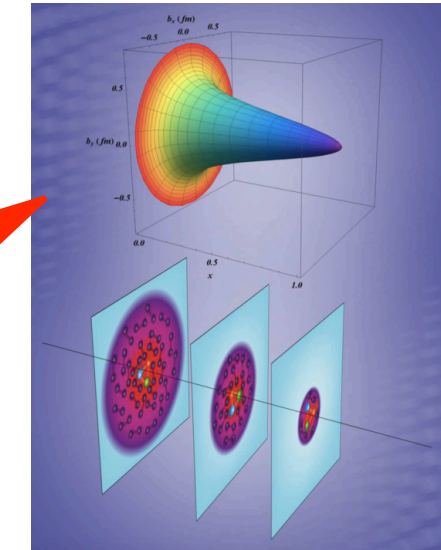
$$\rho^q(x, \mathbf{b}_\perp) = \int \frac{d^2 \Delta_\perp}{(2\pi)^2} e^{-i \mathbf{b}_\perp \cdot \Delta_\perp} H_-^q(x, 0, -\Delta_\perp^2)$$

$$H_-^q(x, 0, t) \equiv H^q(x, 0, t) + H^q(-x, 0, t)$$

Transverse four-momentum transfer to nucleon

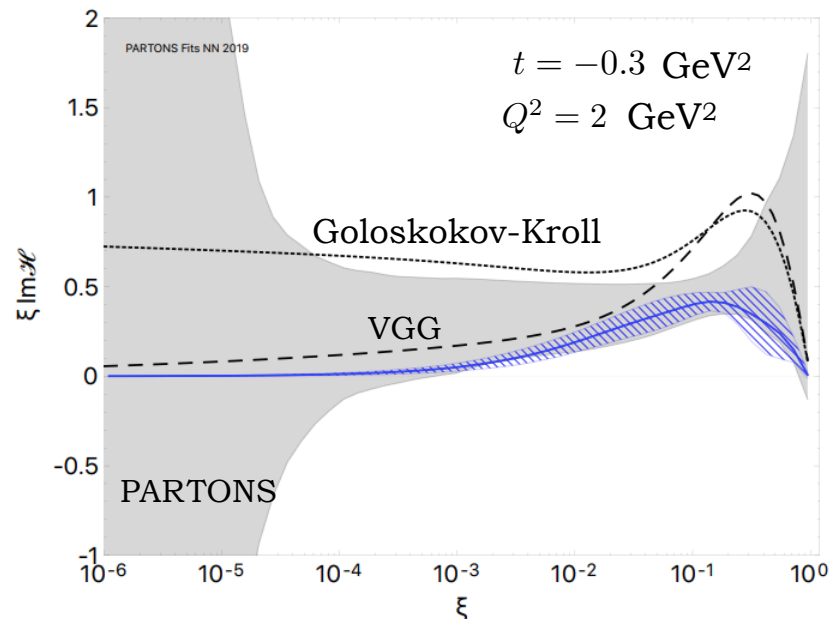
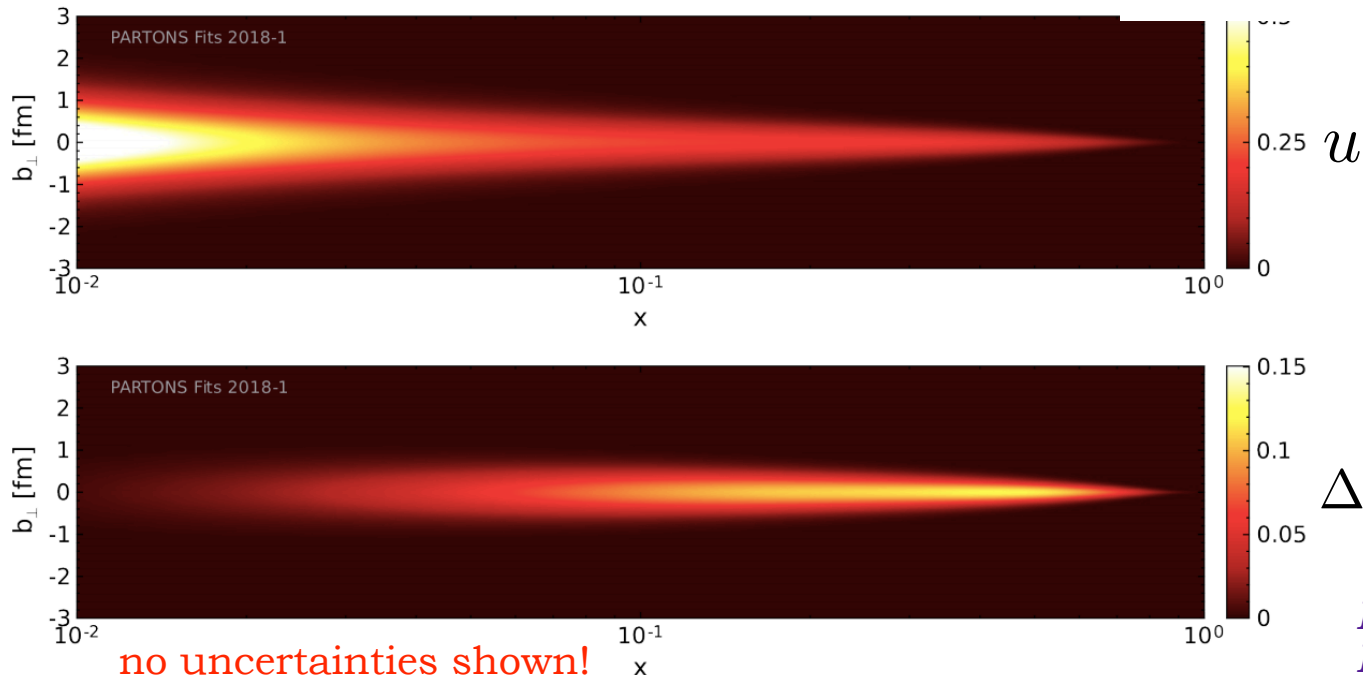


Radius at different momentum fractions x



Towards nucleon tomography: global fits

- * PARTONS framework: global fits and neural networks to minimise model-dependence in the extraction of CFFs.



H. Moutarde *et al.*, Eur. Phys. J C79, 614 (2019)

Inclusion of other channels into PARTONS underway.

Framework in place: more data needed!

Image from Paweł Sznajder,
IWHSS 2019